CHAPTER 9

CONTINUUM-MECHANICS CONCEPTS[1]

In Chapters 6, 7, and 8 we discussed some nonlinear viscoelastic constitutive equations and showed how to use them to solve flow problems. These constitutive equations contained finite strain tensors, rate-of-strain tensors, and the convected derivative of the stress tensor. These various quantities were defined and it was shown how to evaluate them for problem-solving purposes. In this chapter we show how these quantities arise naturally by considering the transformation rules between fixed and convected coordinates; we also discuss why they are needed in order to produce constitutive equations that are "admissible."

The establishment of criteria for admissibility is the subject of §9.1. This subject has been approached in a number of ways in the literature, and the interrelation of the various approaches is by no means easy to understand.[2] We have chosen here to present the criteria for admissibility according to the convected-component method of Oldroyd.[3] Having done this we then turn to the problems of interrelating convected coordinates and fixed coordinates and the tensor components in the two coordinate systems. Thus §9.2 is devoted to the relation between convected coordinates and fixed coordinates, and the relation between the base vectors in the two coordinate systems. Then §9.3 describes the transformation rules for the kinematic tensors used in continuum mechanics; this section culminates in the presentation of a table that is helpful for understanding the notation and the relations among the various kinematic tensors. In §9.4 a discussion of the transformation rules for the stress tensor and its time derivatives is given, and this, too, ends with a table summarizing the notation. Then in §9.5 we return to the subject addressed in §9.1—that of constructing admissible constitutive equations—this time showing how the tables of the two preceding sections can be used to write down constitutive equations in a coordinate system fixed in space. It is at this point that we can understand how the equations given in Chapters 6, 7, and 8 satisfy the criteria of admissibility. In the final section, §9.6, we introduce the very general "memory-integral expansion" and show how it provides important perspectives about constitutive equations, and in particular how the key equations of Chapters 4 through 8 are interrelated.

[1] The authors wish to thank Professor A. S. Lodge for many helpful discussions in connection with this chapter.

[2] For some perspectives on admissibility criteria see A. S. Lodge, *Body Tensor Fields in Continuum Mechanics*, Academic Press, New York (1974), pp. 254–256; this book is recommended for those interested in a more advanced and comprehensive study of the fundamental basis of continuum mechanics.

[3] J. G. Oldroyd, *J. Non-Newtonian Fluid Mech.*, **14**, 9–46 (1984).

This chapter is intended to be only a brief introduction to the subject of continuum mechanics, which is a very large branch of classical mechanics. Those wishing more on this subject should consult one of the many available textbooks or reference works.[4]

§9.1 OLDROYD'S CRITERIA FOR ADMISSIBILITY OF CONSTITUTIVE EQUATIONS[1]

The aim of this section is to obtain the general form of the equations that interrelate the components of the stress and strain tensors (and their time derivatives or integrals) in a material element moving in an arbitrary way as a part of a flowing continuum. In general, this constitutive equation may involve the stress components at time t' for $-\infty < t' \leq t$ and the strain components at time t' for $-\infty < t' \leq t$. Oldroyd proposed that the constitutive equation thus expressed should be independent of (a) any frame of reference, (b) the position in space, the translational motion, and the rotational motion of the fluid element, and (c) the stress and strain in the neighboring fluid elements (except for the continuity requirements on velocity and stress across any surface). In order to construct an equation satisfying these requirements it is most convenient to use a "convected coordinate system," with coordinate surfaces $\hat{x}^i$ = constant ($i = 1, 2, 3$), embedded in the fluid and deforming with it; this kind of coordinate system was first proposed by Hencky.[2] In this kind of coordinate system a fluid particle has by definition the same coordinates $\hat{x}^1$, $\hat{x}^2$, $\hat{x}^3$ for all time. In Fig. 9.1-1 we show how a convected coordinate system moves through space as it is swept along with the moving fluid; for simplicity a two-dimensional flow is depicted.

Next we want to describe the fundamental kinematic and dynamic quantities that should appear in the constitutive equation. The kinematic quantities pertain to the shape and change of shape of fluid elements, and the dynamic quantities have to do with the forces transmitted across fluid surfaces. The next two paragraphs are concerned with the kinematic and dynamic variables central to the formulation of constitutive equations.

We first examine the kinematic description of the flow. At any point in the convected coordinate system we can construct a set of three *convected base vectors* $\hat{\boldsymbol{g}}_i = (\partial/\partial\hat{x}^i)\boldsymbol{r}$, where $\boldsymbol{r}$ is the position vector (see §A.8). A base vector $\hat{\boldsymbol{g}}_i$ is tangent to the $\hat{x}^i$-coordinate curve, and its change in length indicates the extent to which the fluid is stretched in the $\hat{x}^i$-direction. The base vectors depend on the convected coordinates $\hat{x} \equiv \hat{x}^1, \hat{x}^2, \hat{x}^3$ and on the time. The vector between two neighboring fluid particles $\hat{x}$ and $\hat{x} + d\hat{x}$ at time t' is given by

$$\boldsymbol{dr} = \sum_i \hat{\boldsymbol{g}}_i(\hat{x}, t')d\hat{x}^i \tag{9.1-1}$$

[4] Traditional presentations of continuum mechanics have been given by W. Prager, *Introduction to Mechanics of Continua*, Ginn, Boston (1961), and L. E. Malvern, *Introduction to the Mechanics of a Continuous Medium*, Prentice-Hall, Englewood Cliffs, NJ, (1969). An introductory text with a less traditional flavor and with a number of novel viewpoints is A. S. Lodge, *Elastic Liquids*, Academic Press, New York (1964); this book has been particularly influential in the field of rheological measurements, inasmuch as the opening chapters are devoted to homogeneous flows. For extensive bibliographies consult C. Truesdell and R. Toupin, *Encylopedia of Physics*, Vol. III/1, Springer-Verlag, Berlin (1960), pp. 226–793 (with an appendix on tensor fields by J. L. Ericksen, pp. 794–858), and C. Truesdell and W. Noll, *Encyclopedia of Physics*, Vol. III/3, Springer-Verlag, Berlin (1965), pp. 1–579.

[1] J. G. Oldroyd, *Proc. Roy. Soc.*, **A200**, 523–541 (1950); **A202**, 345–358 (1950); **A245**, 278–297 (1958); **A283**, 115–133 (1965); J. G. Oldroyd and B. R. Duffy, *J. Non-Newtonian Fluid Mech.*, **5**, 141–145 (1979). A particularly fine summary of Oldroyd's work is that portion of an essay submitted in competition for the Adams Prize in 1964, which was published posthumously as J. G. Oldroyd, *J. Non-Newtonian Fluid Mech.*, **14**, 9–46 (1984); those wishing to study Oldroyd's approach to continuum mechanics should begin by studying this very readable publication. Much of §9.1 is a paraphrasing of certain portions of pp. 17–24 of this paper.

[2] H. Hencky, *Z. Angew. Math. Mech.*, **5**, 144–146 (1925).

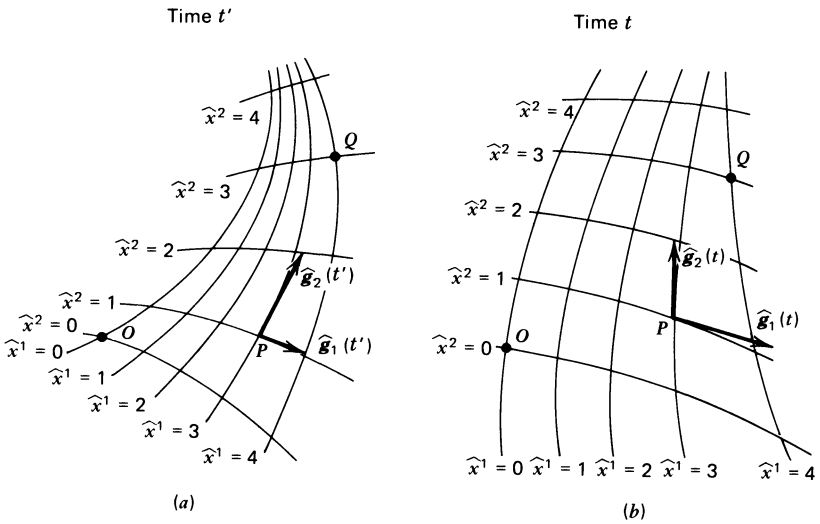

FIGURE 9.1-1. An arbitrarily chosen coordinate system, embedded in a flowing fluid, at two different times (*a*) t' and (*b*) t. Fluid particle P is located at $\hat{x}^1 = 3$, $\hat{x}^2 = 1$ at all times; fluid particle Q is at $\hat{x}^1 = 4$, $\hat{x}^2 = 3$ at all times. The base vectors $\hat{\boldsymbol{g}}_1$ and $\hat{\boldsymbol{g}}_2$ at fluid particle P are also shown.

so that the square of the separation between the particles is given by

$$(\boldsymbol{dr}\cdot\boldsymbol{dr}) = \sum_i \sum_j (\hat{\boldsymbol{g}}_i\cdot\hat{\boldsymbol{g}}_j)d\hat{x}^i\,d\hat{x}^j$$
$$= \sum_i \sum_j \hat{g}_{ij}(\hat{x}, t')d\hat{x}^i\,d\hat{x}^j \tag{9.1-2}$$

in which the $\hat{g}_{ij}(\hat{x}, t)$ are the covariant metric coefficients. These quantities, which describe the relative distances between arbitrary pairs of neighboring particles, contain complete information about the shape of a fluid element at time t'. All the kinematic quantities that may appear in a constitutive equation must be derivable from the metric coefficients $\hat{g}_{ij}(\hat{x}, t)$ for $-\infty < t' \leq t$, which is sometimes called the *deformation history* at the fluid particle $\hat{x}$. Since the $\hat{g}_{ij}$ are obtained by forming scalar products, they do not depend on the instantaneous position or orientation of the fluid element in space.

Next we turn our attention to the dynamical quantities. Let $\hat{\boldsymbol{f}}_i$ be the instantaneous force (per unit area) transmitted across a fluid surface element perpendicular to $\hat{\boldsymbol{g}}_i$. Then according to §1.1b

$$\hat{\boldsymbol{f}}_i = [(\hat{\boldsymbol{g}}_i/|\hat{\boldsymbol{g}}_i|)\cdot\boldsymbol{\pi}] \tag{9.1-3}$$

where $\boldsymbol{\pi}$ is the total stress tensor and $\hat{\boldsymbol{g}}_i/|\hat{\boldsymbol{g}}_i|$ is the unit vector in the $\hat{x}^i$ direction. We now form the scalar product of Eq. 9.1-3 with $\hat{\boldsymbol{g}}_j$

$$(\hat{\boldsymbol{f}}_i\cdot\hat{\boldsymbol{g}}_j) = \frac{1}{|\hat{\boldsymbol{g}}_i|}(\boldsymbol{\pi}:\hat{\boldsymbol{g}}_j\hat{\boldsymbol{g}}_i) \tag{9.1-4}$$

But the double dot product on the right side is just $\hat{\pi}_{ij}$, the ijth component of $\boldsymbol{\pi}$ in the convected coordinate system. Therefore

$$\hat{\pi}_{ij} = \sqrt{(\hat{\boldsymbol{g}}_i\cdot\hat{\boldsymbol{g}}_i)}(\hat{\boldsymbol{f}}_i\cdot\hat{\boldsymbol{g}}_j) \tag{9.1-5}$$

The quantities $\hat{\pi}_{ij}(\hat{x}, t)$ then describe completely the state of stress at a fluid particle at time t, and $\hat{\pi}_{ij}(\hat{x}, t')$ for $-\infty < t' \leq t$ is called the *stress history* at the fluid particle $\hat{x}$. Since the $\hat{\pi}_{ij}$ are obtained by forming scalar products, they are independent of the instantaneous position and orientation of the fluid element in space.

The constitutive equation will generally be some kind of relation containing the stress history and the strain history. If one desires to take into account nonisothermal effects, then the *temperature history*, $T(\hat{x}, t')$ for $-\infty < t' \leq t$, must be included as well. In addition the time difference $t - t'$ may be expected to appear, as well as some material constants (or even material constant tensors whose components are $\hat{\kappa}_{N\,kl\ldots}^{ij\ldots}(\hat{x})$, and whose time derivatives with respect to t' are zero). The constitutive equation might then contain time derivatives such as $\partial\hat{g}_{ij}/\partial t$, $\partial^2\hat{g}_{ij}/\partial t^2$, $\partial\hat{\pi}_{ij}/\partial t, \ldots$ or quantities such as $\hat{g}_{ij}(t')$, $\partial\hat{g}_{ij}/\partial t'$, $\partial\hat{\pi}_{ij}/\partial t', \ldots$ in the integrands of time integrals $\int_{-\infty}^{t} \ldots dt'$. So far we have written only the covariant convected components $\hat{g}_{ij}$ and $\hat{\pi}_{ij}$, but contravariant and mixed components may also be used. For incompressible fluids Oldroyd summarized all of the above in the following way:

The constitutive equation for a flowing continuum can be written as an invariant set of integro-differential equations relating

$$\hat{g}_{ij}(\hat{x}, t'), \quad \hat{\tau}_{ij}(\hat{x}, t'), \quad T(\hat{x}, t'), \quad \hat{\kappa}_{N\,pqr\ldots}^{ijk\ldots}(\hat{x}) \qquad (N = 1, 2, 3\ldots) \tag{9.1-6}$$

for $-\infty < t' \leq t$. Because of the incompressibility constraint it is necessary that

$$\sqrt{\det \hat{g}_{ij}(\hat{x}, t')} = 1 \qquad (-\infty < t' \leq t) \tag{9.1-7}$$

which is equivalent to the statement that the volume of a fluid element is a constant for all t' (see §A.8). The auxiliary relation

$$\hat{\pi}_{ij}(\hat{x}, t) = p(\hat{x}, t)\hat{g}_{ij}(\hat{x}, t) + \hat{\tau}_{ij}(\hat{x}, t) \tag{9.1-8}$$

then gives the total stress tensor components in terms of the $\hat{\tau}_{ij}$ and an isotropic pressure[3] p.

The term "invariant" used above refers to the fact that the equation must have a form independent of the coordinate system; this is accomplished by writing the equations in tensor component form, with the two sides of each equation being tensor components of the same kind (e.g., covariant or contravariant) and order.

Oldroyd pointed out that equations of the above type are *admissible* in the sense that they are (a) form invariant under a change of coordinate system, (b) value invariant under a change of translational or rotational motion of the fluid element as it goes through space, and (c) value invariant under a change of rheological history of neighboring fluid elements. Oldroyd further offered the term *rheological invariance* to describe these three invariances. In this book we use the term "admissible" to indicate that a constitutive equation is rheologically invariant.

The second invariance requirement listed above (labeled (b)) has met with some resistance. It is, however, probably very good for polymer solutions and polymer melts, and indeed almost all molecular theories for polymeric liquids give constitutive equations that

[3] In this text we use the convention that $\hat{\tau}_{ij} = 0$ at equilibrium; this serves to define p.

are consistent with this invariance requirement;[4] this is presumably a consequence of the fact that centrifugal and Coriolis forces can be neglected at the molecular level.[5] It may well be, however, that for a two-phase fluid the invariance requirement (b) will not be appropriate if one wishes to develop a constitutive equation for the equivalent one-phase continuum.

We conclude by writing down several constitutive equations from previous chapters in convected components

Second Order Fluid: (Eq. 6.2-1)

$$\hat{\tau}^{ij} = -b_1 \frac{\partial \hat{g}^{ij}}{\partial t} - b_2 \frac{\partial^2 \hat{g}^{ij}}{\partial t^2} - b_{11} \sum_k \sum_l \frac{\partial \hat{g}^{ik}}{\partial t} \hat{g}_{kl} \frac{\partial \hat{g}^{lj}}{\partial t} \tag{9.1-9}$$

Contravariant Convected Jeffreys Model: (Eq. 7.2-1)

$$\hat{\tau}^{ij} + \lambda_1 \frac{\partial}{\partial t} \hat{\tau}^{ij} = -\eta_0 \left(\frac{\partial \hat{g}^{ij}}{\partial t} + \lambda_2 \frac{\partial^2 \hat{g}^{ij}}{\partial t^2} \right) \tag{9.1-10}$$

Lodge Rubberlike Liquid: (Eq. 8.2-1)

$$\hat{\tau}^{ij} = -\int_{-\infty}^{t} M(t - t')[\hat{g}^{ij}(t') - \hat{g}^{ij}(t)]\, dt' \tag{9.1-11}$$

These equations are all "admissible," in the sense that they satisfy Oldroyd's rules of rheological invariance. In the next several sections we develop the connection between the convected and fixed coordinates and the convected and fixed components of the kinematic and dynamic tensors. Then we will have all the necessary transformation rules to enable us to go back and forth between constitutive equations written in the convected-component form and the fixed-component form. Also we will be able to restate Oldroyd's rules so that we can construct admissible constitutive equations directly using fixed-component notation.

§9.2 CONVECTED COORDINATES AND CONVECTED BASE VECTORS[1]

In §9.1 we introduced the idea of a convected coordinate system embedded in a flowing fluid and deforming with it; in that section no reference was made to any coordinate system fixed in space. In this section we discuss the relation between the convected coordinate system and a specific Cartesian coordinate system fixed in space.[2] We also want to relate the convected base vectors to the unit vectors of the fixed coordinate system.

[4] As one example of a kinetic theory that leads to terms not satisfying this invariance we can cite R. B. Bird, X. J. Fan, and C. F. Curtiss, *J. Non-Newtonian Fluid Mech.*, **15**, 85–92 (1984); even in this theory, however, it was proven that the terms accounting for the deviations from the invariance requirement are negligibly small.

[5] P.-G. de Gennes, *Physica*, **118A**, 44–45 (1983); G. Ryskin, *Phys. Rev.*, **A32**, 1239–1240 (1985).

[1] The presentation in this and the following section has been influenced by L. I. Sedov, *Introduction to the Mechanics of a Continuous Medium*, Addison-Wesley, Reading, MA (1965), and by the first three chapters of A. S. Lodge, *Elastic Liquids*, Academic Press, New York (1964).

[2] One can, of course, choose an orthogonal (or even nonorthogonal) curvilinear coordinate system for the fluid at time t; by using Cartesian coordinates the discussion is simplified somewhat.

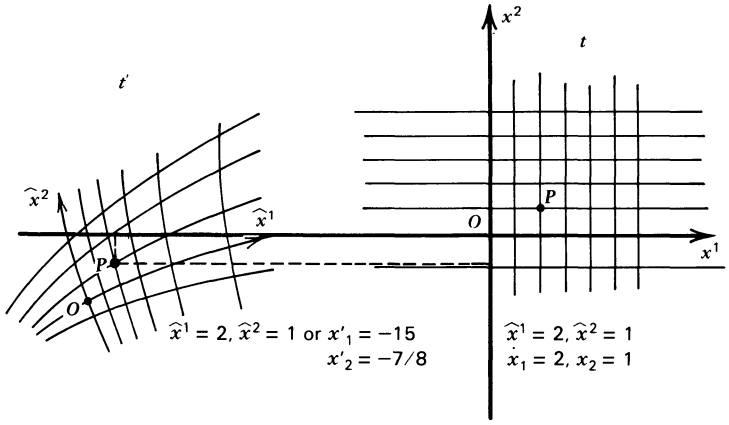

FIGURE 9.2-1. Convected coordinates; the convected coordinates $\hat{x}^i$ exactly coincide with the fixed coordinates x_i at time t.

We consider now the special convected coordinate system $\hat{x}^1$, $\hat{x}^2$, $\hat{x}^3$ in Fig. 9.2-1, which at time t exactly coincides with a Cartesian coordinate system x_1, x_2, x_3. A fluid particle P can be designated by giving its convected coordinates $\hat{x}^i$, which remain the same for all values of the time. The fluid particle P can also be identified by giving its Cartesian coordinates x'_i at time t'; these coordinates are given with respect to the frame $Ox_1x_2x_3$. At time t particle P has coordinates x_i in the frame $Ox_1x_2x_3$. Note that the coordinates x_i at time t have exactly the same numerical values as the particle coordinates $\hat{x}^i$ in the $\hat{O}\hat{x}^1\hat{x}^2\hat{x}^3$ system.[3]

The motion of the fluid is described by giving the location of all fluid particles for all past times t':

$$x'_i = x'_i(\hat{x}^1, \hat{x}^2, \hat{x}^3, t') \qquad i = 1, 2, 3 \tag{9.2-1}$$

The fluid particle given by the convected coordinates $\hat{x}^1$, $\hat{x}^2$, $\hat{x}^3$ is located at x_1, x_2, x_3, at time t. That is we can use either $\hat{x}^1$, $\hat{x}^2$, $\hat{x}^3$ as the "particle label" or alternatively the variables x_1, x_2, x_3, and t. Hence we may rewrite Eq. 9.2-1 as

$$x'_i = x'_i(x_1, x_2, x_3, t, t') \quad \text{or} \quad \boldsymbol{r}' = \boldsymbol{r}'(\boldsymbol{r}, t, t') \tag{9.2-2}$$

These relations may be inverted to give

$$x_i = x_i(x'_1, x'_2, x'_3, t', t) \quad \text{or} \quad \boldsymbol{r} = \boldsymbol{r}(\boldsymbol{r}', t', t) \tag{9.2-3}$$

The functions on the right sides of these equations are the *displacement functions* (cf. Eqs. 8.1-1 and 2).

As pointed out in §9.1 we may define *convected base vectors* $\hat{\boldsymbol{g}}_i$ at each fluid particle. They are functions of the location in the convected coordinate system and also depend on the time t' since the coordinate system itself is changing with time as the fluid moves along.

[3] In comparing the discussion here with that of §A.8 note that the Cartesian coordinates x_i of Appendix A correspond to the x'_i here, and the nonorthogonal, curvilinear coordinates q^i of Appendix A correspond to $\hat{x}^i$ here.

Hence we indicate the dependence on fluid particle and time by writing $\hat{\boldsymbol{g}}_i(\hat{x}^1, \hat{x}^2, \hat{x}^3, t')$ or alternatively $\hat{\boldsymbol{g}}_i(\boldsymbol{r}, t, t')$—that is, we can use the particle label $\hat{x}^i (i = 1, 2, 3)$ or $(\boldsymbol{r}, t)$. Then,

$$\begin{aligned}
\hat{\boldsymbol{g}}_i(\boldsymbol{r}, t, t') &= \frac{\partial}{\partial \hat{x}^i} \boldsymbol{r}' && \text{(Definition of } \hat{\boldsymbol{g}}_i\text{)} \\
&= \frac{\partial}{\partial x_i} \left(\sum_j \boldsymbol{\delta}_j x'_j \right) && \text{(Expand position vector } \boldsymbol{r}' \text{ in its Cartesian components)} \\
&= \sum_j \boldsymbol{\delta}_j \Delta_{ji} && \text{(Use definition of Eq. 8.1-3)} \\
&= [\boldsymbol{\Delta} \cdot \boldsymbol{\delta}_i] && (9.2\text{-}4)
\end{aligned}$$

Note that the tensor $\boldsymbol{\Delta}(\boldsymbol{r}, t, t') = \sum_i \sum_j \boldsymbol{\delta}_i \boldsymbol{\delta}_j \Delta_{ij}$ operates on the ith unit vector $\boldsymbol{\delta}_i$ to give the ith convected base vector $\hat{\boldsymbol{g}}_i$; we can also regard Δ_{ji} as the jth Cartesian component of $\hat{\boldsymbol{g}}_i$. By virtue of the way we define the convected coordinate system, at $t' = t$ we must have $\hat{\boldsymbol{g}}_i(\boldsymbol{r}, t, t) = \boldsymbol{\delta}_i$ and $\boldsymbol{\Delta}(\boldsymbol{r}, t, t) = \boldsymbol{\delta}$. The base vector $\hat{\boldsymbol{g}}_i$ is tangent to the $\hat{x}^i$ coordinate curve; the set of three base vectors $\hat{\boldsymbol{g}}_i(\boldsymbol{r}, t, t')$ describe how the fluid in the neighborhood of the particle $\boldsymbol{r}, t$ is oriented and distorted as it moves through space.

At every fluid particle we may also define a set of *convected reciprocal base vectors*

$$\begin{aligned}
\hat{\boldsymbol{g}}^i(\boldsymbol{r}, t, t') &= \frac{\partial}{\partial \boldsymbol{r}'} \hat{x}^i && \text{(Definition of } \hat{\boldsymbol{g}}^i\text{)} \\
&= \left(\sum_j \boldsymbol{\delta}_j \frac{\partial}{\partial x'_j} \right) x_i && \text{(Expand } \partial/\partial \boldsymbol{r}' \text{ in its Cartesian components)} \\
&= \sum_j \mathrm{E}_{ij} \boldsymbol{\delta}_j && \text{(Use definition of Eq. 8.1-4)} \\
&= [\boldsymbol{\delta}_i \cdot \mathbf{E}] && (9.2\text{-}5)
\end{aligned}$$

Note that the tensor $\mathbf{E}(\boldsymbol{r}, t, t') = \sum_i \sum_j \boldsymbol{\delta}_i \boldsymbol{\delta}_j \mathrm{E}_{ij}$ operates on the ith unit vector to give the ith convected reciprocal base vector $\hat{\boldsymbol{g}}^i$; we can also regard E_{ij} as the jth Cartesian component of $\hat{\boldsymbol{g}}^i$. It should be pointed out that to calculate the components of $\mathbf{E}$, we first differentiate the inverse displacement functions and then eliminate the x'_j in favor of the x_j so that $\mathbf{E}$ finally depends on $\boldsymbol{r}, t$ and t'. At $t' = t$, we have $\hat{\boldsymbol{g}}^i = \boldsymbol{\delta}_i$ and $\mathbf{E} = \boldsymbol{\delta}$. The reciprocal base vector $\hat{\boldsymbol{g}}^i$ is normal to the surface $\hat{x}^i =$ constant; the set of $\hat{\boldsymbol{g}}^i$ gives information about how the fluid is being deformed. We also mention that for an incompressible fluid $\hat{\boldsymbol{g}}^i = [\hat{\boldsymbol{g}}_j \times \hat{\boldsymbol{g}}_k]$ (for $ijk = 123$, 231, and 312). Keep in mind that $(\hat{\boldsymbol{g}}_i \cdot \hat{\boldsymbol{g}}^j) = (\hat{\boldsymbol{g}}^i \cdot \hat{\boldsymbol{g}}_j) = \delta_{ij}$ (see §A.8).

In Fig. 9.2-2 we show the convected base vectors and reciprocal base vectors in a homogeneous flow, and in Fig. 9.2-3 the convected base vectors for four different times in a nonhomogeneous flow. These figures should be helpful in showing how the convected coordinate system and the $\hat{\boldsymbol{g}}_i$ and $\hat{\boldsymbol{g}}^i$ change with time as the fluid flows along. In addition Problems 9B.3 and 4 provide an opportunity for calculating the convected base vectors and various kinematic tensors for the flows depicted in Figs. 9.2-2 and 3.

In the following development we need to know how the convected base vectors and the displacement gradient tensors $\boldsymbol{\Delta}$ and $\mathbf{E}$ change with t' as we follow a fluid particle along

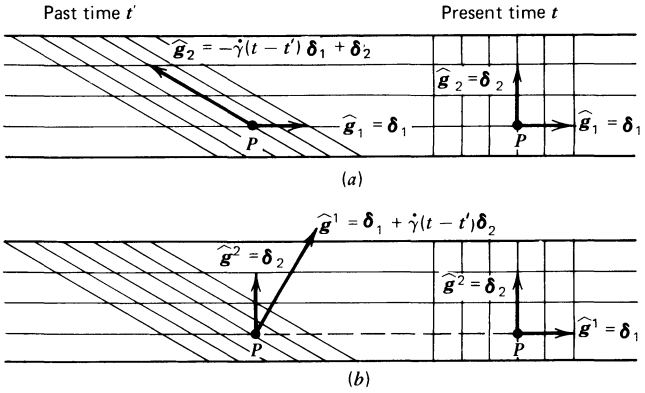

FIGURE 9.2-2. Steady shear flow $v_1 = \dot{\gamma}x_2$, $v_2 = 0$, $v_3 = 0$ showing the convected base vectors and reciprocal base vectors associated with a fluid particle P as it moves along from some past time t' to the present time t. The vectors $\hat{\boldsymbol{g}}_3$ and $\hat{\boldsymbol{g}}^3$ are perpendicular to the plane of the paper and both equal to $\boldsymbol{\delta}_3$. In this *homogeneous* flow the convected base vectors $\hat{\boldsymbol{g}}_i$ are coincident with material lines; that is, they are "embedded" in the fluid. The convected reciprocal base vectors $\hat{\boldsymbol{g}}^i$ are perpendicular to material surfaces.

its trajectory. As we show in Example 9.2-1 the time derivatives of the convected base vectors are

$$\boxed{\frac{\partial}{\partial t'}\hat{\boldsymbol{g}}_i = +[\hat{\boldsymbol{g}}_i \cdot \nabla \boldsymbol{v}]} \tag{9.2-6}$$

$$\boxed{\frac{\partial}{\partial t'}\hat{\boldsymbol{g}}^i = -[(\nabla \boldsymbol{v})\cdot \hat{\boldsymbol{g}}^i]} \tag{9.2-7}$$

Here it is understood that the base vectors and $\nabla \boldsymbol{v}$ are all evaluated at t' for constant $\boldsymbol{r}$ and t (that is, following the fluid particle). From these relations and Eqs. 9.2-4 and 5 it follows that the time derivatives of the displacement gradient tensors are given by

$$\boxed{\frac{\partial}{\partial t'}\boldsymbol{\Delta} = +\{(\nabla \boldsymbol{v})^\dagger \cdot \boldsymbol{\Delta}\}} \tag{9.2-8}$$

$$\boxed{\frac{\partial}{\partial t'}\mathbf{E} = -\{\mathbf{E}\cdot(\nabla \boldsymbol{v})^\dagger\}} \tag{9.2-9}$$

These expressions are needed in §9.3 to get the rate-of-strain tensors.

EXAMPLE 9.2-1 Change of Convected Base Vectors with Time

Derive Eqs. 9.2-6 to 9.

SOLUTION **(a)** First make use of the definition of the $\hat{\boldsymbol{g}}_i$ and write

$$\frac{\partial}{\partial t'}\hat{\boldsymbol{g}}_i(\hat{x}, t') = \frac{\partial}{\partial t'}\left(\frac{\partial}{\partial \hat{x}^i}\boldsymbol{r}'\right) \tag{9.2-10}$$

Next we interchange the order of differentiation:

$$\frac{\partial}{\partial t'}\hat{\boldsymbol{g}}_i(\hat{x}, t') = \frac{\partial}{\partial \hat{x}^i}\left(\frac{\partial}{\partial t'}\boldsymbol{r}'\right) \tag{9.2-11}$$

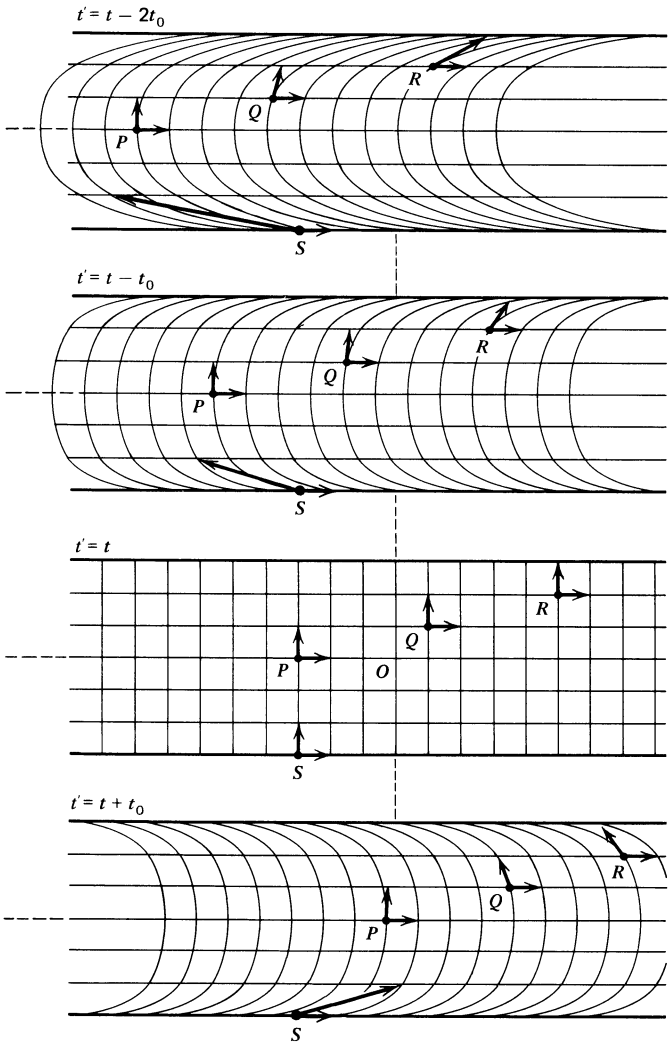

FIGURE 9.2-3. Steady flow between two parallel plates. The fluid viscosity is given by $\eta = m\dot{\gamma}^{n-1}$ with $n = \frac{1}{3}$. At $t' = t$ fluid particle R has coordinates $x_1 = 5, x_2 = 2, x_3 = 0$ with respect to the origin O of a Cartesian coordinate system. At time $t' = t - 2t_0$ its coordinates are $x'_1 = 1, x'_2 = 2, x'_3 = 0$ with respect to the origin O. Its convected coordinates are $\hat{x}^1 = 5, \hat{x}^2 = 2, \hat{x}^3 = 0$ for all times t'. The convected base vectors $\hat{\boldsymbol{g}}_1$ and $\hat{\boldsymbol{g}}_2$ are shown for fluid particles P, Q, R, S; $\hat{\boldsymbol{g}}_3$ is of unit length perpendicular to the plane of the paper. At $t' = t$ the convected base vectors $\hat{\boldsymbol{g}}_1, \hat{\boldsymbol{g}}_2, \hat{\boldsymbol{g}}_3$ coincide with the unit vectors $\boldsymbol{\delta}_1, \boldsymbol{\delta}_2, \boldsymbol{\delta}_3$ of the Cartesian coordinate system. Note that this flow is *nonhomogeneous* and that the convected base vector $\hat{\boldsymbol{g}}_2$ is not coincident with a material line; it is "embedded" in the fluid in the sense that it is always tangent to the same material curve.

But the change of $\boldsymbol{r}'$ with respect to t' at constant fluid particle label $\hat{x}^i$ is the definition of the fluid velocity $\boldsymbol{v}'$ at the time t', so that

$$\frac{\partial}{\partial t'}\hat{\boldsymbol{g}}_i(\hat{x}, t') = \frac{\partial}{\partial \hat{x}^i}\boldsymbol{v}'$$

$$= \sum_j \frac{\partial x'_j}{\partial \hat{x}_i}\left(\frac{\partial}{\partial x'_j}\boldsymbol{v}'\right) \tag{9.2-12}$$

However $\partial x'_j/\partial \hat{x}^i$ is the same as $\partial x'_j/\partial x_i$, and therefore, according to Eq. 9.2-4, is also the same as the jth component of $\hat{\boldsymbol{g}}_i$. Hence Eq. 9.2-6 follows directly.

(b) To get Eq. 9.2-7 we start by differentiating the relation $(\hat{\boldsymbol{g}}_i \cdot \hat{\boldsymbol{g}}^j) = \delta_{ij}$ with respect to t'

$$\left(\left(\frac{\partial}{\partial t'}\hat{\boldsymbol{g}}_i\right)\cdot\hat{\boldsymbol{g}}^j\right) + \left(\hat{\boldsymbol{g}}_i\cdot\left(\frac{\partial}{\partial t'}\hat{\boldsymbol{g}}^j\right)\right) = 0 \tag{9.2-13}$$

Then we use Eq. 9.2-6 in the first term to get

$$([\hat{\boldsymbol{g}}_i\cdot\nabla\boldsymbol{v}]\cdot\hat{\boldsymbol{g}}^j) = -\left(\hat{\boldsymbol{g}}_i\cdot\frac{\partial}{\partial t'}\hat{\boldsymbol{g}}^j\right) \tag{9.2-14}$$

The dot products on the left side may be regrouped:

$$(\hat{\boldsymbol{g}}_i\cdot[(\nabla\boldsymbol{v})\cdot\hat{\boldsymbol{g}}^j]) = -\left(\hat{\boldsymbol{g}}_i\cdot\frac{\partial}{\partial t'}\hat{\boldsymbol{g}}^j\right) \tag{9.2-15}$$

Since $\hat{\boldsymbol{g}}_i$ is arbitrary (i.e., i can be 1, 2, or 3), the quantities dotted into the $\hat{\boldsymbol{g}}_i$ may be equated and Eq. 9.2-7 is obtained.

(c) To get Eq. 9.2-8 we substitute $\hat{\boldsymbol{g}}_i = [\boldsymbol{\Delta}\cdot\boldsymbol{\delta}_i]$ into both sides of Eq. 9.2-6:

$$\left[\frac{\partial\boldsymbol{\Delta}}{\partial t'}\cdot\boldsymbol{\delta}_i\right] = [[\boldsymbol{\Delta}\cdot\boldsymbol{\delta}_i]\cdot\nabla\boldsymbol{v}] \tag{9.2-16}$$

When the right side is rearranged we get:

$$\left[\frac{\partial\boldsymbol{\Delta}}{\partial t'}\cdot\boldsymbol{\delta}_i\right] = [\{(\nabla\boldsymbol{v})^\dagger\cdot\boldsymbol{\Delta}\}\cdot\boldsymbol{\delta}_i] \tag{9.2-17}$$

When the quantities dotted into $\boldsymbol{\delta}_i$ are equated, Eq. 9.2-8 results. Equation 9.2-9 may be derived in a similar way.

§9.3 TRANSFORMATION RULES FOR THE STRAIN TENSOR AND ITS TIME DERIVATIVES

It was pointed out in §9.1 that the quantities $\hat{g}_{ij} = (\hat{\boldsymbol{g}}_i\cdot\hat{\boldsymbol{g}}_j)$ contain complete information about the shape of a fluid element. The same can be said about the quantities $\hat{g}^{ij} = (\hat{\boldsymbol{g}}^i\cdot\hat{\boldsymbol{g}}^j)$. This section is devoted to a study of these quantities and their time derivatives. In particular we want to provide the transformation rules that allow us to write the kinematic quantities, defined in the convected coordinate system, in terms of the Cartesian components in a fixed coordinate system.

In Chapter 5, in the discussion of linear viscoelasticity, we introduced infinitesimal strain tensors describing the strain at time t', relative to the fluid configuration at time t. This suggests that we ought to use the quantity $[\hat{g}_{ij}(\boldsymbol{r}, t, t') - \hat{g}_{ij}(\boldsymbol{r}, t, t)]$ as a measure of the relative strain, where $\boldsymbol{r}$, t is the label for a particular fluid particle. This quantity can be expressed in terms of Cartesian components in the fixed frame by using Eq. 9.2-4:

$$\begin{aligned}[\hat{g}_{ij}(\boldsymbol{r}, t, t') - \hat{g}_{ij}(\boldsymbol{r}, t, t)] &= \left(\left(\sum_m \boldsymbol{\delta}_m\Delta_{mi}\right)\cdot\left(\sum_n \boldsymbol{\delta}_n\Delta_{nj}\right)\right) - (\boldsymbol{\delta}_i\cdot\boldsymbol{\delta}_j)\\ &= \sum_n \Delta^\dagger_{in}(\boldsymbol{r}, t, t')\Delta_{nj}(\boldsymbol{r}, t, t') - \delta_{ij}\\ &= \gamma^{[0]}_{ij}(\boldsymbol{r}, t, t')\end{aligned} \tag{9.3-1}$$

These are the Cartesian components of the *relative (finite) strain tensor* $\boldsymbol{\gamma}^{[0]} = \sum_i \sum_j \boldsymbol{\delta}_i \boldsymbol{\delta}_j \gamma_{ij}^{[0]}$ given earlier in Eq. 8.1-8. In a similar way we can use Eq. 9.2-5 to show that

$$\begin{aligned} -[\hat{g}^{ij}(\boldsymbol{r}, t, t') - \hat{g}^{ij}(\boldsymbol{r}, t, t)] &= (\boldsymbol{\delta}_i \cdot \boldsymbol{\delta}_j) - \left(\left(\sum_m \mathrm{E}_{im}\boldsymbol{\delta}_m\right)\cdot\left(\sum_n \mathrm{E}_{jn}\boldsymbol{\delta}_n\right)\right) \\ &= \delta_{ij} - \sum_n \mathrm{E}_{in}(\boldsymbol{r}, t, t')\mathrm{E}^{\dagger}_{nj}(\boldsymbol{r}, t, t') \\ &= \gamma_{[0]ij}(\boldsymbol{r}, t, t') \end{aligned} \tag{9.3-2}$$

These are the Cartesian components of the *relative (finite) strain tensor* $\boldsymbol{\gamma}_{[0]} = \sum_i \sum_j \boldsymbol{\delta}_i \boldsymbol{\delta}_j \gamma_{[0]ij}$ given in Eq. 8.1-9.

Several comments deserve to be made regarding the relative strain tensors:

- **a.** They are both obtainable from the displacement functions (as shown in §8.1).
- **b.** They both reduce to the infinitesimal strain tensor $\boldsymbol{\gamma}$ for small strains (see Example 9.3-1).
- **c.** They both depend on the particle label $\boldsymbol{r}$, t and on the time t'; when $t' = t$, the relative finite strain tensors vanish.
- **d.** They both arise naturally in molecular theories, and both are used in empirical constitutive equations.

The main point of the above discussion is that we have seen how the finite strain tensors introduced in Chapter 8 are related to the quantities $\hat{g}_{ij}$ and $\hat{g}^{ij}$ that arise in the convected-coordinate formulation of constitutive equations.

EXAMPLE 9.3-1 The Relation of the Relative Strain Tensors to the Infinitesimal Strain Tensor

Let $\boldsymbol{u} = \boldsymbol{r}' - \boldsymbol{r}$ be the location of a fluid particle at time t' relative to its location at time t. Show that both $\boldsymbol{\gamma}^{[0]}$ and $\boldsymbol{\gamma}_{[0]}$ become $\boldsymbol{\gamma} = \nabla\boldsymbol{u} + (\nabla\boldsymbol{u})^{\dagger}$ in the limit of very small displacement gradients.

SOLUTION **(a)** First we substitute $x'_k = x_k + u_k$ into the second line of Eq. 9.3-1 to get

$$\begin{aligned} \gamma_{ij}^{[0]} &= \sum_k \left(\delta_{ik} + \frac{\partial u_k}{\partial x_i}\right)\left(\delta_{jk} + \frac{\partial u_k}{\partial x_j}\right) - \delta_{ij} \\ &= \left(\frac{\partial}{\partial x_i} u_j + \frac{\partial}{\partial x_j} u_i\right) + \sum_k \left(\frac{\partial}{\partial x_i} u_k\right)\left(\frac{\partial}{\partial x_j} u_k\right) \end{aligned} \tag{9.3-3}$$

In the limit of very small displacement gradients, the quadratic terms can be omitted so that

$$\boldsymbol{\gamma}^{[0]} \doteq \nabla\boldsymbol{u} + (\nabla\boldsymbol{u})^{\dagger} \tag{9.3-4}$$

This is the infinitesimal strain tensor $\boldsymbol{\gamma}$ used in Chapter 5.

(b) Similarly if we substitute $x_k = x'_k - u_k$ into Eq. 9.3-2 we get

$$\begin{aligned} \gamma_{[0]ij} &= \delta_{ij} - \sum_k \left(\delta_{ik} - \frac{\partial u_i}{\partial x'_k}\right)\left(\delta_{jk} - \frac{\partial u_j}{\partial x'_k}\right) \\ &= \left(\frac{\partial}{\partial x'_j} u_i + \frac{\partial}{\partial x'_i} u_j\right) + \text{quadratic terms} \end{aligned} \tag{9.3-5}$$

But for very small displacement gradients, the quadratic terms can be omitted; also x'_j and x_j will be indistinguishable in the derivatives. Hence,

$$\boldsymbol{\gamma}_{[0]} \doteq \nabla \boldsymbol{u} + (\nabla \boldsymbol{u})^\dagger \tag{9.3-6}$$

for small displacement gradients.

In linear viscoelasticity we used not only the infinitesimal strain tensor $\boldsymbol{\gamma}$ but also the rate of strain tensor $\dot{\boldsymbol{\gamma}} = \partial\boldsymbol{\gamma}/\partial t$ and higher time derivatives, $\ddot{\boldsymbol{\gamma}} = \partial\dot{\boldsymbol{\gamma}}/\partial t = \partial^2\boldsymbol{\gamma}/\partial t^2$, etc. It is not surprising, then, that in nonlinear viscoelasticity time derivatives of the relative strain tensors have been defined

$$\boldsymbol{\gamma}^{[n]} = \partial^n \boldsymbol{\gamma}^{[0]}(\boldsymbol{r}, t, t')/\partial t'^n \quad \text{and} \quad \boldsymbol{\gamma}_{[n]} = \partial^n \boldsymbol{\gamma}_{[0]}(\boldsymbol{r}, t, t')/\partial t'^n \tag{9.3-7}$$

By way of illustration we show how to get $\boldsymbol{\gamma}^{[1]}$ and $\boldsymbol{\gamma}^{[2]}$.

To get $\boldsymbol{\gamma}^{[1]}$ we take the time derivative of Eq. 9.3-1 and use Eq. 9.2-8 to evaluate $(\partial/\partial t')\boldsymbol{\Delta}$:

$$\begin{aligned}
\boldsymbol{\gamma}^{[1]}(\boldsymbol{r}, t, t') &= \frac{\partial}{\partial t'}\{\boldsymbol{\Delta}^\dagger \cdot \boldsymbol{\Delta} - \boldsymbol{\delta}\} \\
&= \left\{\frac{\partial \boldsymbol{\Delta}^\dagger}{\partial t'} \cdot \boldsymbol{\Delta} + \boldsymbol{\Delta}^\dagger \cdot \frac{\partial \boldsymbol{\Delta}}{\partial t'}\right\} \\
&= \left\{\{\boldsymbol{\Delta}^\dagger \cdot \nabla \boldsymbol{v}\} \cdot \boldsymbol{\Delta} + \boldsymbol{\Delta}^\dagger \cdot \{(\nabla \boldsymbol{v})^\dagger \cdot \boldsymbol{\Delta}\}\right\} \\
&= \{\boldsymbol{\Delta}^\dagger \cdot (\nabla \boldsymbol{v} + (\nabla \boldsymbol{v})^\dagger) \cdot \boldsymbol{\Delta}\} \\
&= \{\boldsymbol{\Delta}^\dagger \cdot \boldsymbol{\gamma}^{(1)} \cdot \boldsymbol{\Delta}\}
\end{aligned} \tag{9.3-8}$$

in which $\boldsymbol{\Delta}$, $\nabla \boldsymbol{v}$, and $\boldsymbol{\gamma}^{(1)}$ are understood to be functions of $\boldsymbol{r}$, t, and t'. The last equality serves to define the tensor $\boldsymbol{\gamma}^{(1)}(\boldsymbol{r}, t, t')$. Note that when $t' = t$, the displacement gradient tensor $\boldsymbol{\Delta}$ becomes the unit tensor and hence $\boldsymbol{\gamma}^{[1]}(\boldsymbol{r}, t, t) = \boldsymbol{\gamma}^{(1)}(\boldsymbol{r}, t)$. The tensor $\boldsymbol{\gamma}^{(1)}(\boldsymbol{r}, t)$ is exactly the same as the rate-of-strain tensor $\dot{\boldsymbol{\gamma}}(\boldsymbol{r}, t) = \nabla \boldsymbol{v} + (\nabla \boldsymbol{v})^\dagger$.

To get $\boldsymbol{\gamma}^{[2]}$ we take the time derivative of Eq. 9.3-8:

$$\begin{aligned}
\boldsymbol{\gamma}^{[2]}(\boldsymbol{r}, t, t') &= \frac{\partial}{\partial t'}\{\boldsymbol{\Delta}^\dagger \cdot \boldsymbol{\gamma}^{(1)} \cdot \boldsymbol{\Delta}\} \\
&= \left\{\frac{\partial \boldsymbol{\Delta}^\dagger}{\partial t'} \cdot \boldsymbol{\gamma}^{(1)} \cdot \boldsymbol{\Delta} + \boldsymbol{\Delta}^\dagger \cdot \frac{\partial \boldsymbol{\gamma}^{(1)}}{\partial t'} \cdot \boldsymbol{\Delta} + \boldsymbol{\Delta}^\dagger \cdot \boldsymbol{\gamma}^{(1)} \cdot \frac{\partial \boldsymbol{\Delta}}{\partial t'}\right\} \\
&= \left\{\{\boldsymbol{\Delta}^\dagger \cdot \nabla \boldsymbol{v}\} \cdot \boldsymbol{\gamma}^{(1)} \cdot \boldsymbol{\Delta} + \boldsymbol{\Delta}^\dagger \cdot \frac{\partial \boldsymbol{\gamma}^{(1)}}{\partial t'} \cdot \boldsymbol{\Delta} + \boldsymbol{\Delta}^\dagger \cdot \boldsymbol{\gamma}^{(1)} \cdot \{(\nabla \boldsymbol{v})^\dagger \cdot \boldsymbol{\Delta}\}\right\} \\
&= \left\{\boldsymbol{\Delta}^\dagger \cdot \left\{\frac{\partial \boldsymbol{\gamma}^{(1)}}{\partial t'} + (\nabla \boldsymbol{v}) \cdot \boldsymbol{\gamma}^{(1)} + \boldsymbol{\gamma}^{(1)} \cdot (\nabla \boldsymbol{v})^\dagger\right\} \cdot \boldsymbol{\Delta}\right\} \\
&= \{\boldsymbol{\Delta}^\dagger \cdot \boldsymbol{\gamma}^{(2)} \cdot \boldsymbol{\Delta}\}
\end{aligned} \tag{9.3-9}$$

Here also $\boldsymbol{\Delta}$, $\nabla \boldsymbol{v}$, and $\boldsymbol{\gamma}^{(2)}$ are understood to be functions of $\boldsymbol{r}$, t, t'—that is, they are evaluated at time t' at the fluid particle $\boldsymbol{r}$, t. The tensor $\boldsymbol{\gamma}^{(2)}(\boldsymbol{r}, t\, t')$ is defined by the last equality above. When $t' = t$, the tensor $\boldsymbol{\Delta}$ becomes the unit tensor, and the derivative $(\partial\boldsymbol{\gamma}^{(1)}/\partial t')_{\boldsymbol{r},t}$ following

the particle $\boldsymbol{r}, t$ becomes identical to the substantial derivative[1] $D\boldsymbol{\gamma}^{(1)}/Dt$. As a result of Eqs. 9.3-8 and 9 and straightforward extensions we have

$$\boldsymbol{\gamma}^{[1]}(\boldsymbol{r}, t, t) = \boldsymbol{\gamma}^{(1)}(\boldsymbol{r}, t) = \nabla\boldsymbol{v} + (\nabla\boldsymbol{v})^{\dagger} \tag{9.3-10}$$

$$\boldsymbol{\gamma}^{[2]}(\boldsymbol{r}, t, t) = \boldsymbol{\gamma}^{(2)}(\boldsymbol{r}, t) = \frac{D\boldsymbol{\gamma}^{(1)}}{Dt} + \{(\nabla\boldsymbol{v})\cdot\boldsymbol{\gamma}^{(1)} + \boldsymbol{\gamma}^{(1)}\cdot(\nabla\boldsymbol{v})^{\dagger}\} \tag{9.3-11}$$

$$\vdots \qquad \vdots \qquad \vdots$$

$$\boldsymbol{\gamma}^{[n]}(\boldsymbol{r}, t, t) = \boldsymbol{\gamma}^{(n)}(\boldsymbol{r}, t) = \frac{D\boldsymbol{\gamma}^{(n-1)}}{Dt} + \{(\nabla\boldsymbol{v})\cdot\boldsymbol{\gamma}^{(n-1)} + \boldsymbol{\gamma}^{(n-1)}\cdot(\nabla\boldsymbol{v})^{\dagger}\} \tag{9.3-12}$$

In this way the higher rate-of-strain tensors are defined. The tensor $\boldsymbol{\gamma}^{(n)}$ is said to be the *covariant convected derivative* of $\boldsymbol{\gamma}^{(n-1)}$; it is also the $(n-1)$th covariant convected derivative of $\boldsymbol{\gamma}^{(1)}$.

The tensors $\boldsymbol{\gamma}_{(n)}$, first introduced in Eqs. 6.1-5 and 6, are obtained by a procedure analogous to that described above. The results may be summarized as follows

$$\boldsymbol{\gamma}_{[1]}(\boldsymbol{r}, t, t) = \boldsymbol{\gamma}_{(1)}(\boldsymbol{r}, t) = \nabla\boldsymbol{v} + (\nabla\boldsymbol{v})^{\dagger} \tag{9.3-13}$$

$$\boldsymbol{\gamma}_{[2]}(\boldsymbol{r}, t, t) = \boldsymbol{\gamma}_{(2)}(\boldsymbol{r}, t) = \frac{D\boldsymbol{\gamma}_{(1)}}{Dt} - \{(\nabla\boldsymbol{v})^{\dagger}\cdot\boldsymbol{\gamma}_{(1)} + \boldsymbol{\gamma}_{(1)}\cdot\nabla\boldsymbol{v}\} \tag{9.3-14}$$

$$\vdots \qquad \vdots \qquad \vdots$$

$$\boldsymbol{\gamma}_{[n]}(\boldsymbol{r}, t, t) = \boldsymbol{\gamma}_{(n)}(\boldsymbol{r}, t) = \frac{D\boldsymbol{\gamma}_{(n-1)}}{Dt} - \{(\nabla\boldsymbol{v})^{\dagger}\cdot\boldsymbol{\gamma}_{(n-1)} + \boldsymbol{\gamma}_{(n-1)}\cdot\nabla\boldsymbol{v}\} \tag{9.3-15}$$

The tensor $\boldsymbol{\gamma}_{(n)}$ is the *contravariant convected derivative* of $\boldsymbol{\gamma}_{(n-1)}$ and the $(n-1)$th contravariant convected derivative of $\boldsymbol{\gamma}_{(1)}$.

The interrelation of the tensors $\boldsymbol{\gamma}^{[n]}$ (with $n \geq 0$) and $\boldsymbol{\gamma}^{(n)}$ with $(n \geq 1)$ is summarized in Table 9.3-1, and also the relation of these quantities to $\hat{g}_{ij}$ and its time derivatives. In addition the same information is shown for the tensors $\boldsymbol{\gamma}_{[n]}$ and $\boldsymbol{\gamma}_{(n)}$. The table is useful for showing how the notation for the kinematic tensors is systematized:

a. The superscript [ ] and ( ) quantities arise from the behavior of the dot products of the convected base vectors $\hat{\boldsymbol{g}}_i$ whereas the subscript [ ] and ( ) quantities result from the dot products of the convected reciprocal base vectors $\hat{\boldsymbol{g}}^i$. The subscript quantities seem to

[1] The tensor $\boldsymbol{\gamma}^{(1)}$ can be regarded either as being a function of the fluid particle label $\boldsymbol{r}, t$ and the time t', or else as a function of the spatial coordinates $\boldsymbol{r}'$ and the time t'. Then by the chain rule of partial differention,

$$\frac{\partial}{\partial t'}\boldsymbol{\gamma}^{(1)}(\boldsymbol{r}, t, t') = \frac{\partial}{\partial t'}\boldsymbol{\gamma}^{(1)}(\boldsymbol{r}', t') + \left\{\left(\frac{\partial}{\partial t'}\boldsymbol{r}'\right)_{\boldsymbol{r},t}\cdot\left(\frac{\partial}{\partial \boldsymbol{r}'}\boldsymbol{\gamma}^{(1)}(\boldsymbol{r}', t')\right)\right\} \tag{9.3-9a}$$

But $(\partial\boldsymbol{r}'/\partial t')$ is just the velocity $\boldsymbol{v}'$ at $\boldsymbol{r}', t'$. When $t' = t$, the right side of Eq. 9.3-9a becomes

$$\frac{D}{Dt}\boldsymbol{\gamma}^{(1)}(\boldsymbol{r}, t) = \frac{\partial\boldsymbol{\gamma}^{(1)}}{\partial t} + \{\boldsymbol{v}\cdot\nabla\boldsymbol{\gamma}^{(1)}\} \tag{9.3-9b}$$

which is the substantial derivative of $\boldsymbol{\gamma}^{(1)}$.

TABLE 9.3-1

Kinematic Tensors and Their Relation to One Another[a–f]

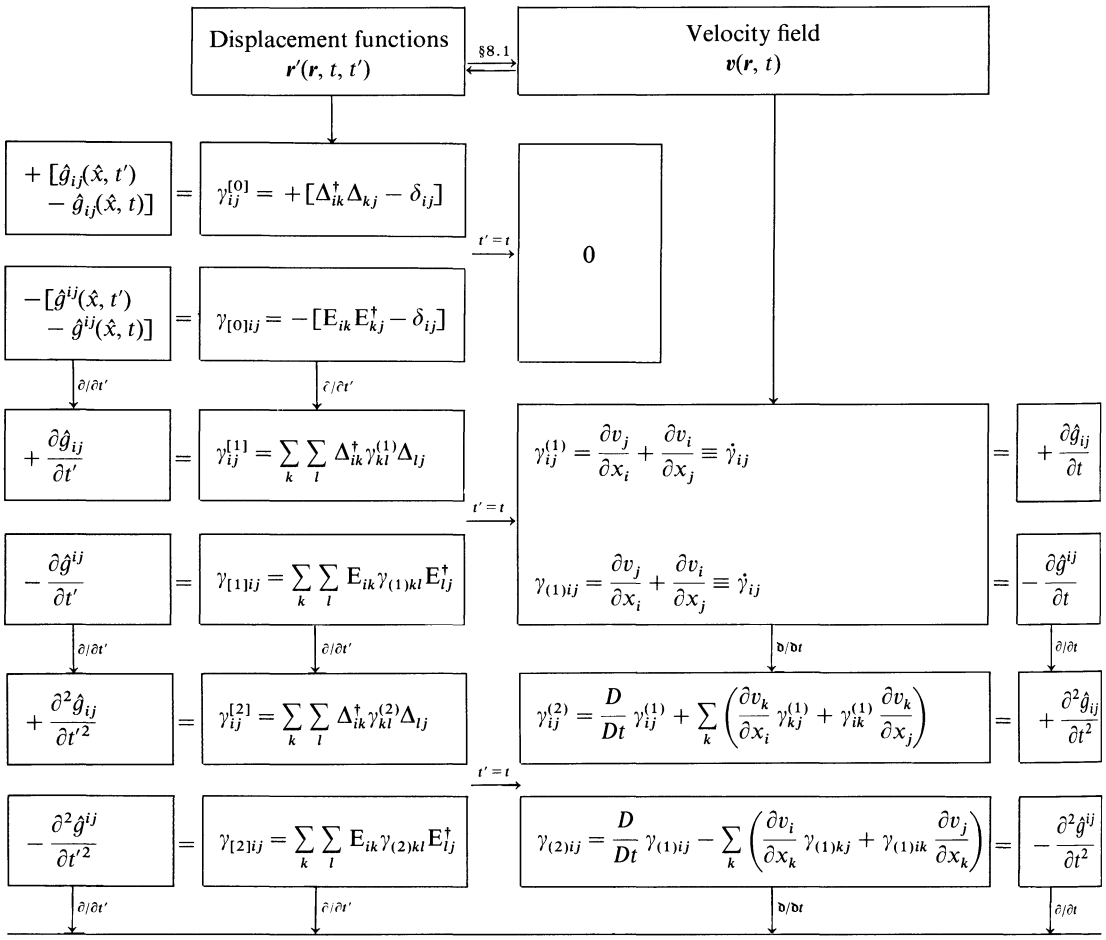

[a] This table is based on the discussion of kinematic tensors given by J. G. Oldroyd, *Proc. Roy. Soc.*, **A200**, 45–63 (1950); *J. Non-Newtonian Fluid Mech.*, **14**, 9–46 (1984).

[b] The symbol $\mathfrak{d}/\mathfrak{d}t$ in the table is Oldroyd's symbol for convected differentiation.

$$\boldsymbol{\gamma}^{(2)} = (\boldsymbol{\gamma}^{(1)})^{(1)} = (\mathfrak{d}/\mathfrak{d}t)\boldsymbol{\gamma}^{(1)} \text{ and } \boldsymbol{\gamma}_{(2)} = (\boldsymbol{\gamma}_{(1)})_{(1)} = (\mathfrak{d}/\mathfrak{d}t)\boldsymbol{\gamma}_{(1)}.$$

Since the meaning of the operator $\mathfrak{d}/\mathfrak{d}t$ depends on whether (1) appears as a superscript or a subscript, the notation $\mathfrak{d}/\mathfrak{d}t$ is not used elsewhere in this book. The $\boldsymbol{\gamma}^{(n)}$ are exactly the same as the Rivlin–Ericksen tensors, and twice Oldroyd's $\boldsymbol{e}^{(n)}$; the tensors $\boldsymbol{\gamma}^{(1)}$ and $\boldsymbol{\gamma}^{(2)}$ were obtained earlier for steady-state flows by Y. Dupont, *Bull. Sci. Acad. Belg.*, **17**, 441–459 (1931), Eq. 27.

[c] The first and fourth columns show the kinematic tensors in terms of covariant and contravariant convected components. The second and third columns show the equivalent tensors given as Cartesian components in a fixed coordinate system.

[d] The partial derivative $\partial/\partial t'$ means $(\partial/\partial t')_{\hat{x}}$ in the first column and $(\partial/\partial t')_{r,t}$ in the second; that is, both represent a differentiation with respect to time following a fluid particle. In the fourth column $\partial\hat{g}_{ij}/\partial t$ means $(\partial\hat{g}_{ij}/\partial t')_{\hat{x}}$ evaluated at $t' = t$.

[e] All tensor components in the second column ($\gamma_{ij}^{[0]}$, $\gamma_{ij}^{(1)}$, Δ_{ij}, etc.) are understood to be functions of r, t, and t'. All tensor components in the third column are understood to be functions of r and t.

[f] For nonorthogonal coordinate systems, the Δ_{ij} and E_{ij} are replaced by $\Delta_j^i = x'^i{}_{,j}$ and $E_j^i = x^i{}_{,j'}$, where "$,j$" denotes covariant differentiation with respect to x^j. In Cartesian coordinates these reduce to partial derivatives: $\Delta_{ij} = \partial x_i'/\partial x_j$ and $E_{ij} = \partial x_i/\partial x_j'$. In generalized coordinates the entries in column two may be calculated by replacing Δ_j^i with $\partial x'^i/\partial x^j$ and E_j^i with $\partial x^i/\partial x'^j$. These latter forms are the most convenient for calculations in geometries where $\boldsymbol{\Delta}$ and $\mathbf{E}$ are not already tabulated in Appendix B.

arise more naturally in the molecular theories and have been used in most of the empirical constitutive equations.

b. The [ ] quantities, which depend on t and t', appear in integral constitutive equations, in integrals over t'. The ( ) quantities appear as functions of t in differential constitutive equations.

c. The [ ] quantities are identical to the corresponding ( ) quantities when $t' = t$; there are, however, no tensors $\gamma^{(0)}$ and $\gamma_{(0)}$ since both $\gamma^{[0]}$ and $\gamma_{[0]}$ go to $\mathbf{0}$ when $t' = t$.

d. Higher order [ ] quantities are obtained by successive *partial* differentiation with respect to t' with $\boldsymbol{r}$, t being held constant. Higher order ( ) quantities are obtained by successive *convected* differentiation.

e. The ( ) quantities are easily obtained from the velocity field since the convected differentiation operators involve only $(\boldsymbol{v}\cdot\nabla)$, $\nabla\boldsymbol{v}$, and $(\nabla\boldsymbol{v})^{\dagger}$. The [ ] quantities require a knowledge of the displacement functions, which are needed to get the displacement gradient tensors $\boldsymbol{\Delta}$ and $\mathbf{E}$.

f. In the limit of very small deformations (i.e., linear viscoelasticity), the relative strain tensors, $\gamma^{[0]}$ and $\gamma_{[0]}$, both simplify to the infinitesimal strain tensor γ as pointed out earlier. In addition in this limit the tensors $\gamma^{[n]}$ and $\gamma_{[n]}$ both simplify to $\partial^n\gamma/\partial t'^n$, and similarly the tensors $\gamma^{(n)}$ and $\gamma_{(n)}$ both simplify to $\partial^n\gamma/\partial t^n$.

g. In Appendix C the most important kinematic tensors are tabulated for homogeneous shear flows and shearfree flows, that is, for those flows encountered in material-function measurements. Table C.1 is particularly useful for evaluating constitutive equations. Appendix B contains tables of the components of various kinematic tensors in cylindrical and spherical coordinates.

The systematic notation shown here should make it easy to remember the meaning of the various kinematic quantities as well as their interrelation. In Chapters 6 and 7 we use the nth rate of strain tensors $\gamma_{(n)}$, and in Chapter 8 we use the relative strain tensors $\gamma_{[0]}$ and $\gamma^{[0]}$. In research publications many of the other tensors in this table (e.g., $\gamma^{(n)}$, $\gamma^{[1]}$, $\gamma_{[1]}$) have been used; unfortunately there seems to be no standard systematic set of symbols for these kinematic tensors in the literature.

§9.4 TRANSFORMATION RULES FOR THE STRESS TENSOR AND ITS TIME DERIVATIVES

Next we turn to the stress tensor τ at time t' evaluated at the fluid particle $\boldsymbol{r}, t$. This tensor may be expanded in terms of unit vectors and Cartesian components as follows:

$$\tau(\boldsymbol{r}, t, t') = \sum_i \sum_j \boldsymbol{\delta}_i\boldsymbol{\delta}_j\tau_{ij}(\boldsymbol{r}, t, t') \tag{9.4-1}$$

It may also be expanded in terms of the base vectors and contravariant components (or alternatively, in terms of the reciprocal base vectors and the covariant components)

$$\tau(\boldsymbol{r}, t, t') = \sum_i \sum_j \hat{\boldsymbol{g}}_i\hat{\boldsymbol{g}}_j\hat{\tau}^{ij}(\boldsymbol{r}, t, t') \tag{9.4-2}$$

$$\tau(\boldsymbol{r}, t, t') = \sum_i \sum_j \hat{\boldsymbol{g}}^i\hat{\boldsymbol{g}}^j\hat{\tau}_{ij}(\boldsymbol{r}, t, t') \tag{9.4-3}$$

where the $\hat{\boldsymbol{g}}_i$ and $\hat{\boldsymbol{g}}^i$ are functions of $\boldsymbol{r}$, t and t'. But the base vectors and the reciprocal base vectors can be written in terms of the unit vectors (as in Eqs. 9.2-4 and 5), and therefore the covariant and contravariant components can be expressed in terms of the Cartesian components as follows:

$$\hat{\tau}_{ij}(\boldsymbol{r}, t, t') = \sum_m \sum_n \tau_{mn}(\boldsymbol{r}, t, t')\Delta_{mi}\Delta_{nj} \equiv \tau^{[0]}_{ij}(\boldsymbol{r}, t, t') \tag{9.4-4}$$

$$\hat{\tau}^{ij}(\boldsymbol{r}, t, t') = \sum_m \sum_n \mathrm{E}_{im}\mathrm{E}_{jn}\tau_{mn}(\boldsymbol{r}, t, t') \equiv \tau_{[0]ij}(\boldsymbol{r}, t, t') \tag{9.4-5}$$

These are the Cartesian components of the tensors $\boldsymbol{\tau}^{[0]} = \sum_i \sum_j \boldsymbol{\delta}_i\boldsymbol{\delta}_j\tau^{[0]}_{ij}$ and $\boldsymbol{\tau}_{[0]} = \sum_i \sum_j \boldsymbol{\delta}_i\boldsymbol{\delta}_j\tau_{[0]ij}$. Note that when $t' = t$, both $\boldsymbol{\tau}^{[0]}$ and $\boldsymbol{\tau}_{[0]}$ become equal to $\boldsymbol{\tau}(\boldsymbol{r}, t)$.

We can now find the derivatives with respect to t', using the procedure of §9.3, to get the quantities $\boldsymbol{\tau}^{[n]} = \partial^n\boldsymbol{\tau}^{[0]}/\partial t'^n$ and $\boldsymbol{\tau}_{[n]} = \partial^n\boldsymbol{\tau}_{[0]}/\partial t'^n$. We illustrate the method by getting $\boldsymbol{\tau}^{[1]}$ and $\boldsymbol{\tau}_{[1]}$:

$$\begin{aligned}\boldsymbol{\tau}^{[1]}(\boldsymbol{r}, t, t') &= \frac{\partial}{\partial t'}\{\boldsymbol{\Delta}^\dagger\cdot\boldsymbol{\tau}\cdot\boldsymbol{\Delta}\} \\ &= \left\{\boldsymbol{\Delta}^\dagger\cdot\left\{\frac{\partial\boldsymbol{\tau}}{\partial t'} + (\boldsymbol{\nabla v})\cdot\boldsymbol{\tau} + \boldsymbol{\tau}\cdot(\boldsymbol{\nabla v})^\dagger\right\}\cdot\boldsymbol{\Delta}\right\} \\ &\equiv \{\boldsymbol{\Delta}^\dagger\cdot\boldsymbol{\tau}^{(1)}\cdot\boldsymbol{\Delta}\}\end{aligned} \tag{9.4-6}$$

$$\begin{aligned}\boldsymbol{\tau}_{[1]}(\boldsymbol{r}, t, t') &= \frac{\partial}{\partial t'}\{\mathbf{E}\cdot\boldsymbol{\tau}\cdot\mathbf{E}^\dagger\} \\ &= \left\{\mathbf{E}\cdot\left\{\frac{\partial\boldsymbol{\tau}}{\partial t'} - (\boldsymbol{\nabla v})^\dagger\cdot\boldsymbol{\tau} - \boldsymbol{\tau}\cdot(\boldsymbol{\nabla v})\right\}\cdot\mathbf{E}^\dagger\right\} \\ &\equiv \{\mathbf{E}\cdot\boldsymbol{\tau}_{(1)}\cdot\mathbf{E}^\dagger\}\end{aligned} \tag{9.4-7}$$

In these relations it is understood that $\boldsymbol{\Delta}$, $\mathbf{E}$, $\boldsymbol{\nabla v}$, $\boldsymbol{\tau}^{(1)}$, and $\boldsymbol{\tau}_{(1)}$ are all functions of t' and the particle label $\boldsymbol{r}, t$. When t' becomes equal to t we get

$$\boldsymbol{\tau}^{[1]}(\boldsymbol{r}, t, t) = \boldsymbol{\tau}^{(1)}(\boldsymbol{r}, t) = \frac{D\boldsymbol{\tau}}{Dt} + \{(\boldsymbol{\nabla v})\cdot\boldsymbol{\tau} + \boldsymbol{\tau}\cdot(\boldsymbol{\nabla v})^\dagger\} \tag{9.4-8}$$

$$\boldsymbol{\tau}_{[1]}(\boldsymbol{r}, t, t) = \boldsymbol{\tau}_{(1)}(\boldsymbol{r}, t) = \frac{D\boldsymbol{\tau}}{Dt} - \{(\boldsymbol{\nabla v})^\dagger\cdot\boldsymbol{\tau} + \boldsymbol{\tau}\cdot(\boldsymbol{\nabla v})\} \tag{9.4-9}$$

The quantities $\boldsymbol{\tau}^{(1)}$ and $\boldsymbol{\tau}_{(1)}$ are the *covariant and contravariant convected derivatives* of the stress tensor $\boldsymbol{\tau}$. The convected derivative $\boldsymbol{\tau}_{(1)}$ has already been encountered in Eq. 7.1-1. In Table 9.4-1 we summarize the notation developed in this section and show how the various quantities are interrelated. We also give the equivalent quantities in the convected-component notation. In the table we also introduce the symbols $\boldsymbol{\tau}^{(0)}$ and $\boldsymbol{\tau}_{(0)}$ (both identical to $\boldsymbol{\tau}$) just to preserve the notational rule that [ ]-suffixed quantities become ( )-suffixed quantities when t' goes to t.

A few words are in order regarding the operation of *convected differentiation* used in both §9.3 and §9.4.

TABLE 9.4-1

The Stress Tensor and Its Time Derivatives[a–f]

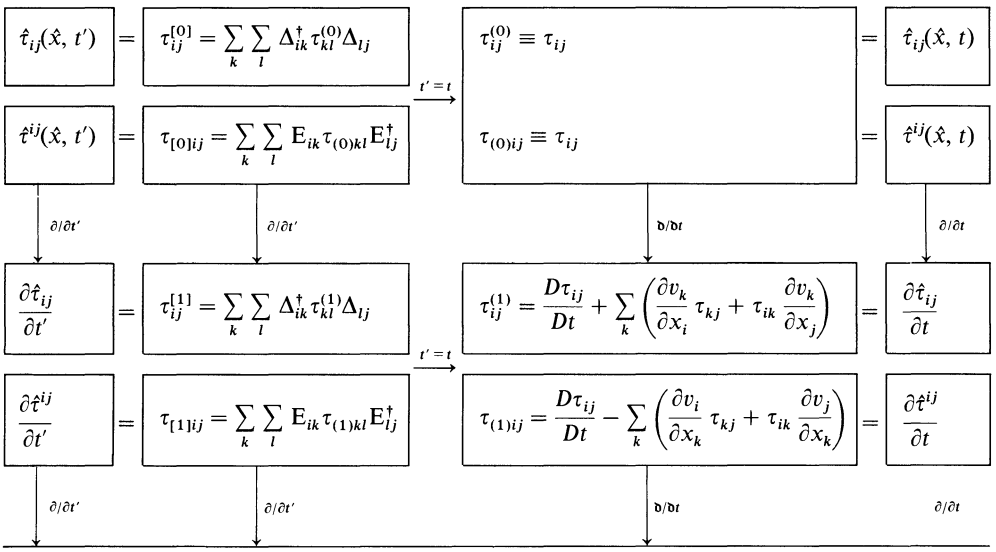

[a] This table is based on J. G. Oldroyd, *Proc. Roy. Soc.*, **A200**, 45–63 (1950); *J. Non-Newtonian Fluid Mech.*, **14**, 9–46 (1984).

[b] The symbol $\mathfrak{d}/\mathfrak{d}t$ is Oldroyd's convected derivative operator: $\boldsymbol{\tau}^{(2)} = (\boldsymbol{\tau}^{(1)})^{(1)} = (\mathfrak{d}/\mathfrak{d}t)\boldsymbol{\tau}^{(1)}$ and $\boldsymbol{\tau}_{(2)} = (\boldsymbol{\tau}_{(1)})_{(1)} = (\mathfrak{d}/\mathfrak{d}t)\boldsymbol{\tau}_{(1)}$. Since the meaning of the operator $\mathfrak{d}/\mathfrak{d}t$ depends on whether (1) appears as a superscript or a subscript, we do not use it elsewhere in this book.

[c] The first and fourth columns are written in terms of convected components. The second and third columns give the tensors in fixed Cartesian components.

[d] The derivative $\partial/\partial t'$ means $(\partial/\partial t')_{\hat{x}}$ in the first column and $(\partial/\partial t')_{r,t}$ in the second.

[e] All tensor components in the second column are understood to be functions of r, t, and t'; in the third column they are functions of r and t.

[f] See Note f of Table 9.3-1.

1. Higher convected derivatives can be obtained by successive application of the convected derivative operator

$$\boldsymbol{\Lambda}^{(n+1)} = (\boldsymbol{\Lambda}^{(n)})^{(1)} \qquad (\boldsymbol{\Lambda} = \text{any second-order tensor}) \tag{9.4-10}$$

2. The convected derivatives of the unit tensor are

$$\boldsymbol{\delta}^{(1)} = \boldsymbol{\gamma}^{(1)}; \quad \boldsymbol{\delta}_{(1)} = -\boldsymbol{\gamma}_{(1)} \tag{9.4-11}$$

It must be emphasized that $\boldsymbol{\gamma}^{(1)}$ and $\boldsymbol{\gamma}_{(1)}$ are *not* the convected derivatives of the infinitesimal strain tensor $\boldsymbol{\gamma}$; see also Eq. 9B.5-5.

3. The convected derivative of the product of a scalar function $a(\boldsymbol{r}, t)$ and a tensor $\boldsymbol{\Lambda}(\boldsymbol{r}, t)$ is

$$(a\boldsymbol{\Lambda})_{(1)} = a\boldsymbol{\Lambda}_{(1)} + (Da/Dt)\boldsymbol{\Lambda} \tag{9.4-12}$$

4. The convected derivative of the tensor product of two tensors, $\boldsymbol{\Lambda}$ and $\boldsymbol{\Theta}$, *does not* obey the simple rule for differentiating a product used in ordinary differential calculus; instead it may be shown that

$$\{\boldsymbol{\Lambda}\cdot\boldsymbol{\Theta}\}_{(1)} = \{\boldsymbol{\Lambda}_{(1)}\cdot\boldsymbol{\Theta}\} + \{\boldsymbol{\Lambda}\cdot\boldsymbol{\Theta}_{(1)}\} + \{\boldsymbol{\Lambda}\cdot\dot{\boldsymbol{\gamma}}\cdot\boldsymbol{\Theta}\} \tag{9.4-13a}$$

$$\{\boldsymbol{\Lambda}\cdot\boldsymbol{\Theta}\}^{(1)} = \{\boldsymbol{\Lambda}^{(1)}\cdot\boldsymbol{\Theta}\} + \{\boldsymbol{\Lambda}\cdot\boldsymbol{\Theta}^{(1)}\} - \{\boldsymbol{\Lambda}\cdot\dot{\boldsymbol{\gamma}}\cdot\boldsymbol{\Theta}\} \tag{9.4-13b}$$

5. The Jaumann (or corotational derivative) is simply related to the convected derivatives as follows:

$$\frac{\mathscr{D}}{\mathscr{D}t}\boldsymbol{\Lambda} = \frac{1}{2}(\boldsymbol{\Lambda}_{(1)} + \boldsymbol{\Lambda}^{(1)}) \tag{9.4-14}$$

This derivative *does* obey the usual differential-calculus rule for the differentiation of products:

$$\frac{\mathscr{D}}{\mathscr{D}t}\{\boldsymbol{\Lambda}\cdot\boldsymbol{\Theta}\} = \left\{\frac{\mathscr{D}\boldsymbol{\Lambda}}{\mathscr{D}t}\cdot\boldsymbol{\Theta}\right\} + \left\{\boldsymbol{\Lambda}\cdot\frac{\mathscr{D}\boldsymbol{\Theta}}{\mathscr{D}t}\right\} \tag{9.4-15}$$

The Jaumann derivative gives the time rate of change in a coordinate system that goes along with a fluid particle and rotates with the instantaneous fluid angular velocity. This derivative can be used for constructing constitutive equations. All of the models discussed in Chapters 6 and 7 can be written in terms of the Jaumann derivatives $\mathscr{D}^n\dot{\boldsymbol{\gamma}}/\mathscr{D}t^n$ and $\mathscr{D}\boldsymbol{\tau}/\mathscr{D}t$ just as conveniently[1] as in terms of the quantities $\boldsymbol{\gamma}_{(n)}$ and $\boldsymbol{\tau}_{(1)}$ (see Problem 9B.9).

EXAMPLE 9.4-1 The Integral Form of the Convected Jeffreys Model (Oldroyd-B Model)

It was pointed out in Chapter 8 that the convected Jeffreys model, introduced in Chapter 7, can be put into integral form. We are now in a position to show how this is done, using Tables 9.3-1 and 9.4-1. First rewrite the differential form of the model (see Eq. 7.2-1) for some past time t' and then integrate the resulting equation.

SOLUTION The convected Jeffreys model in differential form is

$$\boldsymbol{\tau}_{(0)} + \lambda_1\boldsymbol{\tau}_{(1)} = -\eta_0[\boldsymbol{\gamma}_{(1)} + \lambda_2\boldsymbol{\gamma}_{(2)}] \tag{9.4-16}$$

where all tensor quantities are evaluated at the present time t. The equation may also be written for the fluid particle $\boldsymbol{r}, t$ at some past time t' thus,

$$\boldsymbol{\tau}_{[0]} + \lambda_1\boldsymbol{\tau}_{[1]} = -\eta_0[\boldsymbol{\gamma}_{[1]} + \lambda_2\boldsymbol{\gamma}_{[2]}] \tag{9.4-17}$$

But, according to the table this is the same as

$$\boldsymbol{\tau}_{[0]} + \lambda_1\frac{\partial}{\partial t'}\boldsymbol{\tau}_{[0]} = -\eta_0\left[\frac{\partial}{\partial t'}\boldsymbol{\gamma}_{[0]} + \lambda_2\frac{\partial^2}{\partial t'^2}\boldsymbol{\gamma}_{[0]}\right] \tag{9.4-18}$$

[1] In Chapters 7 and 8 of the 1977 edition of this book we based our presentation on the corotating reference frame. See also J. G. Oldroyd, *Proc. Roy. Soc.*, **A245**, 278–297 (1958); J. D. Goddard and C. Miller, *Rheol. Acta*, **5**, 177–184 (1966); J. D. Goddard, *Trans. Soc. Rheol.*, **11**, 381–399 (1967).

This is a first-order differential equation for $\tau_{[0]}$ as a function of t'; it may be integrated to give

$$\tau_{[0]}(\boldsymbol{r}, t, t') = e^{-t'/\lambda_1}\left[\int_{-\infty}^{t'} -\frac{\eta_0}{\lambda_1}\left(\frac{\partial}{\partial t''}\gamma_{[0]} + \lambda_2 \frac{\partial^2}{\partial t''^2}\gamma_{[0]}\right)e^{t''/\lambda_1}\, dt'' + \mathbf{K}\right] \tag{9.4-19}$$

where $\gamma_{[0]}$ is now a function of $\boldsymbol{r}$, t, and t'', and $\mathbf{K}$ is an arbitrary tensor function of t. If we require that the stresses in the fluid be finite at $t' = -\infty$, then $\mathbf{K} = \mathbf{0}$. Subsequently integration by parts gives

$$\tau_{[0]}(\boldsymbol{r}, t, t') = +\int_{-\infty}^{t'} \left\{\frac{\eta_0}{\lambda_1^2}\left[\left(1 - \frac{\lambda_2}{\lambda_1}\right)e^{-(t'-t'')/\lambda_1} + 2\lambda_1\lambda_2 \frac{\partial}{\partial t''}\delta(t' - t'')\right]\right\}\gamma_{[0]}(\boldsymbol{r}, t, t'')dt'' \tag{9.4-20}$$

This gives the stress at particle $\boldsymbol{r}$, t at some past time t' in terms of the deformation history for all times $t'' \leq t'$. If now we let t' become equal to t, we get

$$\tau_{(0)}(\boldsymbol{r}, t) = +\int_{-\infty}^{t} \left\{\frac{\eta_0}{\lambda_1^2}\left[\left(1 - \frac{\lambda_2}{\lambda_1}\right)e^{-(t-t')/\lambda_1} + 2\lambda_1\lambda_2 \frac{\partial}{\partial t'}\delta(t - t')\right]\right\}\gamma_{[0]}(\boldsymbol{r}, t, t')dt' \tag{9.4-21}$$

where the dummy variable of integration has been changed from t'' to t'. Equation 9.4-21 is the same as the integral form of the convected Jeffreys model given by Eqs. 8.2-1 and 3.

§9.5 CONSTRUCTION OF ADMISSIBLE CONSTITUTIVE EQUATIONS IN TERMS OF FIXED COMPONENTS

In §9.1 Oldroyd's criteria for admissibility for constitutive equations were discussed in terms of the convected components of the stress tensor and the metric coefficients of the convected coordinate system. In the intervening sections we showed how to relate convected coordinates to fixed coordinates, and also how to transform convected components to fixed components (including time derivatives and quantities appearing in time integrals). We are now in a position to construct constitutive equations in terms of the tensors given in Tables 9.3-1 and 9.4-1, these equations being admissible in the sense defined in §9.1.

Admissible equations may be created by writing down an algebraic relation among the ( ) quantities and single or multiple time integrals of algebraic relations of the [ ] quantities which may also involve time differences, such as $t - t'$. The unit tensor $\boldsymbol{\delta}$ may also be used. In combining these ( ) and [ ] quantities dot products and multiple dot products may be formed, but the final equation must be such that each term is a second-order tensor. Material constants (or even material constant tensors, whose components are $\kappa_{N\,kl\cdots}^{ij\cdots}(\boldsymbol{r}, t)$, whose convected time derivatives are zero) may appear in the constitutive equation; the temperature history may be included if it is desired to account for nonisothermal effects. No operations may be performed that would violate the admissibility criteria laid down in §9.1; in case of doubt one can transform the proposed constitutive equation back into the convected coordinate form. Inclusion of tensor constants would lead to constitutive equations for materials such as liquid crystals. Since we are interested only in polymers that do not form liquid crystals we include only scalar material constants in constitutive equations in this book.

Constitutive equations have been generated in a number of ways:

1. One can replace the tensors occurring in linear viscoelasticity by the appropriate [ ] and ( ) quantities defined in this chapter to generate "quasi-linear constitutive

equations." There is, however, no unique way to do this. For example, the linear Jeffreys model of Eq. 5.2-9 could be transformed into a nonlinear viscoelastic equation in a number of ways; two possibilities are:

Oldroyd fluid A: $$\boldsymbol{\tau} + \lambda_1 \boldsymbol{\tau}^{(1)} = -\eta_0(\boldsymbol{\gamma}^{(1)} + \lambda_2 \boldsymbol{\gamma}^{(2)}) \tag{9.5-1}$$

Oldroyd fluid B: $$\boldsymbol{\tau} + \lambda_1 \boldsymbol{\tau}_{(1)} = -\eta_0(\boldsymbol{\gamma}_{(1)} + \lambda_2 \boldsymbol{\gamma}_{(2)}) \tag{9.5-2}$$

Only comparison with experimental data or molecular theories can enable one to choose between these two models. Neither model gives a non-Newtonian viscosity or shear-rate dependent normal stress coefficients in steady-state shear flow. Equation 9.5-1 gives $\Psi_2 = -\Psi_1$, whereas Eq. 9.5-2 gives $\Psi_2 = 0$; the latter is somewhat closer to the experimental facts, and therefore Eq. 9.5-2 is preferred.

2. One can put together empirical expressions, using the [ ] and ( ) quantities, in a wide variety of combinations, linear or nonlinear, differential or integral. The models of Oldroyd and Giesekus (Chapter 7) and those of K-BKZ and Rivlin and Sawyers (Chapter 8) are examples of this. Here one proceeds on a try-it-and-see basis until combinations are obtained that are capable of describing experimental data on material functions to the degree desired.

3. One can proceed in a mathematical fashion and make various kinds of ordered expansions. One such attempt leads to the "retarded-motion expansion" discussed in Chapter 6.

4. One can attempt to see how the ordered expansions in (3) simplify for various special categories of flows. An example of this is the CEF equation, for steady shear flows, discussed later in this chapter.

5. One can make use of molecular theories; these theories, of course, involve making some kind of model for the macromolecules in the fluid and some kind of assumptions as to how these molecules interact with one another. If the molecular modeling is sufficiently simple, a complete constitutive equation can be obtained. However, because of the crudeness of the modeling, the final constitutive equation may not be very realistic. If more faithful modeling is done at the molecular level, then it may not even be possible to work all the way through to a constitutive equation, or if it is possible, the resulting constitutive equation may be too complicated for general use in hydrodynamic calculations. In any case, the molecular theories have provided some very useful ideas as to what kinds of terms ought to be included in constitutive equations. Molecular theories are discussed extensively in Volume 2.

§9.6 MEMORY-INTEGRAL EXPANIONS[1,2]

In Chapters 4 through 8 a number of apparently unrelated constitutive equations were proposed and studied. Some assistance in interrelating these models and understanding their limits of applicability can be obtained by looking at a much more general

[1] The presentation in this section has been strongly influenced by K. Walters, *Z. Angew. Math. Phys.*, **21**, 592-600 (1970), and R. S. Rivlin and K. N. Sawyers, *Ann. Rev. Fluid Mech.*, **3**, 117-146 ((1971).

[2] The basis for this section is the fundamental development on materials with memory by A. E. Green and R. S. Rivlin, *Arch. Rat. Mech. Anal.*, **1**, 1-21 (1957), with further developments by A. E. Green, R. S. Rivlin, and A. J. M. Spencer, *Arch. Rat. Mech. Anal.*, **3**, 82-92 (1959); A. E. Green and R. S. Rivlin, *Arch. Rat. Mech. Anal.*, **4**, 387-404 (1960); B. D. Coleman and W. Noll. *Rev. Mod. Phys.*, **33**, 239-249 (1961), errata: *ibid.*, **36**, 1103 (1964); A. C. Pipkin, *Rev. Mod. Phys.*, **36**, 1034-1041 (1964).

constitutive equation, namely the "memory-integral expansion." We postulate that the stress tensor $\tau(r, t)$ is a functional of the strain history $\gamma_{[0]}(r, t, t')$, where $-\infty < t' \leq t$ (this is less general than Oldroyd's constitutive equation in Eqs. 9.1-6 to 8). Then the functional is expanded a Fréchet series (roughly speaking, a Fréchet series is to a functional as a Taylor series is to a function). This gives the stress tensor as a series of integrals of ever-increasing dimensionality:

$$\begin{aligned}\tau(r, t) = &\int_{-\infty}^{t} M_I(t-t')\gamma'_{[0]}\,dt' \\ &+ \int_{-\infty}^{t}\int_{-\infty}^{t} M_{II}(t-t', t-t'')\{\gamma'_{[0]}\cdot\gamma''_{[0]} + \gamma''_{[0]}\cdot\gamma'_{[0]}\}dt''\,dt' \\ &+ \int_{-\infty}^{t}\int_{-\infty}^{t}\int_{-\infty}^{t} [M_{III}(t-t', t-t'', t-t''')\gamma'_{[0]}(\gamma''_{[0]}:\gamma'''_{[0]}) \\ &+ M_{IV}(t-t', t-t'', t-t''')\{\gamma'_{[0]}\cdot\gamma''_{[0]}\cdot\gamma'''_{[0]} + \gamma'''_{[0]}\cdot\gamma''_{[0]}\cdot\gamma'_{[0]}\}]dt'''\,dt''\,dt' + \cdots\end{aligned} \tag{9.6-1}$$

in which $\gamma'_{[0]} \equiv \gamma_{[0]}(r, t, t')$. The expansion is given here in terms of the relative strain tensor $\gamma_{[0]}$, but it could just as well have been given in terms of the other relative strain tensor $\gamma^{[0]}$; or still other kinematic tensors could have been used.[1,3]

A discussion of the convergence of the series in Eq. 9.6-1, the usefulness of a truncated series, and other mathematical questions are outside the scope of this text, inasmuch as we do not use Eq. 9.6-1 for solving fluid dynamics problems. Our main interest in the memory-integral expansion is as a vehicle for explaining how various constitutive equations are related. We do this by means of Fig. 9.6-1 and the illustrative examples that follow.

In Fig. 9.6-1 we see that the memory-integral expansion contains four important constitutive equations, which in turn include other less general equations:

a. If only the first term is retained we get the *Lodge rubberlike liquid*, which has been studied in Chapter 8. This constitutive equation includes all of linear viscoelasticity but is not capable of describing the shear-rate dependence of the viscometric functions, and it gives $\Psi_2 = 0$.

b. If we specialize to a fluid in which the effects on τ at time t of the deformations experienced by a fluid element at different past times t' and t'' are independent of one another, then the *Rivlin–Sawyers fluid* is obtained. Several widely studied integral constitutive equations (including the Lodge rubberlike liquid) fall into this category. The Rivlin-Sawyers fluid has the capability of giving shear-rate-dependent viscometric functions and also $\Psi_2 \neq 0$.

c. If in the memory-integral expansion we expand $\gamma_{[0]}(r, t, t')$ about $t' = t$, then the *retarded-motion expansion* is obtained. Example 9.6-1 shows how the retarded-motion expansion systematically builds up a general description of the stress tensor for flows with small, slowly changing velocity gradients.

[3] A. C. Pipkin, *op cit.*, has shown that a memory-integral expansion equivalent to Eq. 9.6-1 may be obtained by replacing $\gamma_{[0]}$ everywhere by $\gamma_{[1]}$. J. D. Goddard, in *Trans. Soc. Rheol.*, **11**, 381-399 (1967), gave a memory-integral expansion in terms of a corotational rate-of-strain tensor; this expansion was further explored by R. B. Bird, O. Hassager, and S. I. Abdel-Khalik, *AIChE J.*, **20**, 1041-1066 (1975). See also Chapters 8 and 9 of the first edition of this book.

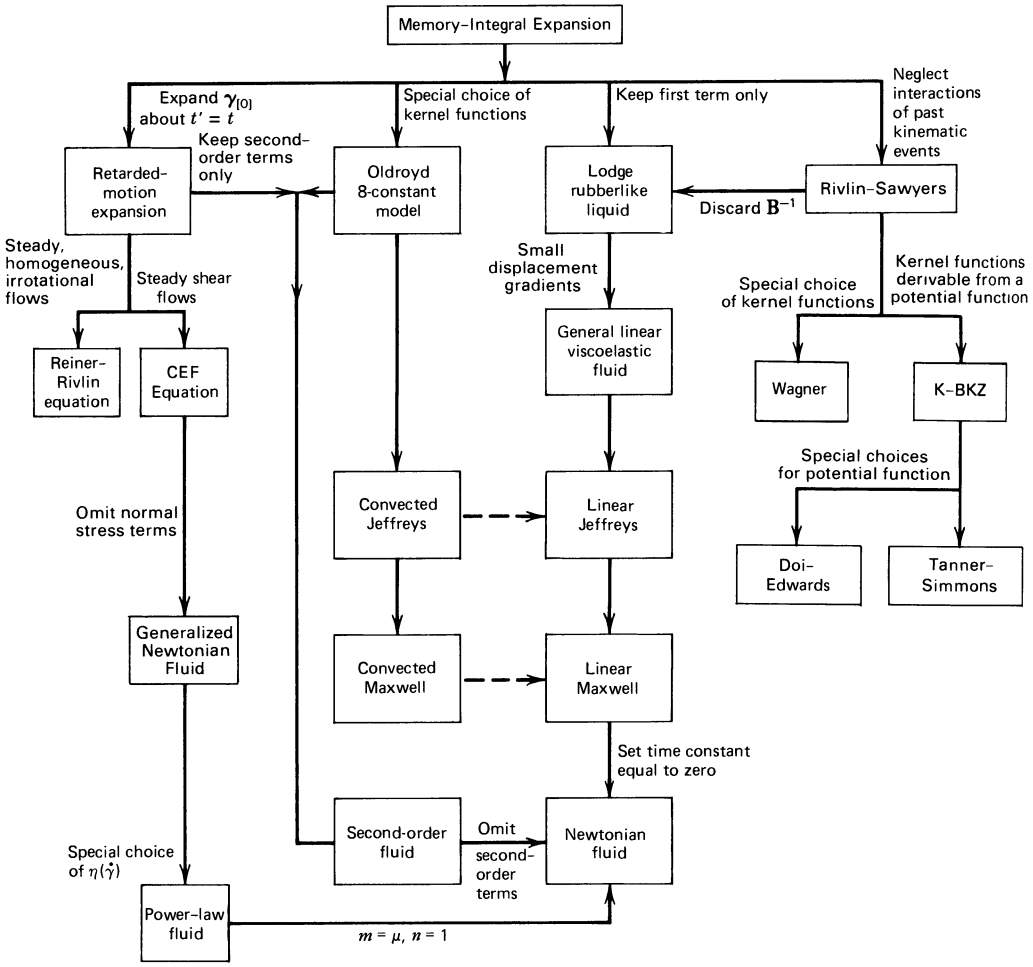

FIGURE 9.6-1. Relations among constitutive equations.

d. For certain classes of flows the memory-integral expansion can be collapsed into rather compact form. For example, for steady shear flows the expansion reduces to the *Criminale–Ericksen–Filbey* (*CEF*) *equation*; for steady, homogeneous, irrotational flows, the *Reiner–Rivlin* equation is obtained. These results are particularly convenient, since we have relatively simple constitutive equations that are exact for flows within these two categories; they are useful in analyzing the flows in rheometric devices (see Chapter 10).

e. Finally, by making very special choices for the kernels M_I, M_{II}, etc., in the memory-integral expansion, one can in principle generate constitutive equations with small numbers of constants. In Example 9.6-2 we show this by taking a differential model and showing how to put it into the form of a memory-integral expansion; in this way we find what M_I, M_{II}, etc. must be.

In addition, constitutive equations generated by molecular theories have been found to fit into the form of the memory-integral expansion or one of the special constitutive equations derived from it. This point is pursued much further in Volume 2.

EXAMPLE 9.6-1 Relation of the Memory-Integral Expansion to the Retarded-Motion Expansion[4]

Expand $\gamma_{[0]}(r, t, t')$ in the memory-integral expansion in a Taylor series about $t' = t$ as is done in Eq. 9B.2-2. Show that this leads to the retarded-motion expansion in Eq 6.2-1.

SOLUTION Let us write the memory-integral expansion as $\tau = \sum_n \tau_n$, where τ_n is the term containing an n-fold integral. When the expansion for $\gamma_{[0]}$ is substituted into τ_1 and the variable of integration is changed from t' to $s = t - t'$, we get

$$\tau_1 = \sum_{p=1}^{\infty} (p!)^{-1}(-1)^p \gamma_{(p)}(r, t) \int_0^{\infty} M_I(s) s^p \, ds \tag{9.6-2}$$

Similarly, for τ_2, with $s' = t - t''$, we have

$$\tau_2 = \sum_{p=1}^{\infty} \sum_{q=1}^{\infty} (p!q!)^{-1}(-1)^{p+q} \{\gamma_{(p)} \cdot \gamma_{(q)}\} \int_0^{\infty} \int_0^{\infty} M_{II}(s, s')(s^p s'^q + s^q s'^p) ds \, ds'$$

$$= 2\{\gamma_{(1)} \cdot \gamma_{(1)}\} \int_0^{\infty} \int_0^{\infty} M_{II}(s, s') s s' \, ds' \, ds$$

$$-\tfrac{1}{2}\{\gamma_{(1)} \cdot \gamma_{(2)} + \gamma_{(2)} \cdot \gamma_{(1)}\} \int_0^{\infty} \int_0^{\infty} M_{II}(s, s')(s s'^2 + s^2 s') ds' \, ds + \cdots \tag{9.6-3}$$

where we have displayed explicitly terms through third order in velocity gradients. Then for τ_3 we can write down a triple sum, which starts out as follows (with $s'' = t - t'''$)

$$\tau_3 = -(\gamma_{(1)} : \gamma_{(1)})\gamma_{(1)} \int_0^{\infty} \int_0^{\infty} \int_0^{\infty} M_{III}(s, s', s'') s s' s'' \, ds'' \, ds' \, ds$$

$$-2\{\gamma_{(1)} \cdot \gamma_{(1)} \cdot \gamma_{(1)}\} \int_0^{\infty} \int_0^{\infty} \int_0^{\infty} M_{IV}(s, s', s'') s s' s'' \, ds'' \, ds' \, ds + \cdots \tag{9.6-4}$$

The Cayley–Hamilton theorem (Eq. A.3-28) enables us to replace $\gamma_{(1)}^3$ in the second term of Eq. 9.6-4 by $\frac{1}{2}(\gamma_{(1)} : \gamma_{(1)})\gamma_{(1)}$; in so doing we make use of the assumption of incompressibility (tr $\gamma_{(1)} = 0$) and an isotropic term (a scalar multiplied by δ) is discarded.

We can now compare the terms generated by the above procedure with those in the retarded-motion expansion in Eq. 6.2-1. This gives expressions for the constants in the expansion:

$$b_p = (p!)^{-1}(-1)^{p+1} \int_0^{\infty} M_I(s) s^p \, ds, \qquad p = 1, 2, 3, \ldots \tag{9.6-5}$$

$$b_{11} = -2 \int_0^{\infty} \int_0^{\infty} M_{II}(s, s') s s' \, ds' \, ds \tag{9.6-6}$$

$$b_{12} = \tfrac{1}{2} \int_0^{\infty} \int_0^{\infty} M_{II}(s, s')(s s'^2 + s^2 s') ds' \, ds \tag{9.6-7}$$

$$b_{1:11} = \int_0^{\infty} \int_0^{\infty} \int_0^{\infty} [M_{III}(s, s', s'') + M_{IV}(s, s', s'')] s s' s'' ds'' \, ds' \, ds \tag{9.6-8}$$

$$\vdots$$

[4] This example is taken from K. Walters, *op cit.*

Higher-order coefficients may be obtained by continuing the process. Since $M_I(s)$ is positive for all s, it is clear that the b_p alternate in sign (see Tables 6.2-1 and 6.2-2).

EXAMPLE 9.6-2 Development of the Oldroyd 6-Constant Model in a Memory-Integral Expansion[4]

Follow the procedure of Example 9.4-1 to put the Oldroyd 6-constant model (see Eq. 7.3-2 with $\lambda_6 = \lambda_7 = 0$) into integral form.

SOLUTION First we rewrite the Oldroyd model at a past time t' thus,

$$\underline{\boldsymbol{\tau}'_{[0]} + \lambda_1 \frac{\partial}{\partial t'} \boldsymbol{\tau}'_{[0]}} + \tfrac{1}{2}\lambda_3\{\boldsymbol{\tau}'_{[0]} \cdot \boldsymbol{\gamma}'_{[1]} + \boldsymbol{\gamma}'_{[1]} \cdot \boldsymbol{\tau}'_{[0]}\} + \tfrac{1}{2}\lambda_5(\text{tr } \boldsymbol{\tau}'_{[0]})\boldsymbol{\gamma}'_{[1]}$$

$$= \underline{-\eta_0(\boldsymbol{\gamma}'_{[1]} + \lambda_2 \frac{\partial}{\partial t'} \boldsymbol{\gamma}'_{[1]}}) + \lambda_4\{\boldsymbol{\gamma}'_{[1]} \cdot \boldsymbol{\gamma}'_{[1]}\}) \tag{9.6-9}$$

The single accent is a reminder that these quantities are functions of the particle label $\boldsymbol{r}$, t and the past time t'. The dashed-underlined terms are those linear in stresses and velocity gradients. We start by considering the differential equation formed by these terms only; this is a first-order differential equation in t' and can be integrated by the method of Example 9.4-1 to give

$$\boldsymbol{\tau}'_{[0]} = -\frac{\eta_0\lambda_2}{\lambda_1}\boldsymbol{\gamma}'_{[1]} - \frac{\eta_0(\lambda_1 - \lambda_2)}{\lambda_1^2}\int_{-\infty}^{t'} e^{-(t'-t'')/\lambda_1}\boldsymbol{\gamma}''_{[1]}dt'' \tag{9.6-10}$$

where $\boldsymbol{\gamma}''_{[1]}$ is a function of $\boldsymbol{r}$, t, and t''.

Next this solution is inserted for $\boldsymbol{\tau}'_{[0]}$ in the nonunderlined (i.e., nonlinear) terms in Eq. 9.6-9. This gives a more complicated first-order differential equation for $\boldsymbol{\tau}'_{[0]}$, which nonetheless can be integrated to give:

$$\begin{aligned}\boldsymbol{\tau}'_{[0]} = {} & \text{(two terms identical to right side of Eq. 9.6-10)} \\ & - \frac{\eta_0(\lambda_2\lambda_3 - \lambda_1\lambda_4)}{\lambda_1^2}\int_{-\infty}^{t'} e^{-(t'-t'')/\lambda_1}\{\boldsymbol{\gamma}''_{[1]} \cdot \boldsymbol{\gamma}''_{[1]}\}dt'' \\ & - \frac{\eta_0(\lambda_1 - \lambda_2)\lambda_3}{2\lambda_1^3}\int_{-\infty}^{t'}\int_{-\infty}^{t''} e^{-(t'-t''')/\lambda_1}\{\boldsymbol{\gamma}'''_{[1]} \cdot \boldsymbol{\gamma}''_{[1]} + \boldsymbol{\gamma}''_{[1]} \cdot \boldsymbol{\gamma}'''_{[1]}\}dt''' \, dt''\end{aligned} \tag{9.6-11}$$

Note that the term containing λ_5 does not appear at second order inasmuch as tr $\boldsymbol{\tau}'_{[0]} = 0$ according to Eq. 9.6-10. This procedure can be continued to third and higher order with triple and higher multiple integrals being generated.

If we stop at second order, Eq. 9.6-11 can be reorganized into the form of a memory-integral expansion; this is done by writing Eq. 9.6-11 for $t' = t$ and then forcing all terms linear in $\boldsymbol{\gamma}'_{[1]}$ to appear in a single-integral term, and all quadratic terms in a double-integral term (by introducing the appropriate δ-functions):

$$\begin{aligned}\boldsymbol{\tau}(t) = {} & -\int_{-\infty}^{t} G_I(t - t')\boldsymbol{\gamma}'_{[1]}dt' \\ & - \int_{-\infty}^{t}\int_{-\infty}^{t} G_{II}(t - t', t - t'')\{\boldsymbol{\gamma}'_{[1]} \cdot \boldsymbol{\gamma}''_{[1]} + \boldsymbol{\gamma}''_{[1]} \cdot \boldsymbol{\gamma}'_{[1]}\}dt'' \, dt'\end{aligned} \tag{9.6-12}$$

in which

$$G_I = \frac{\eta_0(\lambda_1 - \lambda_2)}{\lambda_1^2} e^{-(t-t')/\lambda_1} + \frac{2\eta_0\lambda_2}{\lambda_1}\delta(t-t') \tag{9.6-13}$$

$$G_{II} = \begin{cases} 0 & \text{if } t' < t'' \leq t \\ \dfrac{\eta_0(\lambda_1 - \lambda_2)\lambda_3}{2\lambda_1^3} e^{-(t-t'')/\lambda_1} + \dfrac{\eta_0(\lambda_2\lambda_3 - \lambda_1\lambda_4)}{2\lambda_1^2} e^{-(t-t')/\lambda_1}\delta(t'-t'') & \text{if } -\infty < t'' < t' \end{cases} \tag{9.6-14}$$

We are thus led to a memory-integral expansion in $\gamma_{[1]}$, of which we have worked out the first two terms. The function $G_I(t-t')$ is identical to the relaxation modulus $G(t-t')$ of linear viscoelasticity (see Eq. 5.2-18). The final results may be put in the form of Eq. 9.6-1 (an expansion in $\gamma_{[0]}$) as may be seen in problem 9B.6.

EXAMPLE 9.6-3 The Criminale-Ericksen-Filbey (CEF) Equation and the Reiner-Rivlin Equation

Show how the memory-integral expansion simplifies for **(a)** steady shear flows, and **(b)** steady, homogeneous, irrotational flows.

SOLUTION **(a)** In Example 9.6-1 it is shown how the memory-integral expansion is related to the retarded-motion expansion. If the latter is applied to the steady shear flow $v_x = \dot{\gamma}y$, $v_y = 0$, $v_z = 0$, then from Appendix C

$$\boldsymbol{\gamma}_{(1)} = \begin{pmatrix} 0 & 1 & 0 \\ 1 & 0 & 0 \\ 0 & 0 & 0 \end{pmatrix}\dot{\gamma}, \quad \boldsymbol{\gamma}_{(2)} = -2\begin{pmatrix} 1 & 0 & 0 \\ 0 & 0 & 0 \\ 0 & 0 & 0 \end{pmatrix}\dot{\gamma}^2 \tag{9.6-15}$$

and $\boldsymbol{\gamma}_{(n)} = 0$ for $n \geq 3$. Furthermore terms of third order involve the following products:[5]

$$\begin{aligned} \{\boldsymbol{\gamma}_{(1)}\cdot\boldsymbol{\gamma}_{(2)} + \boldsymbol{\gamma}_{(2)}\cdot\boldsymbol{\gamma}_{(1)}\} &= -2\dot{\gamma}^2\boldsymbol{\gamma}_{(1)} \\ \{\boldsymbol{\gamma}_{(1)}\cdot\boldsymbol{\gamma}_{(1)}\cdot\boldsymbol{\gamma}_{(1)}\} &= \dot{\gamma}^2\boldsymbol{\gamma}_{(1)} \end{aligned} \tag{9.6-16}$$

When these are substituted into the retarded-motion expansion (Eq 6.2-1), we get

$$\begin{aligned} \boldsymbol{\tau} = &-(b_1 - 2b_{12}\dot{\gamma}^2 + 2b_{1;11}\dot{\gamma}^2 + \cdots)\boldsymbol{\gamma}_{(1)} \\ &-(b_2 + \cdots)\boldsymbol{\gamma}_{(2)} \\ &-(b_{11} + \cdots)\{\boldsymbol{\gamma}_{(1)}\cdot\boldsymbol{\gamma}_{(1)}\} \end{aligned} \tag{9.6-17}$$

Here the dots indicate additional terms that arise when one includes terms of fourth, fifth, and higher orders. Thus $\boldsymbol{\tau}$ depends only on the three kinematic tensors $\boldsymbol{\gamma}_{(1)}$, $\boldsymbol{\gamma}_{(2)}$, and $\{\boldsymbol{\gamma}_{(1)}\cdot\boldsymbol{\gamma}_{(1)}\}$, and the coefficients of these tensors are functions of the shear rate $\dot{\gamma}$ alone. We now assign symbols to the scalar coefficients thus,

$$\boxed{\boldsymbol{\tau} = -\eta\boldsymbol{\gamma}_{(1)} + \tfrac{1}{2}\Psi_1\boldsymbol{\gamma}_{(2)} - \Psi_2\{\boldsymbol{\gamma}_{(1)}\cdot\boldsymbol{\gamma}_{(1)}\}} \tag{9.6-18}$$

where $\eta(\dot{\gamma})$, $\Psi_1(\dot{\gamma})$, and $\Psi_2(\dot{\gamma})$ are the three (experimentally measurable) "viscometric functions" defined in §3.3. Equation 9.6-18 is the *Criminale-Ericksen-Filbey ("CEF") equation.*[6]

[5] At fourth and higher order the following two relations are needed:

$$\{\boldsymbol{\gamma}_{(2)}\cdot\boldsymbol{\gamma}_{(2)}\} = -2\dot{\gamma}^2\boldsymbol{\gamma}_{(2)}; \quad \{\boldsymbol{\gamma}_{(1)}^2\cdot\boldsymbol{\gamma}_{(2)} + \boldsymbol{\gamma}_{(2)}\cdot\boldsymbol{\gamma}_{(1)}^2\} = 2\dot{\gamma}^2\boldsymbol{\gamma}_{(2)} \tag{9.6-16a}$$

[6] W. O. Criminale, Jr., J. L. Ericksen, and G. L. Filbey, Jr., *Arch. Rat. Mech. Anal.*, **1**, 410-417 (1958); see also J. L. Ericksen in, J. T. Bergen ed., *Viscoelasticity: Phenomenological Aspects*, Academic Press, New York (1960). The unsteady-state analog of the CEF equation has been derived, but it contains scalar functionals (A. S. Lodge, *Body Tensor Fields in Continuum Mechanics*, Academic Press, New York (1974), Eq. 7.1-11).

Note that the first term in the CEF equation is the generalized Newtonian fluid of Chapter 4; the second and third terms account for the normal-stress effects. The CEF equation is very helpful in the fluid mechanical analysis of standard rheometers.[7]

(b) For flows that are time independent and also homogeneous $D\boldsymbol{\gamma}_{(n)}/Dt$ is exactly zero. For flows that are irrotational $\nabla \boldsymbol{v}$ is the same as $(\nabla \boldsymbol{v})^\dagger$. Therefore, for flows that are steady, homogeneous, and irrotational, it can be shown that

$$\boldsymbol{\gamma}_{(n+1)} = -\tfrac{1}{2}\{\boldsymbol{\gamma}_{(1)} \cdot \boldsymbol{\gamma}_{(n)} + \boldsymbol{\gamma}_{(n)} \cdot \boldsymbol{\gamma}_{(1)}\} \tag{9.6-19}$$

From this recursion relation we can start with $n = 1$ and derive expressions for all the $\boldsymbol{\gamma}_{(n)}$; doing this we find

$$\boldsymbol{\gamma}_{(n)} = (-1)^{n+1}\boldsymbol{\gamma}_{(1)}^n \tag{9.6-20}$$

When this is substituted into the retarded-motion expansion, we find that $\boldsymbol{\tau}$ is a sum of terms containing multiple products of $\boldsymbol{\gamma}_{(1)}$. By repeated application of the Cayley–Hamilton theorem (Eq. A.3-28) these products ultimately yield terms containing $\boldsymbol{\delta}$, $\boldsymbol{\gamma}_{(1)}$, and $\boldsymbol{\gamma}_{(1)}^2$, with scalar coefficients depending only on the invariants of $\boldsymbol{\gamma}_{(1)} \equiv \dot{\boldsymbol{\gamma}}$ (which we call I, II, III). For incompressible fluids we omit the isotropic contributions containing $\boldsymbol{\delta}$ and use the fact that $I = 0$. Then the retarded-motion expansion collapses to

$$\boxed{\boldsymbol{\tau} = -f_1(II, III)\dot{\boldsymbol{\gamma}} - f_2(II, III)\{\dot{\boldsymbol{\gamma}} \cdot \dot{\boldsymbol{\gamma}}\}} \tag{9.6-21}$$

This is the *Reiner–Rivlin* equation[8–10]. When originally proposed this equation was believed to be more generally applicable than it is. Hence there are unfortunately many publications in which the Reiner–Rivlin equation has been applied inappropriately to flows that are not steady, homogeneous, and irrotational.

PROBLEMS

9B.1 Relations Among Kinematic Tensors

a. The tensors $\boldsymbol{\gamma}^{(1)}$ and $\boldsymbol{\gamma}_{(1)}$ are both defined to be identical to $\dot{\boldsymbol{\gamma}} = \nabla \boldsymbol{v} + (\nabla \boldsymbol{v})^\dagger$. Show from the definitions that the higher-order rate-of-strain tensors are related thus

$$\boldsymbol{\gamma}^{(2)} = \boldsymbol{\gamma}_{(2)} + 2\{\boldsymbol{\gamma}_{(1)} \cdot \boldsymbol{\gamma}_{(1)}\} \tag{9B.1-1}$$

$$\boldsymbol{\gamma}_{(2)} = \boldsymbol{\gamma}^{(2)} - 2\{\boldsymbol{\gamma}^{(1)} \cdot \boldsymbol{\gamma}^{(1)}\} \tag{9B.1-2}$$

$$\boldsymbol{\gamma}^{(3)} = \boldsymbol{\gamma}_{(3)} + 3\{\boldsymbol{\gamma}_{(1)} \cdot \boldsymbol{\gamma}_{(2)} + \boldsymbol{\gamma}_{(2)} \cdot \boldsymbol{\gamma}_{(1)}\} + 6\{\boldsymbol{\gamma}_{(1)} \cdot \boldsymbol{\gamma}_{(1)} \cdot \boldsymbol{\gamma}_{(1)}\} \tag{9B.1-3}$$

$$\boldsymbol{\gamma}_{(3)} = \boldsymbol{\gamma}^{(3)} - 3\{\boldsymbol{\gamma}^{(1)} \cdot \boldsymbol{\gamma}^{(2)} + \boldsymbol{\gamma}^{(2)} \cdot \boldsymbol{\gamma}^{(1)}\} + 6\{\boldsymbol{\gamma}^{(1)} \cdot \boldsymbol{\gamma}^{(1)} \cdot \boldsymbol{\gamma}^{(1)}\} \tag{9B.1-4}$$

[7] All of the viscometric flow problems solved in B. D. Coleman, H. Markovitz, and W. Noll, *Viscometric Flows of Non-Newtonian Fluids*, Springer, New York (1966), can be solved using Eq. 9.6-18.

[8] M. Reiner, *Am. J. Math.*, **67**, 350–362 (1945).

[9] R. S. Rivlin, *Proc. Roy. Soc.* (*London*), **A193**, 260–281 (1948); *Proc. Camb. Phil. Soc.*, **45**, 88–91 (1949).

[10] K. Weissenberg, *Arch. Sci. Phys. Nat.* (5), **140**, 44–106, 130–171 (1935), made an earlier attempt to construct a constitutive equation starting with the premise that $\boldsymbol{\tau}$ must be some general function of $\dot{\boldsymbol{\gamma}}$. The unsteady state analog of the Reiner–Rivlin equation has been derived [A. S. Lodge, *Body Tensor Fields in Continuum Mechanics*, Academic Press, New York (1974), Eq. 7.4-5], but it contains scalar functionals.

b. Show that Eqs. 9B.1-2 and 4 can also be obtained from the Walters-Waterhouse relation:[1]

$$\gamma_{(n)} = (-1)^{n+1} n! \begin{vmatrix} \boldsymbol{\gamma}^{(1)} & \boldsymbol{\delta} & \mathbf{0} & \mathbf{0} & \cdots \\ \frac{1}{2!}\boldsymbol{\gamma}^{(2)} & \boldsymbol{\gamma}^{(1)} & \boldsymbol{\delta} & \mathbf{0} & \cdots \\ \frac{1}{3!}\boldsymbol{\gamma}^{(3)} & \frac{1}{2!}\boldsymbol{\gamma}^{(2)} & \boldsymbol{\gamma}^{(1)} & \boldsymbol{\delta} & \cdots \\ \frac{1}{4!}\boldsymbol{\gamma}^{(4)} & \frac{1}{3!}\boldsymbol{\gamma}^{(3)} & \frac{1}{2!}\boldsymbol{\gamma}^{(2)} & \boldsymbol{\gamma}^{(1)} & \cdots \\ \vdots & \vdots & \vdots & \vdots & \end{vmatrix} \tag{9B.1-5}$$

Then show that Eqs. 9B.1-1 and 3 can be obtained from the inverse relation: change all $\boldsymbol{\gamma}^{(n)}$ to $\gamma_{(n)}$ and vice versa, omit the factor $(-1)^{n+1}$, and replace the unit tensor $\boldsymbol{\delta}$ by $-\boldsymbol{\delta}$. In multiplying out the determinant left-to-right multiplication must be preserved.

9B.2 Expansion of the Relative Strain Tensors in Taylor Series

Verify that the relative strain tensors, considered as functions of t', can be expanded in Taylor series about $t' = t$ to give

$$\boldsymbol{\gamma}^{[0]}(\boldsymbol{r}, t, t') = \sum_{k=1}^{\infty} (k!)^{-1} \boldsymbol{\gamma}^{(k)}(\boldsymbol{r}, t)(t' - t)^k \tag{9B.2-1}$$

$$\gamma_{[0]}(\boldsymbol{r}, t, t') = \sum_{k=1}^{\infty} (k!)^{-1} \gamma_{(k)}(\boldsymbol{r}, t)(t' - t)^k \tag{9B.2-2}$$

Table 9.3-1 contains all the information needed to obtain these expansions.

9B.3 Base Vectors and Kinematic Tensors for Steady Shear Flow

For the flow depicted in Fig. 9.2-2 work out the following:

a. From the velocity field find the displacement functions.

b. Display the components of the displacement gradient tensors $\boldsymbol{\Delta}$ and $\mathbf{E}$ in matrix form.

c. Verify that the expressions for $\hat{\boldsymbol{g}}_i$ and $\hat{\boldsymbol{g}}^i$ shown in Fig. 9.2-2 are correct.

d. Next work out the matrix displays for the relative strain tensors $\boldsymbol{\gamma}^{[0]}$ and $\gamma_{[0]}$, and check them against the entries in Table C.1.

e. From **(d)** get $\boldsymbol{\gamma}^{[n]}$ and $\gamma_{[n]}$ for $n = 1, 2$ by differentiating with respect to t'; then set t' equal to t to get the corresponding $\boldsymbol{\gamma}^{(n)}$ and $\gamma_{(n)}$ quantities.

9B.4 Base Vectors and Kinematic Tensors for Flow of a Non-Newtonian Fluid in a Thin Slit

Repeat Problem 9B.3 for the flow shown in Fig. 9.2-3. Verify that the base vectors have been drawn properly for fluid particles P, Q, R, and S.

[1] K. Walters and W. M. Waterhouse, *J. Non-Newtonian Fluid Mech.*, **3**, 293-296 (1977/78).

9B.5 Operations with Kinematic Tensors

Verify the following relations:

a. $\text{tr}\,\gamma_{[1]}(r, t, t') = 0$ for incompressible fluids (9B.5-1)

b. $\{\gamma_{(1)}\cdot\gamma_{(1)}\}_{(1)} = \{\gamma_{(2)}\cdot\gamma_{(1)} + \gamma_{(1)}\cdot\gamma_{(2)} + \gamma_{(1)}\cdot\gamma_{(1)}\cdot\gamma_{(1)}\}$ (9B.5-2)

c. $(s\delta)_{(1)} = \delta\, Ds/Dt - s\gamma_{(1)}$ where s is a scalar (9B.5-3)

d. $(\delta - \gamma_{[0]})_{(1)} = 0$ (9B.5-4)

e. $(\gamma^{[0]})^{(1)} = -\gamma^{(1)}$ (9B.5-5)

9B.6 Interrelation of Two Memory-Integral Expansions

Verify that Eq. 9.6-12 can be transformed into the form of Eq. 9.6-1 and that $M_I(t-t') = \partial G_I(t-t')/\partial t'$ and $M_{II}(t-t', t-t'') = -\partial^2 G_{II}(t-t', t-t'')/\partial t'\partial t''$.

9B.7 A Convected Maxwell Model

a. What are the good and bad features of the following constitutive equation?

$$\tau + \lambda_1[(1-\varepsilon)\tau_{(1)} + \varepsilon\tau^{(1)}] = -\eta_0\dot{\gamma} \tag{9B.7-1}$$

Here η_0, λ_1, and ε are the model parameters. What can be said about the model when $\varepsilon = 0, \frac{1}{2}$, and 1?

b. Is the model in Eq. 9B.7-1 the same as the following integral model?

$$\tau = +\int_{-\infty}^{t}\left\{\frac{\eta_0}{\lambda_1^2}e^{-(t-t')/\lambda_1}\right\}((1-\varepsilon)\gamma'_{[0]} + \varepsilon\gamma^{[0]\prime})dt' \tag{9B.7-2}$$

Here $\gamma'_{[0]} \equiv \gamma_{[0]}(r, t, t')$.

9B.8 The Retarded Motion Expansion for the Factorized Rivlin–Sawyers Fluid

a. Substitute Eq. 8.3-16 for $\phi_1(I_1, I_2)$ and $\phi_2(I_1, I_2)$ into the constitutive equation in Eq. 8.3-12. Then use the expansions in Problem 9B.2 to eliminate the strain tensors in favor of the series involving the nth-order rate-of-strain tensors.

b. Show that for incompressible fluids $\text{tr}\,\gamma^{(2)} = -\text{tr}\,\gamma_{(2)} = \text{tr}\,\{\gamma^{(1)}\cdot\gamma^{(1)}\}$. Next expand the invariants of the Finger tensor as follows:

$$I_1 - 3 = \tfrac{1}{2}(\text{tr}\{\gamma_{(1)}\cdot\gamma_{(1)}\})s^2 + \tfrac{1}{6}(\text{tr}\,\gamma_{(3)})s^3 - \cdots \tag{9B.8-1}$$

$$I_2 - 3 = \tfrac{1}{2}(\text{tr}\{\gamma^{(1)}\cdot\gamma^{(1)}\})s^2 - \text{tr}(\tfrac{1}{6}\gamma^{(3)} + \cdots)s^3 + \cdots \tag{9B.8-2}$$

in which $s = t - t'$. It is thus seen that I_1 and I_2 are identical through terms of second order in s.

c. Then use the condition in Eq. 8.3-14 and the definition of the M_n in Eq. 8.2-12 to get the retarded-motion coefficients in Table 6.2-2.

9B.9 The Jaumann ("Corotational") Derivative[2]

The *Jaumann derivative* of the tensor $\boldsymbol{\tau}$ is defined as

$$\frac{\mathscr{D}}{\mathscr{D}t}\boldsymbol{\tau} = \frac{\partial}{\partial t}\boldsymbol{\tau} + \{\boldsymbol{v}\cdot\nabla\boldsymbol{\tau}\} + \tfrac{1}{2}\{\boldsymbol{\omega}\cdot\boldsymbol{\tau} - \boldsymbol{\tau}\cdot\boldsymbol{\omega}\} \tag{9B.9-1}$$

in which $\boldsymbol{\omega}$ is the vorticity tensor.[2] This derivative has often been used in the rheology and continuum-mechanics literature. Show that

$$\begin{aligned}\frac{\mathscr{D}}{\mathscr{D}t}\dot{\boldsymbol{\gamma}} &= \boldsymbol{\gamma}^{(2)} - \{\boldsymbol{\gamma}^{(1)}\cdot\boldsymbol{\gamma}^{(1)}\} \\ &= \boldsymbol{\gamma}_{(2)} + \{\boldsymbol{\gamma}_{(1)}\cdot\boldsymbol{\gamma}_{(1)}\}\end{aligned} \tag{9B.9-2}$$

$$\begin{aligned}\frac{\mathscr{D}^2\dot{\boldsymbol{\gamma}}}{\mathscr{D}t^2} &= \boldsymbol{\gamma}^{(3)} - \tfrac{3}{2}\{\boldsymbol{\gamma}^{(1)}\cdot\boldsymbol{\gamma}^{(2)} + \boldsymbol{\gamma}^{(2)}\cdot\boldsymbol{\gamma}^{(1)}\} + 2\{\boldsymbol{\gamma}^{(1)}\cdot\boldsymbol{\gamma}^{(1)}\cdot\boldsymbol{\gamma}^{(1)}\} \\ &= \boldsymbol{\gamma}_{(3)} + \tfrac{3}{2}\{\boldsymbol{\gamma}_{(1)}\cdot\boldsymbol{\gamma}_{(2)} + \boldsymbol{\gamma}_{(2)}\cdot\boldsymbol{\gamma}_{(1)}\} + 2\{\boldsymbol{\gamma}_{(1)}\cdot\boldsymbol{\gamma}_{(1)}\cdot\boldsymbol{\gamma}_{(1)}\}\end{aligned} \tag{9B.9-3}$$

9C.1 Time Derivatives of the Displacement Gradient Tensors

a. Start with the definition of E_{ij} in Eq. 9.2-5 and show that

$$\left(\frac{\partial}{\partial t}\mathbf{E}\right)_{\boldsymbol{r}',t'} = \{(\nabla\boldsymbol{v})^{\dagger}\cdot\mathbf{E}\} \tag{9C.1-1}$$

where $\nabla\boldsymbol{v}$ is evaluated at $\boldsymbol{r}$ and t.

b. Knowing that $\{\mathbf{E}\cdot\boldsymbol{\Delta}\} = \boldsymbol{\delta}$, show from Eq. 9C.1-1 that

$$\left(\frac{\partial}{\partial t}\boldsymbol{\Delta}\right)_{\boldsymbol{r}',t'} = -\{\boldsymbol{\Delta}\cdot(\nabla\boldsymbol{v})^{\dagger}\} \tag{9C.1-2}$$

where $\nabla\boldsymbol{v}$ is evaluated at $\boldsymbol{r}$ and t.

9D.1 Relations Among the Tensors $\boldsymbol{\gamma}^{[1]}$, $\boldsymbol{\gamma}_{[1]}$, and $\dot{\boldsymbol{\gamma}}$

a. Consider a fluid particle located at position $\boldsymbol{r}$ at the present time t, and at $\boldsymbol{r}'$ at some past time t'. Show that for homogeneous flows the function $\boldsymbol{r}' = \boldsymbol{r}'(\boldsymbol{r}, t, t')$ is obtained by solving the equation

$$\frac{\partial}{\partial t'}\boldsymbol{r}' = [\boldsymbol{\kappa}'\cdot\boldsymbol{r}'] \tag{9D.1-1}$$

along with the condition that $\boldsymbol{r}'(t) = \boldsymbol{r}$. Here $\boldsymbol{\kappa}' = \boldsymbol{\kappa}(\boldsymbol{r}, t, t')$ is $(\nabla\boldsymbol{v})^{\dagger}$ evaluated at t'.

[2] For an extensive discussion of the corotational formulation of continuum mechanics, the Jaumann derivative, and corotational integration, see J. D. Goddard and C. Miller, *Rheol. Acta*, **5**, 177–184 (1966), and J. D. Goddard, *Trans. Soc. Rheol.*, **11**, 381–399 (1967). See also R. B. Bird, O. Hassager, and S. I. Abdel-Khalik, *AIChE J.*, **20**, 1041–1066 (1975), and J. G. Oldroyd, *Proc. Roy. Soc.*, **A245**, 278–297 (1958).

b. Show that the solution to Eq. 9D.1-1 for $\boldsymbol{\kappa} = \boldsymbol{\kappa}(t)$ is

$$\boldsymbol{r}'(t') = [\boldsymbol{\Omega}_t^{t'}(\boldsymbol{\kappa}) \cdot \boldsymbol{r}(t)] \tag{9D.1-2}$$

where the matrizant[3] $\boldsymbol{\Omega}_t^{t'}(\boldsymbol{\kappa})$ is given by

$$\boldsymbol{\Omega}_t^{t'}(\boldsymbol{\kappa}) = \boldsymbol{\delta} + \int_t^{t'} \boldsymbol{\kappa}''\, dt'' + \int_t^{t'} \int_t^{t''} \{\boldsymbol{\kappa}'' \cdot \boldsymbol{\kappa}'''\} dt'''\, dt'' + \int_t^{t'} \int_t^{t''} \int_t^{t'''} \{\boldsymbol{\kappa}'' \cdot \boldsymbol{\kappa}''' \cdot \boldsymbol{\kappa}''''\} dt''''\, dt'''\, dt'' + \cdots \tag{9D.1-3}$$

in which $\boldsymbol{\kappa}'' \equiv \boldsymbol{\kappa}(\boldsymbol{r}, t, t'')$.

c. Verify that

$$\boldsymbol{\Delta} = \boldsymbol{\delta} - \int_{t'}^{t} \boldsymbol{\kappa}''\, dt'' + \int_{t'}^{t} \int_{t''}^{t} \{\boldsymbol{\kappa}'' \cdot \boldsymbol{\kappa}'''\} dt'''\, dt'' + \cdots \tag{9D.1-4}$$

$$\mathbf{E} = \boldsymbol{\delta} + \int_{t'}^{t} \boldsymbol{\kappa}''\, dt'' + \int_{t'}^{t} \int_{t''}^{t} \{\boldsymbol{\kappa}'' \cdot \boldsymbol{\kappa}'''\} dt'''\, dt'' + \cdots \tag{9D.1-5}$$

d. Then show that:[4]

$$\dot{\boldsymbol{\gamma}}' = \boldsymbol{\gamma}'_{[1]} - \frac{1}{2} \int_{t'}^{t} (\{\boldsymbol{\gamma}'_{[1]} \cdot \boldsymbol{\gamma}''_{[1]} + \boldsymbol{\gamma}''_{[1]} \cdot \boldsymbol{\gamma}'_{[1]}\} - \{\boldsymbol{\omega}'' \cdot \boldsymbol{\gamma}'_{[1]} - \boldsymbol{\gamma}'_{[1]} \cdot \boldsymbol{\omega}''\}) dt'' + \cdots \tag{9D.1-6}$$

and obtain a similar relation giving $\dot{\boldsymbol{\gamma}}'$ in terms of integrals over $\boldsymbol{\gamma}^{[1]}$ and $\boldsymbol{\omega}$ at past times; here $\boldsymbol{\omega} = \nabla \boldsymbol{v} - (\nabla \boldsymbol{v})^{\dagger}$ is the vorticity tensor.

[3] N. R. Amundson, *Mathematical Methods in Chemical Engineering*, Prentice-Hall, Englewood Cliffs, NJ (1966), p. 199.

[4] See R. C. Armstrong and R. B. Bird, *J. Chem. Phys.*, **58**, 2715–2723 (1973); erratum: in Eq. 22, replace 27/280 by 27/980.

CHAPTER 10

FLUID DYNAMICS OF RHEOMETRY

In Chapter 3 we described the material functions that can be used to characterize non-Newtonian fluids. There we introduced the two main types of flows, shear and shearfree, used for this purpose. For each of these flows we considered only homogeneous flow, and we gave definitions for the material functions in terms of the uniform stresses generated in the fluid. In the laboratory we do not usually generate homogeneous flows nor directly measure the material functions. Instead we measure forces and torques exerted on pieces of equipment, rates of rotation in an apparatus, volume flow rates, and so on. It is necessary to be able to relate these measurable quantities to the desired material functions.

We consider here a number of experimental arrangements used for studying shear and shearfree flows. We begin in §10.1 with a discussion of linear viscoelastic property measurements, since these provide the common time-dependent basis to which large deformation shear and shearfree flow results must simplify in the limit of small displacement gradients. Then in §10.2 we consider steady-state shear flows. These are the most commonly performed experiments in rheometry; many standard instruments are available commercially to do these. Next in §10.3 we describe shearfree flow experiments. These methods have been under active development over the past decade and there remain large classes of materials and material functions for which measurements cannot yet be made. Finally, in §10.4 we present several examples of experiments that use complex flows (in the sense of being neither simple shear flow nor shearfree flow) to learn about the material functions.

Although this chapter focuses on mechanical means for measuring material functions, rheo-optical techniques may ultimately prove more useful for certain types of properties, including those involving short-time, transient shear flows and all types of shearfree flows.[1] We do not discuss laboratory techniques or experimental difficulties in any depth here, as these can be found in other references.[2]

[1] A general discussion of birefringence methods is given by H. Janeschitz-Kriegl, *Polymer Melt Rheology and Flow Birefringence*, Elsevier, Amsterdam (1983). Measurement of shearfree flow properties is described by J. A. van Aken and H. Janeschitz-Kriegl, *Rheol. Acta*, **19**, 744–752 (1980); **20**, 419–432 (1981). Transient measurements of the shear stress and first normal stress difference made by birefringence and by standard mechanical methods for shear flow of a polystyrene melt have been shown to agree by F. H. Gortemaker, M. G. Hansen, B. deCindio, H. M. Laun, and H. Janeschitz-Kriegl, *Rheol. Acta*, **15**, 256–267 (1976). The start-up of steady shear flow has been studied by birefringence by A. W. Chow and G. G. Fuller, *J. Non-Newtonian Fluid Mech.*, **17**, 233–243 (1985).

[2] See J. Meissner, *Ann. Rev. Fluid Mech.*, **17**, 45–64 (1985); H. Janeschitz-Kriegl, *Polymer Melt Rheology and Flow Birefringence*, Springer-Verlag, Berlin (1983); J. M. Dealy, *Rheometers for Molten Plastics*, Van Nostrand, New York (1982); R. W. Whorlow, *Rheological Techniques*, Ellis Horwood, Chichester, UK (1980); K. Walters, *Rheometry*, Chapman and Hall, London (1975); S. Oka in F. R. Eirich, ed., *Rheology*, Vol. 3, Academic Press, New York (1960), Chapt. 2.

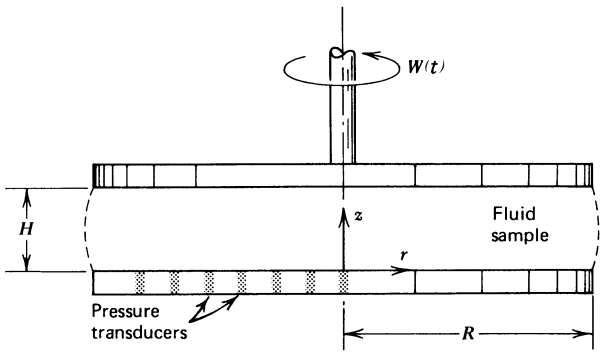

FIGURE 10.1-1. Parallel-disk instrument. In Example 10.1-1, $W(t) = \theta_0 \mathscr{R}e\{i\omega e^{i\omega t}\}$, and in Example 10.2-2, W is a constant.

§10.1 LINEAR VISCOELASTIC MEASUREMENTS[1]

As has been described in Chapter 5, the linear viscoelastic properties of a material can be obtained from a wide variety of experiments. Chapter 5 has further shown how the results of the various experimental measurements can be interrelated. In Example 5.4-3, we worked out the relationships for determining η' and η'' from an oscillating, concentric cylinder device. In this section, we analyze two additional instrumental configurations frequently used to measure these linear viscoelastic material functions. The second example is particularly interesting because we must use a general, nonlinear model, namely the first term of the memory-integral expansion (Eq. 9.6-1), to analyze the flow.

EXAMPLE 10.1-1 The Parallel-Disk Viscometer

A viscoelastic fluid is contained between two parallel disks of radius R separated by a gap H (see Fig. 10.1-1). The upper plate is caused to oscillate in the θ-direction sinusoidally with frequency ω and angular amplitude θ_0, and the time-dependent torque on the fixed, lower plate is measured. Show how the torque measurement can be used to determine η' and η'' from measurements with $\theta_0 \ll 1$. Assume that inertial forces are negligible.

SOLUTION The motion of the top plate is given by the angular displacement θ as a function of the time t

$$\theta = \theta_0 \mathscr{R}e\{e^{i\omega t}\} \tag{10.1-1}$$

where θ_0 is real. The boundary conditions on the fluid velocity are

$$\text{At } z = H, \qquad v_\theta = \theta_0 r \mathscr{R}e\{i\omega e^{i\omega t}\}$$
$$v_r = v_z = 0 \tag{10.1-2}$$

$$\text{At } z = 0, \qquad v_\theta = v_r = v_z = 0 \tag{10.1-3}$$

[1] The standard reference on linear viscoelastic measurement methods is J. D. Ferry, *Viscoelastic Properties of Polymers*, 3rd ed., Wiley, New York (1980). We have also drawn extensively in this section on K. Walters, *Rheometry*, Chapman and Hall, London (1975), Chapts. 6 and 8.

The form of the boundary conditions strongly suggests that we assume $v_r = v_z = 0$ and

$$v_\theta = r\,\mathscr{R}e\{f(z)e^{i\omega t}\} \tag{10.1-4}$$

where $f(z)$ is complex. This form for v_θ satisfies the continuity equation automatically. The boundary conditions on f are

$$f(0) = 0; \quad f(H) = i\omega\theta_0 \tag{10.1-5}$$

The constitutive equation appropriate for small displacement gradients ($\theta_0 \ll 1$) is the general linear viscoelastic model, Eq. 5.2-18. When we combine Eq. 5.2-18 with Eq. 5.3-6, which gives the complex viscosity in terms of $G(s)$, and use the assumed velocity field together with Eqs. B.3-7 through 12 for the rate of strain components, we find that

$$\tau_{\theta z} = \tau_{z\theta} = -r\,\mathscr{R}e\{\eta^* f'(z)e^{i\omega t}\} \tag{10.1-6}$$

and that all other $\tau_{ij} = 0$.

Next we insert the stress tensor into the equation of motion in which the inertial terms are neglected. The r- and z-components show that the pressure is everywhere constant between the plates. The θ-component gives

$$f'' = 0 \tag{10.1-7}$$

The solution to Eq. 10.1-7 that satisfies the boundary conditions is

$$f = i\omega\theta_0 z/H \tag{10.1-8}$$

so that

$$\tau_{\theta z} = -(\theta_0 r/H)\,\mathscr{R}e\{\eta^* i\omega e^{i\omega t}\} \tag{10.1-9}$$

We can now calculate the torque $\mathscr{T}$ that the lower shaft must exert on the bottom plate in order to keep it stationary. This is given by

$$\begin{aligned}
\mathscr{T} &= \mathscr{T}_0\,\mathscr{R}e\{e^{i(\omega t+\delta)}\} \\
&= \mathscr{T}_0\,\mathscr{R}e\{(\cos\delta + i\sin\delta)e^{i\omega t}\} \\
&= \int_0^{2\pi}\int_0^R r\,\mathscr{R}e\{\tau_{\theta z}\}\cdot r dr d\theta \\
&= -(\pi R^4\omega\theta_0/2H)\,\mathscr{R}e\{(i\eta' + \eta'')e^{i\omega t}\}
\end{aligned} \tag{10.1-10}$$

where $\mathscr{T}_0$ is real. By comparing the second and last lines of Eq. 10.1-10 we find the components of the complex viscosity in terms of the measured torque amplitude $\mathscr{T}_0$ and phase shift δ as follows:

$$\eta' = -\frac{2H\mathscr{T}_0\sin\delta}{\pi R^4\omega\theta_0} \tag{10.1-11}$$

$$\eta'' = -\frac{2H\mathscr{T}_0\cos\delta}{\pi R^4\omega\theta_0} \tag{10.1-12}$$

The phase angle δ must vary between $-\pi$ for a purely elastic solid and $-\pi/2$ for a purely viscous fluid.

The most serious assumption involved in the derivation of Eqs. 10.1-11 and 12 is the neglect of inertia. It can be shown that this is a good approximation provided that (see Problem 10B.2)

$$H\left|\frac{i\rho\omega}{\eta^*}\right|^{1/2} \ll 1 \tag{10.1-13}$$

An advantage of the parallel-disk geometry for measuring η^* for low-viscosity liquids is that at fixed frequency ω the gap H can be reduced in order to minimize inertial effects.

EXAMPLE 10.1-2 The Eccentric Rotating Disk Rheometer[2]

The eccentric disk or orthogonal rheometer flow[3] is shown in Fig. 3B.1. The material to be tested is contained between parallel disks of radius R, each of which rotates with angular velocity W. The resulting motion would be a rigid rotation except for the fact that the axes of rotation of the disks are displaced from each other by an amount a. The gap between the disks is b. Show how the linear viscoelastic material functions η' and η'' can be determined from the steady-state forces F_x and F_y exerted by the fluid in the x- and y-directions on the lower plate. Assume that inertial forces are negligible, and take the origin of the xyz-coordinate system to be at the midpoint of the line connecting the centers of the two disks.

SOLUTION (a) Boundary Conditions and Assumed Solution

The boundary conditions for the flow in Fig. 3B.1 (with the coordinate system described above) are

$$\begin{aligned} \text{On } z = b/2, \qquad \boldsymbol{v} &= [W\boldsymbol{\delta}_z \times [\boldsymbol{r} - \tfrac{1}{2}a\boldsymbol{\delta}_y]] \\ &= [W\boldsymbol{\delta}_z \times [r\boldsymbol{\delta}_r - \tfrac{1}{2}a(\sin\theta\,\boldsymbol{\delta}_r + \cos\theta\,\boldsymbol{\delta}_\theta)]] \\ &= \tfrac{1}{2}Wa\cos\theta\,\boldsymbol{\delta}_r + W(r - \tfrac{1}{2}a\sin\theta)\boldsymbol{\delta}_\theta \end{aligned} \tag{10.1-14a}$$

$$\begin{aligned} \text{On } z = -b/2, \qquad \boldsymbol{v} &= [W\boldsymbol{\delta}_z \times [r + \tfrac{1}{2}a\boldsymbol{\delta}_y]] \\ &= -\tfrac{1}{2}Wa\cos\theta\,\boldsymbol{\delta}_r + W(r + \tfrac{1}{2}a\sin\theta)\boldsymbol{\delta}_\theta \end{aligned} \tag{10.1-14b}$$

where $\boldsymbol{\delta}_i$ is the unit vector in the ith coordinate direction. Equations 10.1-14a and b are of the form

$$v_r = aW\,\mathscr{R}e\{v_r^0 e^{i\theta}\} \tag{10.1-15a}$$

$$v_\theta = rW + aW\,\mathscr{R}e\{v_\theta^0 e^{i\theta}\} \tag{10.1-15b}$$

$$v_z = aW\,\mathscr{R}e\{v_z^0 e^{i\theta}\} \tag{10.1-15c}$$

in which the dimensionless complex amplitude functions v_i^0 are given by

$$\begin{aligned} \text{On } z = b/2, \qquad v_r^0 &= 1/2 \\ v_\theta^0 &= i/2 \\ v_z^0 &= 0 \end{aligned} \tag{10.1-16a}$$

$$\begin{aligned} \text{On } z = -b/2, \qquad v_r^0 &= -1/2 \\ v_\theta^0 &= -i/2 \\ v_z^0 &= 0 \end{aligned} \tag{10.1-16b}$$

The factor aW is included in the velocity perturbation definitions in Eq. 10.1-15 because we expect the flow will reduce to a rigid rotation in the limit as $a \to 0$.

[2] This analysis is based on K. Walters, *Rheometry*, Chapman and Hall, London (1975), pp. 164–172.

[3] The kinematics of flow between eccentric rotating disks was discussed in Problems 3B.1 and 3C.2. This flow has also been analyzed in Problems 6B.2, 7B.9, and 8B.5.

The boundary conditions suggest a solution of the form given by Eq. 10.1-15 with $v_r^0 = v_r^0(z)$, $v_\theta^0 = v_\theta^0(z)$, $v_z^0 = 0$. If these are inserted into the continuity equation we obtain the following relation between v_r^0 and v_θ^0:

$$v_r^0 + iv_\theta^0 = 0 \tag{10.1-17}$$

(b) Constitutive Equation

Because the material particles experience rotations through large angles during this experiment, the general linear viscoelastic model cannot be used (see Example 8.1-2). However, the first term of the memory-integral expansion, Eq. 9.6-1 (namely, the Lodge rubberlike liquid constitutive equation), can be used for this analysis if the strain (a/b) imposed on the material is sufficiently small; we have seen in §9.6 that this equation is valid in the limit of small strains for a very broad class of fluids.

To calculate the stress at position $\boldsymbol{r}$ and time t, the Lodge rubberlike liquid requires that we integrate the relative strain tensor $\boldsymbol{\gamma}_{[0]}(\boldsymbol{r}, t, t')$ following a particle that is at position $\boldsymbol{r}$ at time t. This is most easily done if we take the position $\boldsymbol{r}'$ of the particle at past times t' to be the dependent variable and the present location $\boldsymbol{r}$ at which we want to evaluate stress to be the independent variable. Evaluation of $\boldsymbol{\gamma}_{[0]}$ is then accomplished by using the displacement functions $\boldsymbol{r}' = \boldsymbol{r}'(\boldsymbol{r}, t, t')$ to calculate the displacement gradient tensor $\boldsymbol{\Delta}$, by inverting $\boldsymbol{\Delta}$ to obtain $\mathbf{E}$, and then finally by using $\mathbf{E}$ to calculate $\boldsymbol{\gamma}_{[0]}$. The displacement functions are given by the velocities as follows:

$$\begin{aligned}
\frac{\partial r'}{\partial t'} &= v_r = aW\,\mathscr{R}e\{v_r^0 e^{i\theta'}\} \\
r'\frac{\partial \theta'}{\partial t'} &= v_\theta = r'W + aW\,\mathscr{R}e\{v_\theta^0 e^{i\theta'}\} \\
\frac{\partial z'}{\partial t'} &= v_z = 0
\end{aligned} \tag{10.1-18}$$

subject to the condition

$$\text{At } t' = t \qquad r' = r; \quad \theta' = \theta; \quad z' = z \tag{10.1-19}$$

where the velocities $v_i = v_i(r', \theta', z', t')$ are functions of the space coordinates r', θ', z' and we have taken $v_z = 0$. The solution to Eqs. 10.1-18 is made easy by the fact that the amplitudes aWv_i^0 of the perturbations to the rigid rotation are small. Thus we can construct a successive substitution scheme to obtain a solution good to terms linear in the small offset a.

At lowest order we neglect all terms containing a. Thus Eqs. 10.1-18 reduce to

$$\frac{\partial r'}{\partial t'} = 0; \quad \frac{\partial \theta'}{\partial t'} = W; \quad \frac{\partial z'}{\partial t'} = 0 \tag{10.1-20}$$

which have the solutions (when condition Eq. 10.1-19 is applied)

$$r' = r; \quad \theta' = \theta - W(t - t'); \quad z' = z \tag{10.1-21}$$

The terms that were neglected in obtaining Eqs. 10.1-20 are now evaluated by using Eqs. 10.1-21 and the following equations for the next approximation to the displacement functions are obtained:

$$\begin{aligned}
\frac{\partial r'}{\partial t'} &= aW\,\mathscr{R}e\{v_r^0(z)e^{i\theta}e^{-iW(t-t')}\} \\
\frac{\partial \theta'}{\partial t'} &= W + aW\,\mathscr{R}e\left\{\frac{v_\theta^0(z)}{r}e^{i\theta}e^{-iW(t-t')}\right\} \\
\frac{\partial z'}{\partial t'} &= 0
\end{aligned} \tag{10.1-22}$$

The solutions to Eqs. 10.1-22 are

$$\begin{aligned} r' &= r + a\,\mathscr{R}e\{iv_r^0(z)e^{i\theta}[1 - e^{-iW(t-t')}]\} \\ \theta' &= \theta - \mathscr{W}(t-t') + a\,\mathscr{R}e\left\{i\frac{v_\theta^0(z)}{r}e^{i\theta}[1 - e^{-iW(t-t')}]\right\} \\ z' &= z \end{aligned} \tag{10.1-23}$$

Equations 10.1-23 are the desired solution for the displacement functions since the quadratic terms in a obtained in the next iteration are negligibly small.

To calculate $\boldsymbol{\Delta}$ we need the following derivatives which are all evaluated to order a

$$\begin{aligned} \frac{\partial r'}{\partial r} &= \frac{\partial z'}{\partial z} = 1 & \frac{\partial \theta'}{\partial r} &= -a\,\mathscr{R}e\left\{i\frac{v_\theta^0}{r^2}\Omega\right\} \\ \frac{\partial r'}{\partial \theta} &= -a\,\mathscr{R}e\{v_r^0\Omega\} & \frac{\partial \theta'}{\partial \theta} &= 1 - a\,\mathscr{R}e\left\{\frac{v_\theta^0}{r}\Omega\right\} \\ \frac{\partial r'}{\partial z} &= a\,\mathscr{R}e\left\{i\frac{\partial v_r^0}{\partial z}\Omega\right\} & \frac{\partial \theta'}{\partial z} &= a\,\mathscr{R}e\left\{\frac{i}{r}\frac{\partial v_\theta^0}{\partial z}\Omega\right\} \end{aligned} \tag{10.1-24}$$

where we have abbreviated

$$\Omega = e^{i\theta}[1 - e^{-iW(t-t')}] \tag{10.1-25}$$

The displacement gradient tensor $\boldsymbol{\Delta}$ is given in Appendix B, Eqs. B.7-3 and 5 as

$$\Delta_{ij} = \sum_k T_{ik}D_{kj} \qquad (i,j = r,\theta,z) \tag{10.1-26}$$

in which (T_{ij}) is the orthogonal matrix in Eq. B.7-5 which rotates $\boldsymbol{r}$ into $\boldsymbol{r}'$, and (D_{ij}) is given in the present problem (according to Eq. B.7-3) by

$$(D_{ij}) = \begin{pmatrix} 1 & \frac{1}{r}\frac{\partial r'}{\partial \theta} & \frac{\partial r'}{\partial z} \\ r'\frac{\partial \theta'}{\partial r} & \frac{r'}{r}\frac{\partial \theta'}{\partial \theta} & r'\frac{\partial \theta'}{\partial z} \\ 0 & 0 & 1 \end{pmatrix} \tag{10.1-27}$$

The displacement gradient tensor $\mathbf{E}$ then has components

$$\mathrm{E}_{ij} = \Delta_{ij}^{-1} = \sum_k D_{ik}^{-1}T_{jk} \tag{10.1-28}$$

since (T_{ij}) is orthogonal. However, to calculate $\boldsymbol{\gamma}_{[0]}$ we need only the components of the matrix inverse to (D_{ij}), since

$$\gamma_{[0]ij} = \delta_{ij} - \sum_k \mathrm{E}_{ik}\mathrm{E}_{jk} = \delta_{ij} - \sum_k D_{ik}^{-1}D_{jk}^{-1} \tag{10.1-29}$$

It is straightforward to invert (D_{ij}), and in doing so we use the fact that det $(D_{ij}) = 1$ because the fluid is assumed incompressible. In this way we obtain

$$(D_{ij}^{-1}) = \begin{pmatrix} \frac{r'}{r}\frac{\partial\theta'}{\partial\theta} & -\frac{1}{r}\frac{\partial r'}{\partial\theta} & \frac{r'}{r}\left(\frac{\partial r'}{\partial\theta}\frac{\partial\theta'}{\partial z} - \frac{\partial\theta'}{\partial\theta}\frac{\partial r'}{\partial z}\right) \\ -r'\frac{\partial\theta'}{\partial r} & 1 & r'\left(\frac{\partial\theta'}{\partial r}\frac{\partial r'}{\partial z} - \frac{\partial\theta'}{\partial z}\right) \\ 0 & 0 & 1 \end{pmatrix} \tag{10.1-30}$$

Equations 10.1-24, 29, and 30 can now be combined to give $\boldsymbol{\gamma}_{[0]}$. If we retain only terms through first order in a, then the only nonzero components of $\boldsymbol{\gamma}_{[0]}$ are

$$\gamma_{[0]rz} = \gamma_{[0]zr} = a\,\mathscr{R}e\left\{i\Omega\frac{\partial v_r^0}{\partial z}\right\} \tag{10.1-31}$$

$$\gamma_{[0]\theta z} = \gamma_{[0]z\theta} = a\,\mathscr{R}e\left\{i\Omega\frac{\partial v_\theta^0}{\partial z}\right\} \tag{10.1-32}$$

where we have made use of the continuity equation, Eq. 10.1-17, in showing that $\gamma_{[0]rr}$ and $\gamma_{[0]r\theta}$ are zero.

When combined with the Lodge rubberlike liquid, Eqs. 10.1-31 and 32 give the stress components up to and including linear terms in a:

$$\tau_{rz} = \tau_{zr} = \mathscr{R}e\left\{\left[-\int_0^\infty \frac{iM(s)}{W}(1 - e^{-iWs})ds\right]\left[-aWe^{i\theta}\frac{\partial v_r^0}{\partial z}\right]\right\} = -aW\,\mathscr{R}e\left\{\eta^* e^{i\theta}\frac{\partial v_r^0}{\partial z}\right\} \tag{10.1-33}$$

$$\tau_{\theta z} = \tau_{z\theta} = -aW\,\mathscr{R}e\left\{\eta^* e^{i\theta}\frac{\partial v_\theta^0}{\partial z}\right\} \tag{10.1-34}$$

where we have used Eq. 5.3-6, after integration by parts, to replace the Fourier transform of the relaxation modulus with the complex viscosity (see also Problem 5B.7). All other stress components are zero to the present order of approximation.

(c) Equation of Motion

Since the stresses are periodic in θ, it is reasonable also to assume that the pressure varies periodically in θ so we write

$$p = p_0 + \mathscr{R}e\{\bar{p}(r, z)e^{i\theta}\} \tag{10.1-35}$$

where p_0 is a constant. When Eqs. 10.1-15 and 33 through 35 are put into the equation of motion written in cylindrical coordinates we find to first order in the offset a:

$$r\text{-component:} \qquad 0 = -\mathscr{R}e\left\{\frac{\partial\bar{p}}{\partial r}\right\} + aW\,\mathscr{R}e\left\{\eta^*\frac{d^2v_r^0}{dz^2}\right\} \tag{10.1-36}$$

$$0\text{-component:} \qquad 0 = -\mathscr{R}e\left\{i\frac{\bar{p}}{r}\right\} + aW\,\mathscr{R}e\left\{\eta^*\frac{d^2v_\theta^0}{dz^2}\right\} \tag{10.1-37}$$

$$z\text{-component:} \qquad 0 = -\mathscr{R}e\left\{\frac{\partial\bar{p}}{\partial z}\right\} \tag{10.1-38}$$

where we have made use of the continuity equation and the fact that inertial terms are negligible. Equation 10.1-38 shows that $\bar{p} = \bar{p}(r)$. Note that Eqs. 10.1-36 through 38 are the same as the creeping flow Navier-Stokes equations for the assumed velocity and pressure fields except that the constant Newtonian viscosity μ is replaced by the complex viscosity η^*. This means, of course, that *the material behavior in the eccentric rotating disk flow is completely determined by the complex viscosity η^* for small eccentricity and that no other material functions enter.*[4] To use this experiment to measure η^* we must complete finding the details of the velocity field.

(d) Velocity Field and Forces on the Lower Plate

It is easy to see that the equations of continuity and motion and the boundary conditons are satisfied by

$$v_r^0 = z/b \tag{10.1-39}$$

$$v_\theta^0 = iz/b \tag{10.1-40}$$

$$\bar{p} = 0 \tag{10.1-41}$$

In the eccentric rotating disk experiment, two orthogonal components of the force in the xy-plane on one of the plates are measured. If we let F_x and F_y be the components of this force in the x- and y-directions, respectively, then we have for the bottom plate ($z = -b/2$)

$$F_x = -\int_0^{2\pi}\int_0^R [\tau_{zr}\cos\theta - \tau_{z\theta}\sin\theta]_{z=-b/2}\, r\, dr\, d\theta \tag{10.1-42}$$

$$F_y = -\int_0^{2\pi}\int_0^R [\tau_{zr}\sin\theta + \tau_{z\theta}\cos\theta]_{z=-b/2}\, r\, dr\, d\theta \tag{10.1-43}$$

The necessary stresses are found by substituting Eqs. 10.1-39 and 40 into Eqs. 10.1-33 and 34, and these can then be put back into the force expressions. When we replace η^* by $\eta' - i\eta''$ we obtain the rheological properties:

$$\eta' = \left[\frac{b}{\pi WaR^2}\right]F_x \tag{10.1-44}$$

$$\eta'' = \frac{G'}{\omega} = \left[\frac{b}{\pi WaR^2}\right]F_y \tag{10.1-45}$$

Equations 10.1-44 and 45 show how measurements of the (steady) forces F_x and F_y can be converted immediately into the linear viscoelastic material functions.

Throughout this analysis we have used the fact that the disturbance velocities v_r^0 and v_θ^0 were small. To be certain that this condition is satisfied, it is necessary to vary a in the experiments. In the limit as $a \to 0$, the quantity Wa can be made small enough for the theory to be satisfied, in which case F_x/a and F_y/a approach constant values which yield the complex viscosity according to Eqs. 10.1-44 and 45.

[4] K. Walters, *loc cit.*, gives a more general result valid for other eccentric geometries.

§10.2 STEADY-STATE SHEAR FLOWS

In this section we focus our attention on the determination of the viscometric functions. The usual geometries for achieving steady shear flow were introduced in §3.7, where viscometric flows were defined. The most important arrangements are the cone-and-plate, parallel-disk, circular tube, rectangular slit, and concentric cylinder apparatuses. For each, the equations of motion must be used together with the experimentally applied boundary conditions in order to relate the steady shear flow material functions to the measured forces and velocities. Several relations obtainable in this way are tabulated in Table 10.2-1 for reference purposes along with a listing of the quantities measured for each type of experiment.[1] The derivations of these relations are treated in detail in the examples at the end of this section and in problems at the end of the chapter.

The most widely used geometry for complete characterization of the viscometric functions is the cone-and-plate configuration; the angle between the cone and plate is very small, typically less than 4°. It is available in a variety of commercial rheological instruments. At high rates of rotation in the cone-and-plate apparatus, a steady shear flow is not possible because of inertial, viscoelastic, and possibly other effects. A particularly severe limitation results from the tendency of viscoelastic samples to fracture[2] at the free surface in cone-and-plate flow at moderate to high rotation rates. Thus, this geometry cannot be used to obtain rheological data at very high shear rates. The cone-and-plate instrument is also convenient for measuring unsteady unidirectional shear flow material functions.

Because of its freedom from inertial effects (see Example 10.2-3) and edge fracture, the capillary viscometer is used to determine viscosity at very high shear rates ($\dot{\gamma} > 10^2\ s^{-1}$). However, flow in the capillary viscometer yields no information on the normal stress coefficients.[3] The rectangular slit is similarly useful for high shear rate measurements of the viscosity, and by using a combination of flush-mounted and hole-mounted pressure transducers it is possible to measure the first normal stress coefficient with this instrument at high shear rates.[4]

A parallel-disk configuration can also be used to obtain all of the viscometric functions. This arrangement has the same drawback as the cone-and-plate that at high rotation rates edge fracture and/or inertial forces become important. It has the advantage, however, that the fluid motion is viscometric at all low rates of rotation, whereas the cone-and-plate flow is steady shear only in the limit of small cone angles. Moreover, high shear rates can be obtained in the parallel-plate device at moderate rotation rates by using very small gaps. From Table 10.2-1, we see that to find either of the normal stress coefficients separately from torsional flow measurements, we must know values of the pressure exerted against one of the disks at specific positions. Many early local pressure measurements were

[1] A review of experimental geometries and appropriate equations for determining the viscometric functions is given by A. C. Pipkin and R. I. Tanner, *Mech. Today*, **1**, 262–321 (1972). H. Markovitz in F. R. Eirich, ed., *Rheology*, Vol. 4, Academic Press, New York (1967), Chapt. 6, pp. 347–410. R. W. Whorlow, *Rheological Techniques*, Ellis Horwood, Chichister, UK (1980). See also R. I. Tanner, *Engineering Rheology*, Oxford University Press (1985), Chapter 3.

[2] J. F. Hutton, *Rhoel, Acta*, **8**, 54–59 (1969); R. I. Tanner and M. Keentok, *J. Rheol.*, **27**, 47–57 (1983).

[3] Measurements have been made of the thrust of the fluid exiting from the capillary tube on a wall, and attempts have been made to relate these measurements to the normal stress coefficients. For a summary of errors in the literature associated with the measurement of normal stresses in capillaries and slits, see J. M. Davies, J. F. Hutton, and K. Walters, *J. Phys. D.: Appl. Phys.*, **6**, 2259–2266 (1973), and K. Walters, *Rheometry*, Chapman and Hall, London (1975), pp. 96–105. For a discussion of the use of the exit pressure in capillaries and slits to determine normal stresses, see D. V. Boger and M. M. Denn, *J. Non-Newtonian Fluid Mech.*, **6**, 163–185 (1980).

[4] A. S. Lodge and L. deVargas, *Rheol. Acta*, **22**, 151–170 (1983); A. S. Lodge, *Polym. News*, **9**, 242–246 (1984); A. S. Lodge, *Chem. Eng. Commun.*, **32**, 1–60 (1985).

TABLE 10.2-1

Examples of Relations for Determining the Viscometric Functions (η, Ψ_1, Ψ_2) in Standard Experimental Arrangements

A. *Capillary Viscometer* (Table 3.7-2*a* and Example 10.2-3)

Q = Volume rate of flow
$\Delta\mathscr{P}$ = Pressure drop through tube
R = Tube radius
L = Tube length
$\dot{\gamma}_R$ = Shear rate at tube wall
τ_R = Shear stress at tube wall

$$\eta(\dot{\gamma}_R) = \frac{\tau_R}{(Q/\pi R^3)}\left[3 + \frac{d \ln (Q/\pi R^3)}{d \ln \tau_R}\right]^{-1} \tag{A-1}$$

$$\dot{\gamma}_R = \frac{1}{\tau_R^2}\frac{d}{d\tau_R}(\tau_R^3 Q/\pi R^3) \tag{A-2}$$

$$\tau_R = \Delta\mathscr{P}R/2L \tag{A-3}$$

B. *Cone-and-Plate Instrument* (Table 3.7-2*d* and Example 10.2-1)

R = Radius of circular plate
ϑ_0 = Angle between cone and plate (usually less than 4°)
W_0 = Angular velocity of cone
$\mathscr{T}$ = Torque on plate
$\mathscr{F}$ = Force required to keep tip of cone in contact with circular plate
$\pi_{\theta\theta}(r)$ = Pressure measured by flush-mounted pressure transducers located on plate
p_a = Atmospheric pressure

$$\eta(\dot{\gamma}) = \frac{3\mathscr{T}}{2\pi R^3 \dot{\gamma}} \tag{B-1}$$

$$\Psi_1(\dot{\gamma}) = \frac{2\mathscr{F}}{\pi R^2 \dot{\gamma}^2} \tag{B-2}$$

$$\Psi_1(\dot{\gamma}) + 2\Psi_2(\dot{\gamma}) = -\frac{1}{\dot{\gamma}^2}\frac{\partial \pi_{\theta\theta}}{\partial \ln r} \tag{B-3}$$

$$\Psi_2(\dot{\gamma}) = \frac{p_a - \pi_{\theta\theta}(R)}{\dot{\gamma}^2} \tag{B-4}$$

$$\dot{\gamma} = W_0/\vartheta_0 \tag{B-5}$$

C. *Parallel-Disk Instrument* (Table 3.7-2*c* and Example 10.2-2)

R = Radius of disks
H = Separation of disks
W_0 = Angular velocity of upper disk

$$\eta(\dot{\gamma}_R) = \frac{(\mathscr{T}/2\pi R^3)}{\dot{\gamma}_R}\left[3 + \frac{d \ln (\mathscr{T}/2\pi R^3)}{d \ln \dot{\gamma}_R}\right] \tag{C-1}$$

$\mathscr{T}$ = Torque required to rotate upper disk
$\mathscr{F}$ = Force required to keep separation of two disks constant
$\dot{\gamma}_R$ = Shear rate at edge of system
$\pi_{zz}(0)$, $\pi_{zz}(R)$ = Normal pressure measured on disk at center and at rim
p_a = Atmospheric pressure

$$\Psi_1(\dot{\gamma}_R) - \Psi_2(\dot{\gamma}_R) = \frac{(\mathscr{F}/\pi R^2)}{\dot{\gamma}_R^2}\left[2 + \frac{d \ln (\mathscr{F}/\pi R^2)}{d \ln \dot{\gamma}_R}\right] \tag{C-2}$$

$$\Psi_1(\dot{\gamma}_R) + \Psi_2(\dot{\gamma}_R) = \frac{1}{\dot{\gamma}_R^2}\frac{d\pi_{zz}(0)}{d \ln \dot{\gamma}_R} \tag{C-3}$$

$$\Psi_2(\dot{\gamma}_R) = \frac{p_a - \pi_{zz}(R)}{\dot{\gamma}_R^2} \tag{C-4}$$

$$\dot{\gamma}_R = \frac{W_0 R}{H} \tag{C-5}$$

D. *Couette Viscometer* (Table 3.7-2*b*) *Narrow Gap*

R_1, R_2 = Radii of inner and outer cylinders
H = Height of cylinders
W_1, W_2 = Angular velocities of inner and outer cylinders
$\mathscr{T}$ = Torque on inner cylinder
$\pi_{rr}(R_1)$, $\pi_{rr}(R_2)$ = Normal pressures measured on inner and outer cylinders

$$\eta(\dot{\gamma}) = \frac{\mathscr{T}(R_2 - R_1)}{2\pi R_1^3 H |W_2 - W_1|} \tag{D-1}$$

$$\Psi_1(\dot{\gamma}) = \frac{-[\pi_{rr}(R_2) - \pi_{rr}(R_1)]R_1}{(R_2 - R_1)\dot{\gamma}^2} + \frac{\rho R_1^2}{3\dot{\gamma}^2}(W_1^2 + W_2^2 + W_1 W_2) \tag{D-2}$$

$$\dot{\gamma} = \frac{|W_2 - W_1|R_1}{R_2 - R_1} \tag{D-3}$$

E. *Axial Annular Flow* (Problem 2B.5)

R_1, R_2 = Radii of inner and outer cylinders
$(\pi_{rr})_i$ = Reading of a flush-mounted pressure transducer at R_i

$$(\pi_{rr})_1 - (\pi_{rr})_2 = -\int_{R_1}^{R_2} \frac{\Psi_2 \dot{\gamma}^2}{r}\, dr \tag{E-1}$$

(*Continued*)

TABLE 10.2-1 (*Continued*)

F. *Torsional Flow between Two Disks, the Upper One of Which is Rotating and Attached to a Vertical Tube* (Problem 10B.6)

h = Height of rise of fluid in tube
R_1 = Radius of tube
R_2 = Radius of disks
W_0 = Angular velocity of tube-disk assembly
H = Gap between disks
g = Gravitational acceleration

$$h = \frac{W_0^2}{\rho g H}\int_{R_1}^{R_2}(\Psi_1 + \Psi_2) r\, dr - \frac{W_0^2}{6g}(R_2^2 - R_1^2) \tag{F-1}$$

G. *Truncated Cone-and-Plate Instrument* (Problem 10B.7)

R = Radius of circular plate
R_0 = Radius of truncated section of cone
ϑ_0 = Angle between cone and plate (usually less than 4°)
H = Gap between truncated section of cone and circular plate
$\pi'_{\theta\theta}(r)$ = Pressure measured by transducers mounted at the bottom of holes along bottom disk
$\pi_{\theta\theta}(r)$ = Normal stress on bottom circular disk
W = Angular velocity of truncated cone
$\dot{\gamma}_0$ = Shear rate for $R_0 \le r \le R$
p^* = Hole pressure
p_a = Atmospheric pressure

$$\pi_{\theta\theta}(0) = \pi'_{\theta\theta}(0) \tag{G-1}$$

$$\Psi_1(\dot{\gamma}_0) + 2\Psi_2(\dot{\gamma}_0) = -\frac{1}{\dot{\gamma}_0^2}\frac{\partial \pi'_{\theta\theta}}{\partial \ln r} \quad (R_0 \le r \le R) \tag{G-2}$$

$$\Psi_1(\dot{\gamma}_0) + \Psi_2(\dot{\gamma}_0) = \frac{1}{\dot{\gamma}_0}\frac{d}{d\dot{\gamma}_0}\left\{(\pi_{\theta\theta}(0) - p_a) - [\Psi_1(\dot{\gamma}_0) + 2\Psi_2(\dot{\gamma}_0)]\dot{\gamma}_0^2 \ln\frac{R}{R_0}\right\} \tag{G-3}$$

$$p^*(\dot{\gamma}_0) = p_a - \pi'_{\theta\theta}(R) - \Psi_2(\dot{\gamma}_0)\dot{\gamma}_0^2 \tag{G-4}$$

$$\dot{\gamma}_0 = \frac{WR_0}{H} \tag{G-5}$$

misinterpreted because of the hole pressure effect. Note, on the other hand, that with a cone-and-plate instrument, the first normal stress coefficient can be determined by measuring the total force required to keep the cone and plate together; this gives Ψ_1 directly without interference from the presence of holes.

The Couette viscometer, which utilizes the concentric cylinder geometry, allows a straightforward determination of viscosity when the gap between the cylinders is small. For large gaps the analysis is complicated because the velocity field depends on the viscosity function. Finally, the hole pressure can cause significant errors in this instrument, making measurement of the normal stresses difficult.

With most of the above devices it is difficult to make measurements in the zero-shear-rate region because the instrument forces become very small. To get the zero-shear-rate viscosity, a parallel-plate "sandwich" viscometer[5] or a falling sphere experiment (see §10.4 and Example 8.5-2) is useful. If the linear viscoelastic properties can be measured to lower frequencies, then the equality between η' and η at low ω and $\dot{\gamma}$ can be used to get η_0. Similarly, $\Psi_{1,0}$ can be evaluated if low-frequency η'' data are available (cf. Eq. 3.6-21).

In the following examples, we show how a few of the systems mentioned here are analyzed. Some of the operational difficulties encountered with each are also discussed. Analysis of these flow problems is sometimes simplified by the fact that for steady-state shear flow, the constitutive equation is known to be the CEF equation, Eq. 9.6-18.

EXAMPLE 10.2-1 Measurement of Viscosity and Normal Stress Coefficients in the Cone-and-Plate Instrument

A cone-and-plate geometry is shown in Fig. 10.2-1. The fluid to be tested is placed in the gap between the cone and plate; the cone is rotated with an angular velocity W. Three measurements can be made: the torque $\mathscr{T}$ on the plate, the total normal thrust $\mathscr{F}$ on the plate, and the "pressure distribution," $(p + \tau_{\theta\theta})|_{\theta=\pi/2}$ across the plate. From these measurements we want to get the material

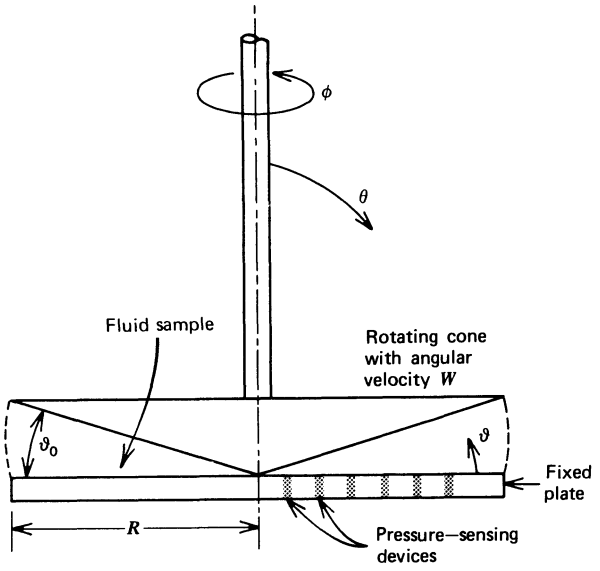

FIGURE 10.2-1. Cone-and-plate device; ϑ_0 is quite small, of the order of several degrees.

[5] H. M. Laun and J. Meissner, *Rheol. Acta*, **19**, 60–67 (1980).

functions, η, Ψ_1, and Ψ_2. Assume that inertial forces can be neglected. Recall that in Example 1.3-4 it was shown how to find the viscosity of a Newtonian fluid from cone-and-plate viscometer data.

SOLUTION **(a)** The Shear Rate

The small cone angle analysis of Example 1.3-4 can be taken over directly here to show that the shear rate $\dot{\gamma}$ is uniform throughout the gap and is equal to

$$\dot{\gamma} = -\dot{\gamma}_{\theta\phi} = \frac{W}{\vartheta_0} \tag{10.2-1}$$

Since η, Ψ_1, and Ψ_2 are functions of $\dot{\gamma}$ alone, the CEF equation tells us that the stress tensor τ is also uniform throughout the gap.

(b) The Shear Stress

Since the shear stress is constant in the fluid, we can immediately take over Eqs. 1.3-36 and 37 to give the shear stress and viscosity in terms of the measured torque and rotation rate of the cone

$$\boxed{\eta(\dot{\gamma}) = \frac{3\mathscr{T}\vartheta_0}{2\pi R^3 W}} \tag{10.2-2}$$

(c) The Radial Pressure Distribution

From the radial component of the equation of motion (neglecting the centrifugal force term $-\rho v_\phi^2/r$) we get

$$0 = -\frac{\partial p}{\partial r} - \frac{1}{r^2}\frac{\partial}{\partial r}(r^2\tau_{rr}) + \frac{\tau_{\theta\theta} + \tau_{\phi\phi}}{r} \tag{10.2-3}$$

Since $\tau_{\theta\theta}$ is constant, we can replace $\partial p/\partial r$ by $\partial \pi_{\theta\theta}/\partial r$; we do this beca ıse pressure transducers will measure $\pi_{\theta\theta}$ rather than p. The normal stress terms can be rewritten in terms of the material functions to give

$$\frac{\partial}{\partial \ln r}\pi_{\theta\theta} = -(\Psi_1 + 2\Psi_2)\dot{\gamma}^2 \tag{10.2-4}$$

Hence, if $\pi_{\theta\theta}$ is measured on the plate (where $\theta = \pi/2$) and plotted against $\ln r$, the slope will yield the indicated combination of normal stress coefficients. Since data in §3.3 indicate that Ψ_1 is positive and Ψ_2 is roughly $-0.1\Psi_1$, we would expect the above slope to be negative; this is illustrated in Fig. 10A.2.

The pressure at the edge of the plate $\pi_{\theta\theta}(R)$ can be related to the second normal stress coefficient by means of a normal force balance across the fluid–air interface at the rim. If we assume the liquid surface at $r = R$ to be spherical, then $\pi_{rr}(R) = p_a$ where p_a is atmospheric pressure. When this is combined with the definition of the second normal stress coefficient we find

$$\Psi_2 = (p_a - \pi_{\theta\theta}(R))/\dot{\gamma}^2 \tag{10.2-5}$$

Equation 10.2-4 may be integrated over the plate from R to r and combined with Eq. 10.2-5 to give

$$\begin{aligned}\pi_{\theta\theta} &= \pi_{\theta\theta}(R) - (\Psi_1 + 2\Psi_2)\dot{\gamma}^2 \ln\left(\frac{r}{R}\right) \\ &= p_a - \Psi_2\dot{\gamma}^2 - (\Psi_1 + 2\Psi_2)\dot{\gamma}^2 \ln\left(\frac{r}{R}\right)\end{aligned} \tag{10.2-6}$$

This result gives the radial distribution of the force per unit area measured by pressure transducers on the bottom plate.

(d) Total Thrust on the Lower Plate

The total thrust of the fluid on the plate minus the thrust associated with atmospheric pressure p_a is $\mathscr{F} = 2\pi \int_0^R \pi_{\theta\theta}\, rdr - \pi R^2 p_a$. Insertion of $\pi_{\theta\theta}$ from Eq. 10.2-6 then gives after integration

$$\boxed{\Psi_1 = \frac{2\mathscr{F}}{\pi R^2 \dot{\gamma}^2}} \tag{10.2-7}$$

Many commercially available cone-and-plate instruments are equipped to measure the total thrust $\mathscr{F}$, and thus it is possible to determine the first normal stress difference by means of Eq. 10.2-7. On a few instruments it is also possible to measure the local pressure distribution along the plate; for these devices both Ψ_1 and Ψ_2 can be measured.[6]

There are several assumptions that have been made in the derivations of the material functions given above that can introduce error into interpretation of experimental measurements.[1,6] First, the fluid inertia,[7] which tends to throw the fluid out of the gap, has been neglected. Consequently, when inertial effects are important the total thrust measured will be less than that given by Eq. 10.2-7 for the true first normal stress difference, and Ψ_1 will be underestimated. In practice, the best way to correct for the centrifugal force is to calibrate the instrument using Newtonian liquids. Inertial effects can also be accounted for approximately by theoretical means (see Problem 10B.3).

Second, the assumed rim condition is that the fluid–air interface is spherical, and experimentally this is not found exactly. The nonspherical free surface implies that the flow is not viscometric all the way to the edge of the instrument. However, varying the free surface shape does not seem to affect the total thrust measurements,[8] and errors associated with the nonspherical interface appear to be no more than 5%. To achieve reproducibility the cone-and-plate device is sometimes operated in a sea of liquid to avoid a free surface.

Third, for large cone angles and high speeds of rotation, secondary flows are observed in the gap as a result of the competing centrifugal and normal stress effects.[9] Secondary flows may occur for cone angles as small as 10°. If secondary flows are present, the overall fluid motion will not be viscometric and the analysis presented here is invalid.

Fourth, the temperature of the fluid in the gap may not be uniform due to viscous heating. An approximate analysis of nonisothermal effects in the cone-and-plate viscometer gives a maximum temperature rise within the gap[10]

$$(T - T_0)_{\max} = \frac{3\mathscr{T}W\vartheta_0}{16\pi kR} \tag{10.2-8}$$

[6] See, for example, S. Ramachandran, H. W. Gao, and E. B. Christiansen, *Macromolecules*, **18**, 695–699 (1985); H. W. Gao, S. Ramachandran, and E. B. Christiansen, *J. Rheol.*, **25**, 213–235 (1981); E. B. Christiansen and W. R. Leppard, *Trans. Soc. Rheol.*, **18**, 65–86 (1974).

A method that has been suggested for measuring Ψ_2 in a cone-and-plate geometry without small pressure transducers is to vary the gap between the cone and plate. See R. Jackson and A. Kaye, *Br. J. Appl. Phys.*, **17**, 1355–1360 (1966); B. D. Marsh and J. R. A. Pearson, *Rheol. Acta*, **7**, 326–331 (1968); K. Walters, *Rheometry*, Chapman and Hall, London (1975), pp. 56–58.

[7] Neglect of fluid inertia can also lead to errors in the measurement of small-amplitude oscillatory shear properties in the cone-and-plate geometry. The errors can be serious at high frequencies, particularly for η''. See K. Walters and R. A. Kemp in R. E. Wetton and R. W. Whorlow, eds., *Polymer Systems*, Macmillan, London (1968), pp. 237–250.

[8] E. Ashare, Ph.D. Thesis, University of Wisconsin, Madison (1968), pp. 50–52, 67–68, 105.

[9] H. Giesekus, *Rheol. Acta*, **4**, 85–101 (1965); W. H. Hoppmann II and C. E. Miller, *Trans. Soc. Rheol.*, **7**, 181–193 (1963); K. Walters and N. D. Waters in R. E. Wetton and R. W. Whorlow, eds., *Polymer Systems*, Macmillan, London (1968), pp. 211–235; R. M. Turian, *Ind. Eng. Chem. Fundam.*, **11**, 361–368 (1972).

[10] This result was obtained by R. B. Bird and R. M. Turian, *Chem. Eng. Sci.*, **17**, 331–334 (1961), by using a variational method.

where T_0 is the temperature at which the cone-and-plate surfaces are held constant, and k is the thermal conductivity of the fluid. Equation 10.2-8 can be used to estimate the importance of viscous heating; if a temperature rise of 1 or 2 K is predicted, then serious errors can result from use of the isothermal analysis presented here. Viscous heating for some simple non-Newtonian fluid models is discussed in §4.4.

Finally, there are other problems associated with polymer degradation,[11] melt fracture, bubble inclusion, solvent evaporation, possible slip at the wall, balling of the material, and alignment of the instrument that add uncertainty to the reported values.

EXAMPLE 10.2-2 Measurement of the Viscometric Functions in the Parallel-Disk Instrument

The parallel-disk system (Fig. 10.1-1) is very similar in operation to the cone-and-plate device discussed in the preceding example. As before, when the upper disk is rotated with constant angular velocity W, the torque $\mathscr{T}$ required to achieve this rotation as well as the total force $\mathscr{F}$ required to maintain the disks at a separation H, and the pressure distribution $(p + \tau_{zz})|_{z=0}$ across one of the plates can be measured. Show how to obtain the viscometric functions in terms of these measurements when inertial effects are unimportant. (See Problem 1B.5 for Newtonian flow in this system.)

SOLUTION **(a)** Governing Equations

We begin by postulating that a fluid plane of constant z rotates with an angular velocity $w(z)$ that depends on its position between the two disks. The velocity field is then $v_\theta = rw(z)$, $v_r = 0$, and $v_z = 0$; accordingly, the shear rate is $\dot\gamma = r\,dw/dz = rw'$. Unlike the cone-and-plate rheometer, the shear rate is not constant throughout the fluid. Since the flow is steady-state shearing, the CEF equation, Eq. 9.6-18, can be used as the constitutive equation.

To evaluate the stress tensor with the CEF equation, we need the following kinematic tensors derived from the postulated velocity field

$$\nabla \boldsymbol{v} = \begin{pmatrix} 0 & w & 0 \\ -w & 0 & 0 \\ 0 & rw' & 0 \end{pmatrix}; \qquad \boldsymbol{\gamma}_{(1)} = \dot\gamma \begin{pmatrix} 0 & 0 & 0 \\ 0 & 0 & 1 \\ 0 & 1 & 0 \end{pmatrix}; \qquad \dot\gamma = rw' \tag{10.2-9}$$

$$\boldsymbol{\gamma}_{(1)}^2 = \dot\gamma^2 \begin{pmatrix} 0 & 0 & 0 \\ 0 & 1 & 0 \\ 0 & 0 & 1 \end{pmatrix} \tag{10.2-10}$$

$$\boldsymbol{\gamma}_{(2)} = -2\dot\gamma^2 \begin{pmatrix} 0 & 0 & 0 \\ 0 & 1 & 0 \\ 0 & 0 & 0 \end{pmatrix} \tag{10.2-11}$$

When these contributions are assembled into the CEF equation the stress tensor is

$$\boldsymbol{\tau} = -\begin{pmatrix} 0 & 0 & 0 \\ 0 & (\Psi_1 + \Psi_2)\dot\gamma^2 & \eta\dot\gamma \\ 0 & \eta\dot\gamma & \Psi_2\dot\gamma^2 \end{pmatrix} \tag{10.2-12}$$

[11] J. M. Lipson and A. S. Lodge, *Rheol. Acta*, **7**, 364-379 (1968); W. G. Pritchard, *Phil. Trans. Roy. Soc. London*, **A270**, 507-556 (1971).

If fluid inertia and gravity are neglected, the equation of motion in cylindrical coordinates takes the form

$$r\text{-Component:} \qquad 0 = -\frac{\partial p}{\partial r} - \frac{(\Psi_1 + \Psi_2)\dot{\gamma}^2}{r} \tag{10.2-13}$$

$$\theta\text{-Component:} \qquad 0 = \frac{\partial}{\partial z}\eta\dot{\gamma} \tag{10.2-14}$$

$$z\text{-Component:} \qquad 0 = -\frac{\partial p}{\partial z} + \frac{\partial}{\partial z}\Psi_2\dot{\gamma}^2 \tag{10.2-15}$$

Equation 10.2-14 says that the shear stress, and hence the shear rate, is independent of z. Thus the expression for the shear rate given in Eq. 10.2-9 can be integrated to yield w, which in turn gives

$$v_\theta = \frac{rWz}{H} \tag{10.2-16}$$

Thus the shear rate is a function of r alone:

$$\dot{\gamma} = \frac{rW}{H} = \dot{\gamma}_R r/R \tag{10.2-17}$$

where $\dot{\gamma}_R = RW/H$ is the shear rate at the rim.

(b) The Viscosity

In order to find the viscosity of the sample, we consider the total torque $\mathscr{T}$ required to rotate the upper disk:

$$\begin{aligned}\mathscr{T} &= 2\pi\int_0^R (-r\tau_{z\theta})r\,dr \\ &= 2\pi\int_0^R \eta\dot{\gamma}r^2\,dr \\ &= \frac{2\pi R^3}{\dot{\gamma}_R^3}\int_0^{\dot{\gamma}_R}\eta(\dot{\gamma})\dot{\gamma}^3\,d\dot{\gamma}\end{aligned} \tag{10.2-18}$$

In going from the second to third line of Eq. 10.2-18 we have made the change of variable indicated by Eq. 10.2-17. Because of the inhomogeneity of the shear rate in torsional flow, the viscosity is not an explicit function of the applied torque. However by differentiating this last result with respect to $\dot{\gamma}_R$ we find[12]

$$\boxed{\eta(\dot{\gamma}_R) = \frac{(\mathscr{T}/2\pi R^3)}{\dot{\gamma}_R}\left[3 + \frac{d\ln(\mathscr{T}/2\pi R^3)}{d\ln\dot{\gamma}_R}\right]} \tag{10.2-19}$$

Thus by varying $\dot{\gamma}_R$ and computing the change in torque as indicated above, the viscosity may be determined explicitly.

[12] Use the "Leibniz formula" for differentiating an integral:

$$\frac{d}{dt}\int_{a_1(t)}^{a_2(t)} f(x,t)dx = \int_{a_1(t)}^{a_2(t)}\frac{\partial f}{\partial t}dx + f(a_2,t)\frac{da_2}{dt} - f(a_1,t)\frac{da_1}{dt} \tag{10.2-19a}$$

(c) The Radial Pressure Distribution

The r-component of the equation of motion suggests that we can get the sum of the first and second normal stress coefficients from the radial pressure distribution. To see this we integrate this equation from a position r to the rim $r = R$ to obtain

$$p(r) - p_a = \int_{\dot{\gamma}}^{\dot{\gamma}_R} (\Psi_1 + \Psi_2)\dot{\gamma}\, d\dot{\gamma} \tag{10.2-20}$$

where we have set $p(R) = p_a$, since $\tau_{rr} = 0$, and we have changed the integration variable from r to $\dot{\gamma}$. The quantity measured by pressure transducers along the bottom plate is π_{zz} rather than p, so we add τ_{zz} as given by the CEF equation to both sides of Eq. 10.2-20. The result is

$$\pi_{zz}(\dot{\gamma}) - p_a = \int_{\dot{\gamma}}^{\dot{\gamma}_R} (\Psi_1 + \Psi_2)\dot{\gamma}\, d\dot{\gamma} - \Psi_2\dot{\gamma}^2 \tag{10.2-21}$$

To obtain an explicit expression for the normal stress coefficients we evaluate this last result at the center of the disk ($\dot{\gamma} = 0$), and then differentiate the result with respect to $\dot{\gamma}_R$ as we did in Eq. 10.2-19. In this way we obtain

$$\frac{d}{d\dot{\gamma}_R}(\pi_{zz}(0) - p_a) = (\Psi_1(\dot{\gamma}_R) + \Psi_2(\dot{\gamma}_R))\dot{\gamma}_R \tag{10.2-22}$$

This shows how one combination of normal stresses can be obtained from measurements of π_{zz} at the center of the disk at different shear rates. Note that since the shear rate is zero at $r = 0$, then $\pi_{zz}(0)$ can be measured with a hole mounted pressure transducer without having to corrrect for the hole pressure.

(d) The Second Normal Stress Coefficient

The second normal stress coefficient can easily be found by evaluating Eq. 10.2-21 at the rim:

$$\pi_{zz}(R) - p_a = -\Psi_2(\dot{\gamma}_R)\dot{\gamma}_R^2 \tag{10.2-23}$$

Accurate measurement of the rim pressure $\pi_{zz}(R)$ requires use of flush-mounted pressure transducers or careful correction for the hole pressure if hole-mounted transducers are used.

(e) The Total Thrust on the Lower Plate

The total force $\mathscr{F}$ that must be applied to keep the disks from separating is found by integrating $\pi_{zz}(r) - p_a$ over the area of one of the disks. Using π_{zz} from Eq. 10.2-21 gives

$$\begin{aligned}
\mathscr{F} &= \frac{2\pi R^2}{\dot{\gamma}_R^2}\int_0^{\dot{\gamma}_R}\left[\int_{\dot{\gamma}}^{\dot{\gamma}}[\Psi_1(x) + \Psi_2(x)]x\,dx - \Psi_2(\dot{\gamma})\dot{\gamma}^2\right]\dot{\gamma}\, d\dot{\gamma} \\
&= \frac{2\pi R^2}{\dot{\gamma}_R^2}\left[\int_0^{\dot{\gamma}_R}\int_0^{x}[\Psi_1(x) + \Psi_2(x)]\dot{\gamma}\, d\dot{\gamma}\, x\,dx - \int_0^{\dot{\gamma}_R}\Psi_2(\dot{\gamma})\dot{\gamma}^3\, d\dot{\gamma}\right] \\
&= \frac{\pi R^2}{\dot{\gamma}_R^2}\int_0^{\dot{\gamma}_R}(\Psi_1 - \Psi_2)\dot{\gamma}^3\, d\dot{\gamma}
\end{aligned} \tag{10.2-24}$$

Solving Eq. 10.2-24 for the normal stress coefficients gives

$$\boxed{\Psi_1 - \Psi_2 = \frac{1}{\dot{\gamma}_R^2}\left(\frac{\mathscr{F}}{\pi R^2}\right)\left[2 + \frac{d\ln(\mathscr{F}/\pi R^2)}{d\ln\dot{\gamma}_R}\right]} \tag{10.2-25}$$

Thus in a parallel-disk rheometer, one can determine the non-Newtonian viscosity and both normal stress coefficients by varying the angular velocity of the upper disk and the separation of the disks.

EXAMPLE 10.2-3 Obtaining the Non-Newtonian Viscosity from the Capillary Rheometer

Show how the viscosity as a function of shear rate can be determined from measurements of volume flow rate and pressure drop in a capillary tube.

SOLUTION **(a)** The Shear Stress

It is not difficult to show from the equation of motion that for steady tube flow the shear stress varies linearly with distance from the center of the tube (see Example 4.2-1)

$$\tau_{rz} = \tau_R r/R \tag{10.2-26}$$

where τ_R is the shear stress at the tube wall and is given by

$$\tau_R = (\mathscr{P}_0 - \mathscr{P}_L)R/2L \tag{10.2-27}$$

Note that, unlike the situation for the rotational instruments discussed above, the inertial terms in the equation of motion are identically zero for the capillary viscometer. This means that the results from this example can be applied to obtain the viscosity irrespective of the flow rate, provided only that the flow is laminar.

(b) The Shear Rate[13]

The volume rate of flow is given by

$$Q = 2\pi \int_0^R v_z r \, dr \tag{10.2-28}$$

Integration by parts gives

$$Q = -\pi \int_0^R \left(\frac{dv_z}{dr}\right) r^2 \, dr = \pi \int_0^R \dot{\gamma} r^2 \, dr \tag{10.2-29}$$

In Eq. 10.2-29 we have introduced the shear rate $\dot{\gamma} = -dv_z/dr$. Next we change the variable of integration from r to τ_{rz} according to Eq. 10.2-26:

$$\left(\frac{Q}{\pi R^3}\right) = \frac{1}{\tau_R^3} \int_0^{\tau_R} \dot{\gamma} \tau_{rz}^2 \, d\tau_{rz} \tag{10.2-30}$$

The shear rate is to be regarded as a function of shear stress in this last equation. Equation 10.2-30 indicates that data taken in tubes of different lengths and radii should collapse onto a single curve when plotted as $(Q/\pi R^3)$ vs. τ_R. To obtain the desired expression for the shear rate at the wall, we differentiate Eq. 10.2-30 with respect to τ_R

$$\dot{\gamma}_R = \frac{1}{\tau_R^2} \frac{d}{d\tau_R} \left[\tau_R^3 \frac{Q}{\pi R^3} \right] \tag{10.2-31}$$

[13] K. Weissenberg as cited by B. Rabinowitsch, *Z. Phys. Chem.*, **A145**, 1–26 (1929), and R. Eisenschitz, *Kolloid-Z.*, **64**, 184–195 (1933).

This well-known result is sometimes called the "Weissenberg–Rabinowitsch equation." It tells how the wall shear rate $\dot{\gamma}_R$ can be obtained by differentiating pressure drop-flow rate data. Once $\dot{\gamma}_R$ and τ_R are known the viscosity is easily found to be

$$\eta(\dot{\gamma}_R) = \frac{\tau_R}{\dot{\gamma}_R} = \frac{\tau_R}{(Q/\pi R^3)}\left[3 + \frac{d \ln (Q/\pi R^3)}{d \ln \tau_R}\right]^{-1} \tag{10.2-32}$$

Equation 10.2-32 gives the viscosity as a function of shear rate at the wall. If we in addition assume that $\eta(\dot{\gamma}_R)$ obtained at the wall is the same as $\eta(\dot{\gamma})$ throughout the tube, then Eq. 10.2-32 can be used to plot $\eta(\dot{\gamma})$. This assumption appears to be valid for typical polymeric fluids. However, for fluids where the wall may cause changes in the microstructure, for example, preferential orientation of fibers in suspensions of long fibers, Eq. 10.2-32 may not yield information about the viscosity away from the wall.

(c) End Effects

We now know how to calculate the viscosity, given data on the volume flow rate and pressure gradient for fully developed steady shear flow in a tube. The volume rate of flow is obtained in standard capillary viscometer measurements; however, the steady shear flow pressure gradient needed to compute the wall shear stress is not. Figure 10.2-2 illustrates a typical experimental arrangement for this instrument. The test fluid is pushed from a reservoir (barrel) through the tube by a ram which is driven at a specified constant velocity. The load on the ram, and thus the pressure p in the fluid

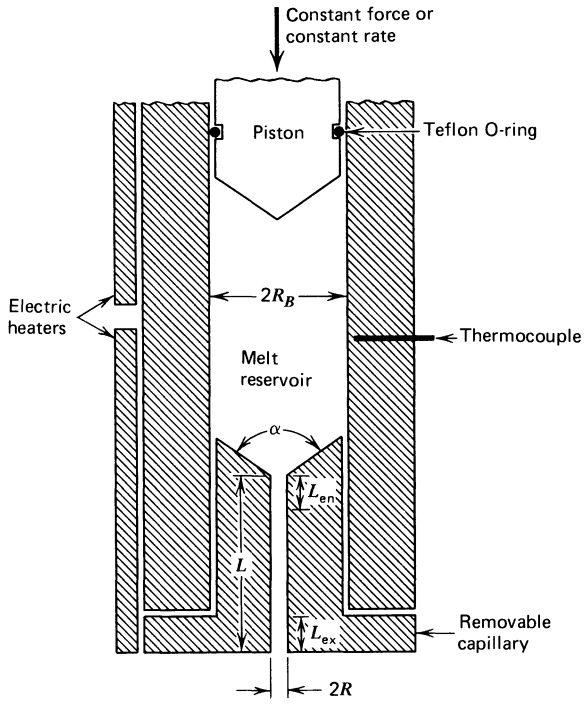

FIGURE 10.2-2. Schematic diagram of a capillary viscometer. The capillary test section is a tube of length L and radius R. Polymer is maintained in a fluid state in an upstream barrel of radius R_B; the converging, transition region between the barrel and capillary has an included angle α. The steady shear flow velocity profile develops over an entrance length L_{en}; the exit may disturb the fully developed velocity profile over a distance L_{ex} from the capillary end.

adjacent to the ram, is the measured pressure. Thus, in order to use the formulas just developed we must know how to compute the steady shear flow pressure gradient (or equivalently τ_R) from p.

The desired wall shear stress can be obtained by performing two experiments,[14] one with a capillary of length L_A attached to the barrel and the other with a capillary of length L_B. Both capillaries have radius R and are longer than the sum of the entrance length L_{en} required for the establishment of fully developed velocity profiles and the exit length L_{ex} over which the velocity profiles may be influenced by the end of the tube. This requirement ensures that there will be steady shear flow in some section of each capillary. The ram pressures p_A and p_B are then measured for the two capillaries for the same volume flow rate Q. The pressure gradient that exists in the steady shear flow portions of the two capillaries may then be computed by applying the macroscopic mechanical energy balance[15] to the two systems (see Problem 10C.1). By subtracting these two results, one can show that

$$\tau_R = \left[\frac{p_B - p_A}{L_B - L_A} + \underline{\rho g \cos\beta}\right]\frac{R}{2} = -\left(\frac{d\mathscr{P}}{dz}\right)\frac{R}{2} \qquad \begin{matrix} L_A > L_{en} + L_{ex} \\ L_B > L_{en} + L_{ex} \end{matrix} \tag{10.2-33}$$

where β is the angle between the tube axis and the vertical. This is then the corrected wall shear stress to be used with a flow rate Q through a capillary tube of radius R. On the right-hand side of Eq. 10.2-33, $d\mathscr{P}/dz$ is the constant pressure gradient corresponding to τ_R. Under ordinary operating conditions, the gravitational (dashed-underlined) term is negligible and $d\mathscr{P}/dz$ is very nearly equal to dp/dz. It is customary to measure the ram pressure for a series of tubes of radius R and different lengths L. The steady shear flow pressure gradient is then found from the slope of the linear region of a plot of p vs. L by replacing $(p_B - p_A)/(L_B - L_A)$ by dp/dL. The linear region is usually reached by L/R of about 10.

In addition to end effects, viscous dissipation heating, fluid compressibility, change of viscosity with pressure, and flow instabilities can introduce errors into capillary viscometer measurements. The temperature rise associated with viscous dissipation can be reduced by using a smaller diameter capillary, since for shear-thinning fluids the rate of heat conduction to the wall increases more rapidly than viscous heat generation with decreasing tube radius. The influence of pressure on viscosity can be seen as a concave-up shape to the pressure drop versus L/D curve at large L/D. If this upward curvature is observed it is necessary to use shorter or wider capillaries. At present, the best practice is to design and operate the viscometer so that these effects can be minimized.

§10.3 SHEARFREE FLOWS[1]

Methods for measuring material functions are not nearly so well developed for shearfree flows as for shearing flows. The primary difficulty is that of mechanically generating the flow because of the fact that in steady shearfree flow, neighboring particles move apart exponentially in time (cf. Eq. 3.1-4). This difficulty has led to many approximate methods for measuring shearfree flow material functions.

It is convenient to divide the measurement techniques for shearfree flows into those methods that yield material functions defined in Chapter 3 and those that do not.[2] We

[14] B. A. Toms in F. R. Eirich, ed., *Rheology*, Vol. 2, Academic Press (1958), pp. 475–501. The correction given in Eq. 10.2-33 was first suggested by Couette.

[15] A. G. Fredrickson, *Principles and Applications of Rheology*, Prentice-Hall, Englewood Cliffs, NJ (1964), pp. 196–200.

[1] For recent reviews of experimental methods for measuring shearfree flow material functions, see J. Meissner, *Chem. Eng. Commun.*, **33**, 159–180 (1985); *Ann. Rev. Fluid Mech.*, **17**, 45–64 (1985). We have drawn heavily on these reviews in this section.

[2] The terms *controllable* and *noncontrollable* have also been used to categorize shearfree flow experiments by F. Nazem and C. T. Hill, *Trans. Soc. Rheol.*, **18**, 87–101 (1974); see also K. Walters, *Rheometry*, Chapman and Hall, London (1975). These terms have also been applied with a different meaning to the description of shear flows by A. C. Pipkin, *Quart. Appl. Math.*, **26**, 87–100 (1968) and A. C. Pipkin and R. I. Tanner, *Mech. Today*, **1**, 262–321 (1972).

introduce this distinction here because, unlike the situation for shear flows where there are numerous methods available for measuring material functions of a wide variety of polymeric liquids, techniques for measuring the kinds of shearfree flow material functions defined in Chapter 3 have been developed only for polymer melts and high-viscosity solutions. Thus complex flows that are predominantly shearfree flows have been used to obtain qualitative information about the shearfree flow properties of low-viscosity polymer solutions.

We first consider uniaxial elongational flows given by Eq. 3.1-3 with $b = 0$ and $\dot{\varepsilon} > 0$. Then in the following two subsections, we look at methods for generating biaxial stretching flow (Eq. 3.1-3 with $b = 0$ and $\dot{\varepsilon} < 0$) and general shearfree flows (Eq. 3.1-3 with arbitrary b).

a. Uniaxial Elongational Flow ($b = 0$, $\dot{\varepsilon} > 0$)

We begin by discussing methods that yield material functions for uniaxial elongational flows. Two basic methods have been used for this purpose: one in which the ends of the sample are clamped and the clamps separated so as to generate either a known elongation rate or a known tensile stress in the material; and the second in which known velocities are applied to two places along the sample so as to achieve a controlled elongation rate or tensile stress.

The first method in which fixed ends are clamped is similar to the operation of a tensile testing apparatus. It is necessary, of course, that the cross head that moves the clamp(s) be programmable. In order to perform start-up of steady-state elongational flow the clamps must be separated exponentially in time. The most serious restriction resulting from this exponential motion is that only modest (Hencky) strains $\varepsilon_{max} = \dot{\varepsilon} t_{max} = \ln(L_{max}/L_0)$ can be achieved because of the size limitations of the instrument. Here L_0 and L_{max} are the initial and maximum sample lengths. For vertical configurations the sample must be surrounded by a density matching medium which also serves to maintain temperature uniformity. It is necessary to be sure that this surrounding fluid does not interact chemically with the test specimen over the time scale of the experiments. Figure 10.3-1 shows two examples of this type of elongational viscometer.[3,4] In one, a cam is used to vary the force on the sample in such a way that the tensile stress remains constant; the other uses a servocontrolled motor to achieve either fixed kinematics or, through feedback control, a constant stress. Total extension ratios L_{max}/L_0 of 50, corresponding to $\varepsilon_{max} = 3.9$, have been achieved with this latter device.[5] A variation on the configurations shown in Fig. 10.3-1 has been used in which the sample is floated horizontally on a supporting liquid.[6] The horizontal configuration does not require the density of the supporting liquid to be matched as closely to that of the sample as does the vertical arrangement.

The second arrangement for generating a uniaxial elongational flow is illustrated in Fig. 10.3-2. The sample is floated horizontally on a supporting liquid that does not interact chemically with it. The elongation is produced by one or two sets of counter-rotating gears through which the sample is pulled.[7] Since the gears do not move relative to one another,

[3] F. N. Cogswell, *Plast. Polym.*, **36**, 109–111 (1968).

[4] H. Münstedt, *Rheol. Acta*, **14**, 1077–1088 (1975); *J. Rheol.*, **23**, 421–436 (1979).

[5] H. M. Laun and H. Münstedt, *Rheol. Acta*, **15**, 517–524 (1976).

[6] G. V. Vinogradov, B. V. Radushkevich, and V. D. Fikhman, *J. Polym. Sci. Part A-2*, **8**, 1–17 (1970); G. V. Vinogradov, V. D. Fikhman, and B. V. Radushkevich, *Rheol. Acta*, **11**, 286–291 (1972); A. Franck and J. Meissner, *Rheol. Acta*, **23**, 117–123 (1984).

[7] J. Meissner, *Rheol. Acta*, **10**, 230–242 (1971); *Trans. Soc. Rheol.*, **16**, 405–420 (1972); J. Meissner, T. Raible, and S. E. Stephenson, *J. Rheol.*, **25**, 1–28 (1981).

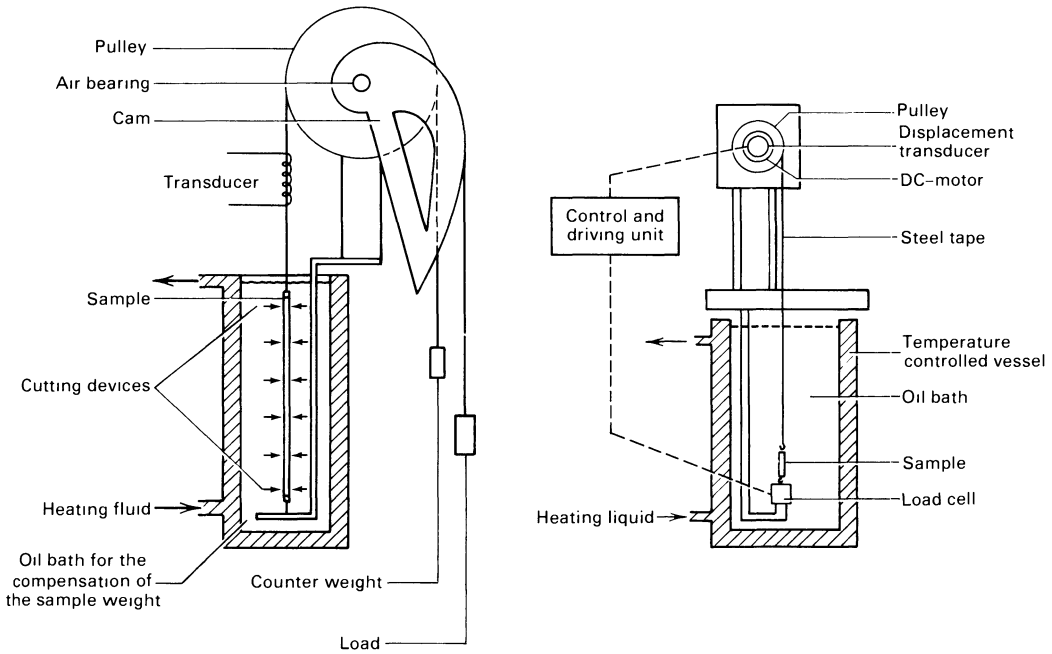

FIGURE 10.3-1. Schematic diagrams for two devices used to generate uniaxial elongational flows by separating clamped ends of the sample. The device on the left uses a cam to maintain mechanically a constant tensile stress on the sample. [H. Münstedt, *Rheol. Acta*, **14**, 1077-1088 (1975).] The device on the right uses a servocontrol system to maintain either a specified (positive) elongation rate or a specified tensile stress. [H. Münstedt, *J. Rheol.*, **23**, 421-436 (1979).]

this method has the advantage over the geometries in Fig. 10.3-1 that the maximum strain ε_{max} is not device-limited. Hencky strains ε_{max} as large as seven (corresponding to an extension ratio L_{max}/L_0 of 1100) have been obtained.[8] The disadvantage of the rotating gear method relative to the moving clamps is that larger samples are required. This is a serious limitation inasmuch as the samples must be very nearly free of inhomogeneities.

With either of the two methods, analysis of the force-extension data to obtain the elongational material functions is straightforward. We assume that the surroundings are at

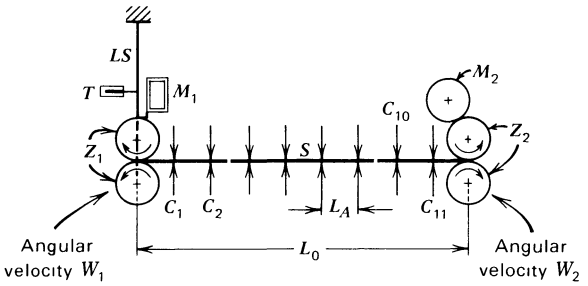

FIGURE 10.3-2. Schematic diagram of an elongational viscometer which uses two sets of rotary clamps (Z_1 and Z_2) to elongate the sample (S). The clamps are driven by two independent motors (M_1 and M_2) at constant rotation rates W_1 and W_2. The force in the sample is measured by the transducer (T) mounted on a leaf spring (LS). At the end of the test the sample can be cut into small segments by the scissors C_i in order to test for uniformity of the elongation throughout the sample and to obtain the true strain rate for the test. [J. Meissner, *Rheol. Acta*, **10**, 230-242 (1971).]

[8] J. Meissner, T. Raible and S. E. Stephenson, *op. cit.*

atmospheric pressure p_a. The total force per unit area exerted by the load cell and atmospheric pressure on the sample must be balanced by π_{zz}. Thus if the load cell indicates a tensile force F:

$$\pi_{zz} = -(F(t)/A(t)) + p_a \tag{10.3-1}$$

where A is the instantaneous cross-sectional area of the sample. A force balance in the radial direction gives

$$\pi_{rr} = p_a \tag{10.3-2}$$

Subtracting these last two results gives the normal stress difference as a function of time

$$\boxed{\tau_{zz} - \tau_{rr} = -F(t)/A(t)} \tag{10.3-3}$$

The material functions can then be calculated from the normal stress difference. For example, in start-up of steady elongational flow with elongation rate $\dot{\varepsilon}_0$, the cross-sectional area varies with time according to $A(t) = A_0 e^{-\dot{\varepsilon}_0 t}$, where A_0 is the initial cross-sectional area of the sample, and we have

$$\bar{\eta}^+ = \frac{F(t)e^{\dot{\varepsilon}_0 t}}{A_0 \dot{\varepsilon}_0} \tag{10.3-4}$$

This expression makes it clear that when steady state is reached, F will be an exponentially decreasing function of time and will thus become very difficult to measure at large strains.

Particularly for large strains ($\varepsilon > 4$), extreme care must be taken to be sure that the sample is deformed homogeneously.[8] This can be checked by cutting the sample into small sections of uniform length at the end of the test, and then weighing them to check for uniformity. Small errors in strain rate are found to be amplified in the stress as strain is increased. It is also found that temperature uniformity must be maintained to within 0.1 °C throughout the rheometer to achieve uniform elongations. In addition interfacial tension between the sample and supporting fluid can be important for low-strain-rate experiments[9] and for recovery experiments.[8]

Both of the test methods described above are limited to polymer melts. In order to investigate the elongational properties of polymer solutions, a variety of experiments have been used that do not yield the material functions defined in Chapter 3. These include fiber spinning,[10] the tubeless siphon,[11] converging flow,[12] and the triple-jet method.[13]

[9] H. M. Laun and H. Münstedt, *Rheol. Acta*, **17**, 415-425 (1978).

[10] J. Ferguson and K. Missaghi, *J. Non-Newtonian Fluid Mech.*, **11**, 269-281 (1982); N. E. Hudson, J. Ferguson, and P. Mackie, *Trans. Soc. Rheol.*, **18**, 541-562 (1974); J. Mewis and A. B. Metzner, *J. Fluid Mech.*, **62**, 593-600 (1974); J. A. Spearot and A. B. Metzner, *Trans. Soc. Rheol.*, **16**, 495-518 (1972); D. Acierno, J. N. Dalton, J. M. Rodriguez, and J. L. White, *J. Appl. Polym. Sci.*, **15**, 2395-2415 (1971). See also Example 7.4-3.

[11] S. T. J. Peng and R. F. Landel in G. Astarita, G. Marrucci, and L. Nicolais, eds., *Rheology*, Vol. 2, Plenum Press, New York (1980), pp. 385-391; S. T. J. Peng and R. F. Landel, *J. Appl. Phys.*, **47**, 4255-4260 (1976); J. R. A. Pearson and T. J. F. Pickup, *Polymer*, **14**, 209-214 (1973); F. A. Kanel, Ph.D Thesis, University of Delaware, Newark (1972); G. Astarita and L. Nicodemo, *Chem. Eng. J.*, **1**, 57-00 (1970). See also §2.5b.

[12] T. Kizior and F. A. Seyer, *Trans. Soc. Rheol.*, **18**, 271-285 (1974); D. R. Oliver and R. Bragg, *Can. J. Chem. Eng.*, **51**, 287-290 (1973); D. R. Oliver, *Chem. Eng. J.*, **6**, 265-271 (1973); F. N. Cogswell, *Polym. Eng. Sci.*, **12**, 64-73 (1972); A. P. Metzner and A. B. Metzner, *Rheol. Acta*, **9**, 174-181 (1970); G. Marrucci and R. E. Murch, *Ind. Eng. Chem. Fundam.*, **9**, 498-499 (1970); H. Giesekus, *Rheol. Acta*, **7**, 127-138 (1968); **8**, 411-421 (1969); A. B. Metzner, E. A. Uebler, and C. F. Chan Man Fong, *AIChE J.*, **15**, 750-758 (1969).

[13] R. Bragg and D. R. Oliver, *Nature*, **241**, 371 (1973); D. R. Oliver and R. Bragg, *Rheol. Acta*, **13**, 830-835 (1974).

b. Biaxial Stretching Flow ($b = 0$, $\dot{\varepsilon} < 0$)

Several methods have been used to obtain biaxial stretching flow for polymer melts: sheet inflation, axisymmetric stagnation flow, lubricated squeezing flow, and sheet stretching. All of these experiments yield shearfree flow material functions.

In the sheet inflation method, a circular sample is clamped around its perimeter and then inflated by applying a differential pressure to the two sides. Both inert gas[14] and silicone oil[15] have been used to inflate the bubble. A biaxial stretching flow occurs in the region near the pole of the bubble, and the elongation rate is determined by measuring the deformation of a grid printed on the sample. By controlling the applied pressure, either a constant stress or constant elongation rate can be achieved.

An axisymmetric stagnation flow, obtained by impinging two polystyrene melt streams through lubricated hyperboloid-shaped walls, has been used to obtain constant elongation rates in biaxial stretching.[16] Birefringence was used to determine the stresses.

The two most promising techniques at this time for biaxial stretching measurements appear to be lubricated squeezing flow[17] and film stretching with rotary clamps. These are illustrated in Figs. 10.3-3 and 4. The rotary clamp method will be discussed in the next subsection on general shearfree flows. The lubricated squeeze flow is accomplished by placing a disk of polymer sample of radius R_0 in the center of two lubricated plates of radius $R(> R_0)$. The lubricant is chosen so that its viscosity is between 500 and 1000 times smaller than the zero-shear-rate viscosity of the polymer melt at the test temperature. After the

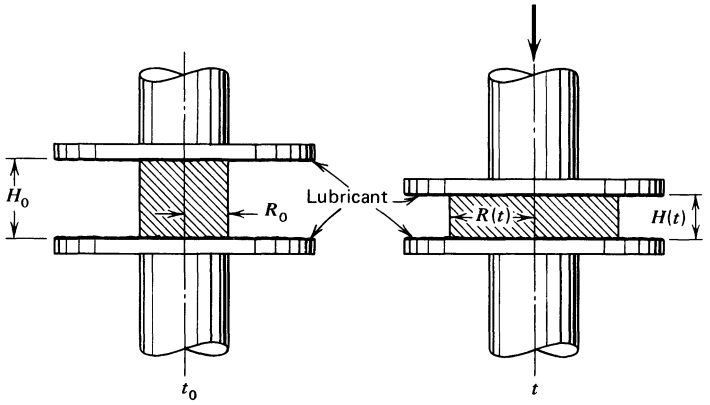

FIGURE 10.3-3. Lubricated squeeze flow device used to generate biaxial stretching flow. The left side of the figure (t_0) shows the initial configuration of the sample; the right side shows the sample at some other time $t > t_0$. The top plate can be driven downward at a programmable rate and the total normal force on the bottom plate measured. [P. R. Soskey and H. H. Winter, *J. Rheol.*, **29**, 493-517 (1985).]

[14] C. D. Denson and R. J. Gallo, *Polym. Eng. Sci.*, **11**, 174-176 (1971); D. D. Joye, G. W. Poehlein, and C. D. Denson, *Trans. Soc. Rheol.*, **16**, 421-449 (1972); **17**, 287-302 (1973); E. D. Baily, *Trans. Soc. Rheol.*, **18**, 635-640 (1974); J. M. Maerker and W. R. Schowalter, *Rheol. Acta*, **13**, 627-638 (1974); A. J. DeVries, C. Bonnebat, and J. Beautemps, *J. Polym. Sci. Polym. Symp.*, **58** 109-156 (1977).

[15] C. D. Denson and D. C. Hylton, *Polym. Eng. Sci.*, **20**, 535-539 (1980); J. Rhi-Sausi and J. M. Dealy, *Polym. Eng. Sci.*, **21**, 227-232 (1981).

[16] J. A. van Aken and H. Janeschitz-Kriegl, *Rheol. Acta*, **19**, 744-752 (1980); **20**, 419-432 (1981); H. H. Winter, C. W. Macosko, and K. E. Bennet, *Rheol. Acta.*, **18**, 323-334 (1979).

[17] S. Chatraei, C. W. Macosko, and H. H. Winter, *J. Rheol.*, **25**, 433-443 (1981).

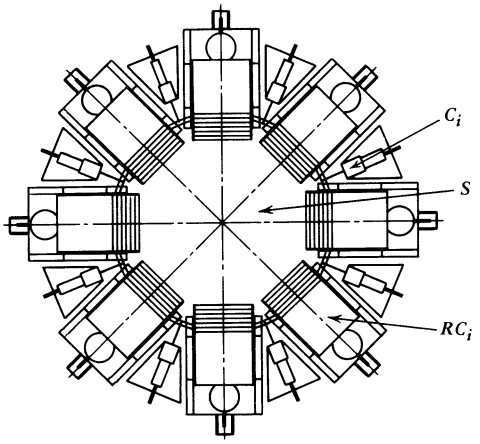

(*a*)

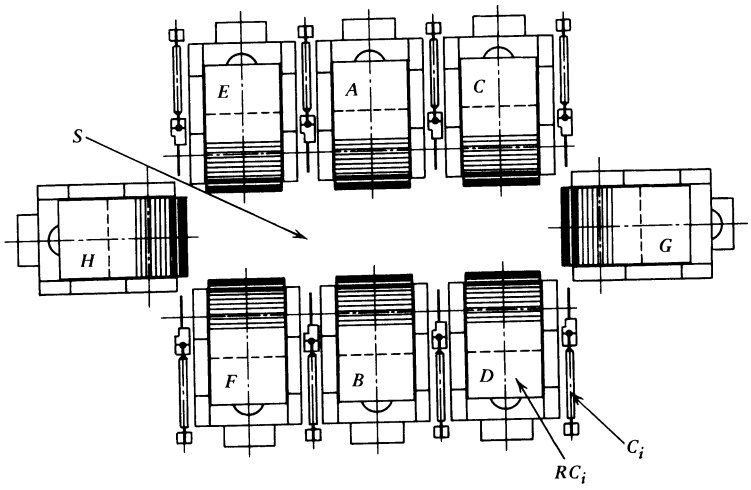

(*b*)

FIGURE 10.3-4. Two arrangements of the rotary clamp device which can be used to generate a wide variety of shearfree flows. The rotary clamps RC_i are capable of pulling the sample S at a programmed rate and of measuring the force in the direction of pulling. Scissors C_i located between the clamps are used to cut sample after it has been pulled outside the central region outlined by the clamps. (*a*) The rotary clamps are located in a circular arrangement and all driven at the same rate to produce biaxial stretching flow ($b = 0$, $\dot{\varepsilon} < 0$). (*b*) The clamps are located in a rectangular arrangement. By rotating clamps A–F and keeping G and H fixed, planar elongational flow ($b = 1$) can be achieved. [J. Meissner, *Chem. Eng. Commun.*, **33**, 159–180 (1985).]

sample is melted, squeezing is produced by moving the top plate downward in a programmable manner. The elongation rate is given by

$$\dot{\varepsilon} = \frac{1}{H}\frac{dH}{dt} \tag{10.3-5}$$

(note that $\dot{\varepsilon}$ is negative) so that to achieve a constant elongation rate, the gap H between the two plates must decrease exponentially in time. Since the sample is surrounded by atmospheric pressure, the normal stress difference $\tau_{zz} - \tau_{rr}$ is given by the total downward force F on the bottom plate by

$$\boxed{\tau_{zz} - \tau_{rr} = \frac{F(t)}{\pi[R(t)]^2}} \tag{10.3-6}$$

provided that the radius $R(t)$ of the deforming sample is less than the radius of the plates. Once the sample fills the region between the two plates, the plate radius is substituted for $R(t)$ in Eq. 10.3-6. Equations 10.3-5 and 6 can be combined to calculate biaxial stretching material functions (cf. Table 3.5-1) for specific $\dot{\varepsilon}(t)$. This geometry has proven particularly convenient for step strain stress relaxation experiments[18] after a suddenly applied strain ε:

$$\varepsilon = \ln\left(\frac{H}{H_0}\right) \tag{10.3-7}$$

where H_0 and H are the gaps before and after the strain is applied. The lubricated squeeze flow is a particularly simple design and has the advantages of small sample size and ability to cover a wide range of temperatures for polymer melts.

c. General Shearfree Flow (Arbitrary b)

The only currently available method for generating well defined, variable shearfree flows is one in which a sheet of polymer is stretched along its periphery by means of specially designed rotary clamps.[19] This device is illustrated in Fig. 10.3-4 in two configurations capable of generating biaxial stretching and planar elongational flow; other configurations have also been used to produce different values of b. It is also possible to pivot the clamps during the experiment and thus generate a shearfree flow with b and $\dot{\varepsilon}$ both functions of time.

§10.4 COMPLEX FLOWS

It is not always possible to measure material functions in one of the well-defined geometries described in the previous sections. For example, we have pointed out that it is presently impossible to measure elongational flow properties of polymer solutions in geometries where either the stresses or the velocity field can be precisely controlled.

[18] P. R. Soskey and H. H. Winter, *J. Rheol.*, **29**, 493–517 (1985); A. C. Papanastasiou, L. E. Scriven, and C. W. Macosko, *J. Rheol.*, **27**, 387–410 (1983).

[19] J. Meissner, *Chem. Eng. Commun.*, **33**, 159–180 (1985); J. Meissner, *Ann. Rev. Fluid Mech.*, **17**, 45–64 (1985); J. Meissner, S. E. Stephenson, A. Demarmels, and P. Portmann, *J. Non-Newtonian Fluid Mech.*, **11**, 221–237 (1982).

Similarly sample fracture often prohibits the use of the cone-and-plate or parallel-plate instruments at shear rates high enough for normal stresses to be appreciable. The capillary viscometer fails to provide data on the low-shear-rate viscosity behavior or to give any normal stress information at all.

Shortcomings such as these of standard instruments coupled with the practical necessity of having some material measurements (even though perhaps qualitative in nature), particularly on the "elastic" properties of polymeric fluids, have fostered the use of a variety of "complex" flows for rheological characterization. By complex we mean that the measureable features of the flow and stress fields cannot be related to the material functions defined in Chapter 3 without an unjustified, a priori assumption about the constitutive equation. This is in contrast to the situation we have dealt with in the previous sections where either no constitutive equation had to be assumed (e.g., the capillary viscometer) or the flow was simple enough so that an exact constitutive equation was known (e.g., the CEF equation for the parallel-plate instrument in steady shear flow). Generally, the complexity in the flow results from its being nonhomogeneous and from its involving some mixture of shear and shearfree flow.

As one example we cite the falling-ball viscometer which is a standard device for measuring the viscosity of Newtonian fluids (by means of Eq. 1.4-31).[1] Creeping flow around a sphere is very complicated, inasmuch as it is nonhomogeneous, is unsteady from the material point of view, and contains elements of both shear and shearfree flows. However, for very small Deborah numbers (De $= \lambda v_\infty / R$, where λ is a characteristic time for the fluid; v_∞, the terminal velocity of the sphere; and R, the sphere radius), it is reasonable to expect that we might be able to extract information on the zero-shear-rate properties from this experiment. This is because for very small De we can use the retarded-motion expansion. In the limit De $= 0$, the Newtonian fluid is recovered and when the first-order terms in De are retained, the second-order fluid, whose constants are simply related to the zero-shear-rate viscometric functions, is obtained (see §6.2).

When wall effects can be neglected, the perturbation analysis of Leslie[2] can be used to calculate the zero-shear-rate viscosity in terms of the terminal velocity of the sphere (see Problem 7A.2). The result of Leslie can also be used to estimate a characteristic time for the fluid if the liquid is assumed to be described by a convected Maxwell model. An empirical approach to estimating a time constant from falling-ball viscometry is also available.[3]

In typical laboratory implementations of the falling-ball viscometer, the walls and bottom of the fluid container can substantialy influence the terminal velocity of the sphere. Wall corrections to the equations for determining the viscosity can be appreciably larger in non-Newtonian fluids than in Newtonian fluids.[4] As was shown in Example 8.5-2, numerical simulations for a sphere falling through a viscoelastic fluid in a cylinder can be very useful in obtaining the zero-shear-rate viscometric functions. There comparison of numerical simulations[5] with experimentally measured terminal velocities allowed quantitative determination of η_0 and $\Psi_{1,0}$. Present methods are not capable of yielding information

[1] A description of many of the standard techniques for measuring μ for Newtonian fluids is contained in J. R. Van Wazer, J. W. Lyons, K. Y. Kim, and R. E. Colwell, *Viscosity and Flow Measurement*, Wiley, New York (1963). See also R. W. Whorlow, *Rheological Techniques*, Ellis Horwood, Chichester, UK (1980).

[2] F. M. Leslie, *Q. J. Mech. Appl. Math.*, **14**, 36-48 (1961); erratum: H. Giesekus, *Rheol. Acta*, **3**, 59-71 (1963), p. 69, footnote 16. See also K. Adachi, N. Yoshioka, and K. Sakai, *J. Non-Newtonian Fluid Mech.*, **3**, 107-125 (1977/78).

[3] Y. I. Cho and J. P. Hartnett, *Lett. Heat Mass Transfer*, **6**, 335-342 (1979); Y. I. Cho, J. P. Hartnett, and W. Y. Lee, *J. Non-Newtonian Fluid Mech.*, **15**, 61-74 (1984).

[4] Y. I. Cho, J. P. Hartnett, and E. Y. Kwack, *Chem. Eng. Commun.*, **6**, 141-149 (1980). A theoretical analysis of wall effects is given by B. Caswell, *Chem. Eng. Sci.*, **25**, 1167-1176 (1970). For an experimental study see M. Gottlieb, *J. Non-Newtonian Fluid Mech.*, **6**, 97-109 (1979).

[5] O. Hassager and C. Bisgaard, *J. Non-Newtonian Fluid Mech.*, **12**, 153-164 (1983).

outside of the zero-shear-rate regime.[6] Numerical simulation techniques have also been developed for flow of a Bingham plastic around a sphere,[7] and these methods could be used to determine the viscosity and yield stress of a Bingham plastic by means of falling-ball viscometry.

A closely related geometry is the rolling-ball viscometer.[8] A rolling-ball viscometer consists of an inclined tube containing a sphere whose diameter is slightly smaller than the diameter of the tube (see Fig. 10.4-1). For a power-law fluid the following formula[9] has been derived to allow the power-law constants m and n to be determined from the speed V with which the ball rolls down the tube inclined at an angle β with respect to the horizontal:

$$\tfrac{1}{3}(2R)^{n+1}(\rho_s - \rho)g \sin\beta = m\left[\pi V\left(\frac{2n+1}{n}\right)\right]^n \left(\frac{R}{R-r}\right)^{2n+(1/2)} J_n \tag{10.4-1}$$

where R and r are the tube and sphere radii, respectively, and ρ_s and ρ are the densities of the sphere and fluid. The quantities J_n are

$$J_n = 2\int_0^\infty \frac{d\xi}{[I_n(\xi^2)]^n} \tag{10.4-2}$$

where

$$I_n(\alpha) = \int_{-\pi}^{\pi} (\cos^2 \tfrac{1}{2}\theta + \alpha)^{2+(1/n)}\, d\theta \tag{10.4-3}$$

An extensive table of J_n has been prepared by Sestak and Ambros.[10] A few sample values are given in Table 10.4-1. Equation 10.4-1 has been found to be satisfactory for aqueous solutions of carboxymethylcellulose and polyacrylamide.[9]

Still other geometries have been used. Several additional systems suggested for determining the second-order fluid constants (and thus η_0, $\Psi_{1,0}$, and $\Psi_{2,0}$) are listed in Table 6.5-1. These include rod-climbing, radial flow between parallel disks, and flow around a rotating sphere. The falling cylinder viscometer is discussed in Problem 1C.2.

Finally we mention the parallel-plate plastometer which involves squeezing flow between parallel disks. This system has been shown in Examples 1.3-5 and 4.2-7 to be useful in obtaining the viscosity of a Newtonian fluid and the power-law constants m and n. In Example 10.4-1 we show that this system can also be used to obtain information about the normal stresses under fast squeezing conditions.

[6] R. P. Chhabra, P. H. T. Uhleherr, and D. V. Boger, *J. Non-Newtonian Fluid Mech.*, **6**, 187–199 (1980).
[7] A. N. Beris, J. A. Tsamopoulos, R. C. Armstrong, and R. A. Brown, *J. Fluid Mech.*, **158**, 219–244 (1985).
[8] J. R. Van Wazer, J. W. Lyons, K. Y. Kim, and R. E. Colwell, *op. cit.*, pp. 276–281.
[9] R. B. Bird and R. M. Turian, *Ind. Eng. Chem. Fundam.*, **3**, 87 (1964). The corresponding formula for a Newtonian fluid with viscosity μ was given by H. W. Lewis, *Anal. Chem.*, **25**, 507–508 (1953)

$$\mu = \frac{4}{9\pi J}\frac{R^2(\rho_s - \rho)g\sin\beta}{V}\left(\frac{R-r}{R}\right)^{5/2} \tag{10.4-1a}$$

where J is a constant:

$$J = \frac{4}{3}\left[\sqrt{2} - \frac{1}{\sqrt{5}}(\sqrt{10}+2)^{1/2}\right] = 0.531 \tag{10.4-2a}$$

[10] J. Šesták and F. Ambros, *Rheol. Acta*, **12**, 70–76 (1973).

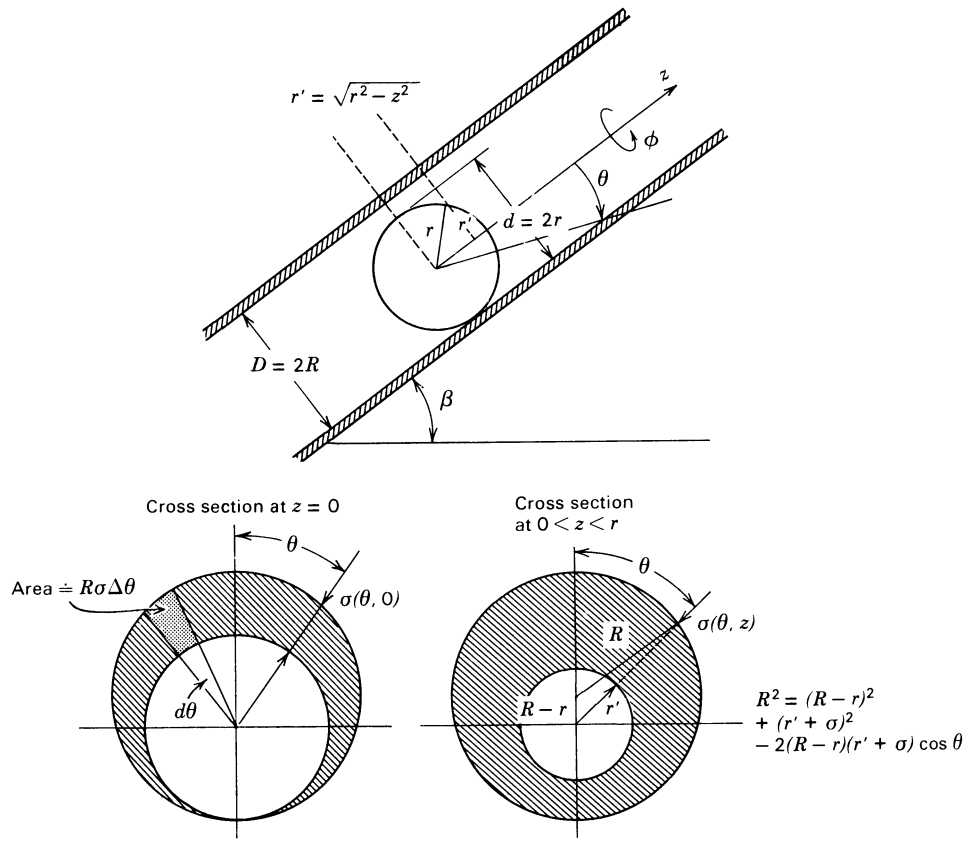

FIGURE 10.4-1 The rolling-ball viscometer. A tightly fitting ball of radius r rolls inside of a tube of radius R filled with fluid. The tube makes an angle β with the horizontal. The local gap $\sigma(\theta, z)$ between the sphere surface and tube wall is given approximately by

$$\sigma \doteq 2(R - r)\left[\cos^2 \tfrac{1}{2}\theta + \frac{R - \sqrt{R^2 - z^2}}{2(R - r)}\right]$$

TABLE 10.4-1

Values of the Quantity J_n Defined by Eq. 10.4-2 as a Function of the Power-Law Index n

n	J_n
0.20	1.8698
0.30	1.5317
0.40	1.2778
0.50	1.0812
0.60	0.9249
0.70	0.7979
0.80	0.6930
0.90	0.6052
1.00	0.5308

EXAMPLE 10.4-1. Squeezing Flow of Viscoelastic Fluids between Parallel Disks[11]

A viscoelastic liquid is contained in the gap between two parallel disks that are initially separated by a gap $2h_0$ (see Fig. 1.3-5). A constant normal force F is applied to the plates to cause the fluid in the gap to be squeezed out. For very small gaps ($h/R \ll 1$) it is reasonable to assume that the flow is sufficiently close to steady shear flow that the CEF equation can be used for the constitutive equation. With the additional assumption that the quasi-steady-state approximation can be used, obtain a relation between the force F applied to the plates, the instantaneous rate of movement of the plates $\dot{h}$, and the viscometric properties of the fluid. Assume gravitational and inertial effects are negligible.

SOLUTION It is reasonable to take $v_r = v_r(r, z)$, $v_z = v_z(r, z)$, $v_\theta = 0$, and $p = p(r, z)$. The continuity equation and the r- and z-components of the equation of motion are then

$$\frac{1}{r}\frac{\partial}{\partial r}(rv_r) + \frac{\partial}{\partial z}v_z = 0 \tag{10.4-4}$$

$$0 = -\frac{\partial p}{\partial r} - \left(\frac{1}{r}\frac{\partial}{\partial r}(r\tau_{rr}) - \frac{\tau_{\theta\theta}}{r} + \frac{\partial \tau_{rz}}{\partial z}\right) \tag{10.4-5}$$

$$0 = -\frac{\partial p}{\partial z} - \left(\frac{1}{r}\frac{\partial}{\partial r}(r\tau_{rz}) + \frac{\partial \tau_{zz}}{\partial z}\right) \tag{10.4-6}$$

These equations are to be solved together with the constitutive equation, Eq. 9.6-18. To evaluate the three terms that contribute to the CEF equation we need first

$$\nabla \boldsymbol{v} = \begin{pmatrix} \frac{\partial v_r}{\partial r} & 0 & \frac{\partial v_z}{\partial r} \\ 0 & \frac{v_r}{r} & 0 \\ \frac{\partial v_r}{\partial z} & 0 & \frac{\partial v_z}{\partial z} \end{pmatrix} \tag{10.4-7}$$

where matrix entries are written in the order r, θ, z. The rate-of-strain tensor is then

$$\gamma_{(1)} = \begin{pmatrix} 2\frac{\partial v_r}{\partial r} & 0 & \frac{\partial v_z}{\partial r} + \frac{\partial v_r}{\partial z} \\ 0 & 2\frac{v_r}{r} & 0 \\ \frac{\partial v_z}{\partial r} + \frac{\partial v_r}{\partial z} & 0 & 2\frac{\partial v_z}{\partial z} \end{pmatrix} \tag{10.4-8}$$

[11] This example is motivated by M. A. McClelland and B. A. Finlayson, *J. Non-Newtonian Fluid Mech.*, **13**, 181–201 (1983). The authors are indebted to L. M. Quinzani and L. E. Wedgewood for valuable contributions to this example.

The Ψ_2 term in Eq. 9.6-18 involves $\{\boldsymbol{\gamma}_{(1)}\cdot\boldsymbol{\gamma}_{(1)}\}$, the components of which are

$$\{\boldsymbol{\gamma}_{(1)}\cdot\boldsymbol{\gamma}_{(1)}\}_{rr} = 4\left(\frac{\partial v_r}{\partial r}\right)^2 + \left(\frac{\partial v_r}{\partial z} + \frac{\partial v_z}{\partial r}\right)^2 \tag{10.4-9a}$$

$$\{\boldsymbol{\gamma}_{(1)}\cdot\boldsymbol{\gamma}_{(1)}\}_{\theta\theta} = 4\left(\frac{v_r}{r}\right)^2 \tag{10.4-9b}$$

$$\{\boldsymbol{\gamma}_{(1)}\cdot\boldsymbol{\gamma}_{(1)}\}_{zz} = 4\left(\frac{\partial v_z}{\partial z}\right)^2 + \left(\frac{\partial v_r}{\partial z} + \frac{\partial v_z}{\partial r}\right)^2 \tag{10.4-9c}$$

$$\{\boldsymbol{\gamma}_{(1)}\cdot\boldsymbol{\gamma}_{(1)}\}_{rz} = \{\boldsymbol{\gamma}_{(1)}\cdot\boldsymbol{\gamma}_{(1)}\}_{zr} = 2\left(\frac{\partial v_r}{\partial z} + \frac{\partial v_z}{\partial r}\right)\left(\frac{\partial v_r}{\partial r} + \frac{\partial v_z}{\partial z}\right) \tag{10.4-9d}$$

and all other components are zero. Similarly for the Ψ_1-term in the CEF equation we need to know the components of $\boldsymbol{\gamma}_{(2)}$:

$$\gamma_{(2)rr} = 2\left(v_r\frac{\partial^2 v_r}{\partial r^2} + v_z\frac{\partial^2 v_r}{\partial r\partial z}\right) - 4\left(\frac{\partial v_r}{\partial r}\right)^2 - 2\frac{\partial v_r}{\partial z}\left(\frac{\partial v_r}{\partial z} + \frac{\partial v_z}{\partial r}\right) \tag{10.4-10a}$$

$$\gamma_{(2)\theta\theta} = 2v_r\frac{\partial}{\partial r}\left(\frac{v_r}{r}\right) + 2v_z\frac{\partial}{\partial z}\left(\frac{v_r}{r}\right) - 4\left(\frac{v_r}{r}\right)^2 \tag{10.4-10b}$$

$$\gamma_{(2)zz} = 2v_r\frac{\partial^2 v_z}{\partial r\partial z} + 2v_z\frac{\partial^2 v_z}{\partial z^2} - 2\frac{\partial v_z}{\partial z}\left(\frac{\partial v_r}{\partial z} + \frac{\partial v_z}{\partial r}\right) - 4\left(\frac{\partial v_z}{\partial z}\right)^2 \tag{10.4-10c}$$

$$\begin{aligned}\gamma_{(2)rz} = \gamma_{(2)zr} &= v_r\left(\frac{\partial^2 v_r}{\partial r\partial z} + \frac{\partial^2 v_z}{\partial r^2}\right) + v_z\left(\frac{\partial^2 v_r}{\partial z^2} + \frac{\partial^2 v_z}{\partial r\partial z}\right)\\ &\quad - \left(\frac{\partial v_r}{\partial z} + \frac{\partial v_z}{\partial r}\right)\left(\frac{\partial v_r}{\partial r} + \frac{\partial v_z}{\partial z}\right) - 2\frac{\partial v_r}{\partial r}\frac{\partial v_z}{\partial r} - 2\frac{\partial v_z}{\partial z}\frac{\partial v_r}{\partial z}\end{aligned} \tag{10.4-10d}$$

with all other components being zero. Finally for the CEF equation we need the shear rate

$$\begin{aligned}\dot\gamma &= \sqrt{\tfrac{1}{2}(\boldsymbol{\gamma}_{(1)}:\boldsymbol{\gamma}_{(1)})} = \sqrt{\tfrac{1}{2}\,\mathrm{tr}\{\boldsymbol{\gamma}_{(1)}\cdot\boldsymbol{\gamma}_{(1)}\}}\\ &= \sqrt{\tfrac{1}{2}\left(2\left(\frac{\partial v_r}{\partial z} + \frac{\partial v_z}{\partial r}\right)^2 + 4\left(\frac{v_r}{r}\right)^2 + 4\left(\frac{\partial v_r}{\partial r}\right)^2 + 4\left(\frac{\partial v_z}{\partial z}\right)^2\right)}\end{aligned} \tag{10.4-11}$$

No approximations have been made in writing down Eqs. 10.4-4 through 11 except for the form of the velocity field given above Eq. 10.4-4 and the quasi-steady-state, creeping flow, and negligible gravity assumptions listed in the problem statement.

We now seek a perturbation solution to these equations, in which we take advantage of the fact that $\varepsilon = h/R \ll 1$. We begin by estimating the orders of magnitude of the velocity components. Since the plates move with speed $-\dot h$, we have

$$v_z \sim O(-\dot h) \tag{10.4-12}$$

Then from the continuity equation it follows that

$$v_r \sim O(-\dot h R/h) \tag{10.4-13}$$

so that v_r will be larger than v_z by a factor of $\varepsilon^{-1} \gg 1$. As a convenient shorthand let us denote the order of magnitude of v_r by $V = -\dot h R/h$. Then Eqs. 10.4-12 and 13 suggest that we expand v_r and v_z thus

$$v_r = V[\hat v_{r0} + \varepsilon\hat v_{r1} + \cdots] \tag{10.4-14}$$

$$v_z = V[\varepsilon\hat v_{z1} + \cdots] \tag{10.4-15}$$

where the $\hat{}$ denotes dimensionless quantities. In addition we define dimensionless radial and axial variables as

$$\xi = r/R; \qquad \zeta = z/h \tag{10.4-16}$$

Then by combining Eqs. 10.4-11, 14 and 15 we obtain the dimensionless shear rate $\dot{\Gamma}$

$$\dot{\Gamma} = \frac{\dot{\gamma}h}{V} = -\frac{\partial \hat{v}_{r0}}{\partial \zeta}\left[1 + \varepsilon \frac{(\partial \hat{v}_{r1}/\partial \zeta)}{(\partial \hat{v}_{r0}/\partial \zeta)} + \cdots\right] \qquad (0 \le \zeta \le 1) \tag{10.4-17}$$

so that at lowest order the shear rate is $(-\partial v_r/\partial z)$. The restriction to $0 \le \zeta \le 1$ in Eq. 10.4-17 arises from the fact that the shear rate must be positive. It is also assumed that the ε-term in Eq. 10.4-17 is sufficiently small that the term in brackets is positive. For the remainder of this example we will consider only the region $0 \le \zeta \le 1$; the flow for $-1 \le \zeta \le 0$ can be obtained from symmetry.

We can now obtain expansions for the components of the stress tensor. In doing this it is convenient to make the stress tensor, viscosity, and normal stress coefficients dimensionless as follows:

$$\mathbf{T} = \frac{\boldsymbol{\tau}}{\eta^0 V/h}; \qquad \hat{\eta} = \frac{\eta}{\eta^0}; \qquad \hat{\Psi}_1 = \frac{\Psi_1}{\eta^0 h/V}; \qquad \hat{\Psi}_2 = -q\hat{\Psi}_1 \tag{10.4-18}$$

where η^0 is a characteristic viscosity and q is a constant. The relation between Ψ_2 and Ψ_1 is supported by data in Fig. 3.7-7. To get expansions for T_{ij} it is necessary to expand $\hat{\eta}$ and $\hat{\Psi}_1$ thus

$$\begin{aligned}\hat{\eta} &= \hat{\eta}(\dot{\Gamma}_0) + \varepsilon\left(\frac{d\hat{\eta}}{d\dot{\Gamma}}\frac{d\dot{\Gamma}}{d\varepsilon}\right)_{\varepsilon=0} + \cdots \\ &= \hat{\eta}(\dot{\Gamma}_0) - \varepsilon\left(\frac{d\hat{\eta}}{d\dot{\Gamma}}\right)_{\Gamma=\Gamma_0}\frac{\partial \hat{v}_{r1}}{\partial \zeta} + O(\varepsilon^2)\end{aligned} \tag{10.4-19}$$

$$\hat{\Psi}_1 = \hat{\Psi}_1(\dot{\Gamma}_0) - \varepsilon\left(\frac{d\hat{\Psi}_1}{d\dot{\Gamma}}\right)_{\dot{\Gamma}=\dot{\Gamma}_0}\frac{\partial \hat{v}_{r1}}{\partial \zeta} + O(\varepsilon^2) \tag{10.4-20}$$

where $\dot{\Gamma}_0 = |\partial \hat{v}_{r0}/\partial \zeta| = -\partial \hat{v}_{r0}/\partial \zeta$. When Eqs. 10.4-14 through 20 are combined with the shear stress expression from the CEF equation we obtain

$$\begin{aligned}T_{rz} = &-\hat{\eta}(\dot{\Gamma}_0)\frac{\partial \hat{v}_{r0}}{\partial \zeta} + \varepsilon\left\{-\left[\hat{\eta}(\dot{\Gamma}_0)\frac{\partial \hat{v}_{r1}}{\partial \zeta} - \left(\frac{d\hat{\eta}}{d\dot{\Gamma}}\right)_{\dot{\Gamma}=\dot{\Gamma}_0}\frac{\partial \hat{v}_{r1}}{\partial \zeta}\frac{\partial \hat{v}_{r0}}{\partial \zeta}\right]\right. \\ &+ \tfrac{1}{2}\hat{\Psi}_1(\dot{\Gamma}_0)\left[\hat{v}_{r0}\frac{\partial^2 \hat{v}_{r0}}{\partial \zeta \partial \xi} + \hat{v}_{z1}\frac{\partial^2 \hat{v}_{r0}}{\partial \zeta^2} - (3-4q)\frac{\partial \hat{v}_{r0}}{\partial \zeta}\frac{\partial \hat{v}_{z1}}{\partial \zeta}\right. \\ &\left.\left. - (1-4q)\frac{\partial \hat{v}_{r0}}{\partial \zeta}\frac{\partial \hat{v}_{r0}}{\partial \xi}\right]\right\} + O(\varepsilon^2)\end{aligned} \tag{10.4-21}$$

For convenience and to facilitate comparison with the results of Example 4.2-7, let us assume that the viscosity and first normal stress coefficients are given by power-law expressions (see text below Eq. 4.2-68). Then we take the characteristic viscosity η^0 to be

$$\eta^0 = m(V/h)^{n-1} \tag{10.4-22}$$

That is, we will take η^0 to be the power-law viscosity evaluated at the characteristic shear rate V/h. It then follows that

$$\hat{\eta} = \dot{\Gamma}^{n-1}; \qquad \hat{\Psi}_1 = M\dot{\Gamma}^{n'-2} \tag{10.4-23}$$

where M is a dimensionless parameter

$$M = \left(\frac{m'}{m}\right)\left(\frac{V}{h}\right)^{n'-n} \tag{10.4-24}$$

In the expansion for $\hat{\eta}$ we then find

$$\left.\frac{d\hat{\eta}}{d\hat{\dot{\Gamma}}}\right|_{\hat{\dot{\Gamma}}=\hat{\dot{\Gamma}}_0} = (n-1)\hat{\dot{\Gamma}}_0^{n-2} \tag{10.4-25}$$

Combining Eqs. 10.4-21 through 25 gives

$$\begin{aligned} \mathrm{T}_{rz} = &\left(-\frac{\partial \hat{v}_{r0}}{\partial \zeta}\right)^n + \varepsilon\left[-n\left(-\frac{\partial \hat{v}_{r0}}{\partial \zeta}\right)^{n-1}\frac{\partial \hat{v}_{r1}}{\partial \zeta}\right. \\ &+ \tfrac{1}{2}M\left(-\frac{\partial \hat{v}_{r0}}{\partial \zeta}\right)^{n'-2}\left(\hat{v}_{r0}\frac{\partial^2 \hat{v}_{r0}}{\partial \zeta \partial \xi} + \hat{v}_{z1}\frac{\partial^2 \hat{v}_{r0}}{\partial \zeta^2} - (3-4q)\frac{\partial \hat{v}_{r0}}{\partial \zeta}\frac{\partial \hat{v}_{z1}}{\partial \zeta}\right. \\ &\left.\left. - (1-4q)\frac{\partial \hat{v}_{r0}}{\partial \zeta}\frac{\partial \hat{v}_{r0}}{\partial \xi}\right)\right] + O(\varepsilon^2) \end{aligned} \tag{10.4-26}$$

By a similar procedure we find expansions for the other dimensionless stress components:

$$\mathrm{T}_{rr} = -(1-q)M\left(-\frac{\partial \hat{v}_{r0}}{\partial \zeta}\right)^{n'} + O(\varepsilon) \tag{10.4-27}$$

$$\mathrm{T}_{\theta\theta} = -2\varepsilon\left(\frac{\hat{v}_{r0}}{\xi}\right)\left(-\frac{\partial \hat{v}_{r0}}{\partial \zeta}\right)^{n-1} + O(\varepsilon^2) \tag{10.4-28}$$

$$\mathrm{T}_{zz} = qM\left(-\frac{\partial \hat{v}_{r0}}{\partial \zeta}\right)^{n'} - 2\varepsilon\left[\left(-\frac{\partial \hat{v}_{r0}}{\partial \zeta}\right)^{n-1}\frac{\partial \hat{v}_{z1}}{\partial \zeta} - \tfrac{1}{2}M\left(-\frac{\partial \hat{v}_{r0}}{\partial \zeta}\right)^{n'-1}\left(\frac{\partial \hat{v}_{z1}}{\partial \zeta}\right)\right] + O(\varepsilon^2) \tag{10.4-29}$$

In these expansions we assume that the stress ratio is of order unity, and this implies that M is also of order unity.

The last variable that needs to be scaled and expanded is the pressure. From an order of magnitude analysis of the r-component of the equation of motion we see that at lowest order in ε the $\partial p/\partial r$ and $\partial \tau_{rz}/\partial z$ terms must balance. Hence the pressure must be of order $(\eta^0 V/h)\varepsilon^{-1}$, which suggests an expansion of the form

$$P = \frac{p}{(\eta^0 V/h)} = P_{-1}\varepsilon^{-1} + P_0 + O(\varepsilon) \tag{10.4-30}$$

Note that the pressure is singular and will be much larger than any of the stresses as $\varepsilon \to 0$.

Dimensionless forms of the equation of motion are obtained by multiplying Eqs. 10.4-5 and 6 by $h/(\eta^0 V/h)$:

$$r\text{-component} \quad 0 = -\varepsilon\frac{\partial P}{\partial \xi} - \left(\varepsilon\frac{1}{\xi}\frac{\partial}{\partial \xi}(\xi \mathrm{T}_{rr}) - \varepsilon\frac{\mathrm{T}_{\theta\theta}}{\xi} + \frac{\partial \mathrm{T}_{rz}}{\partial \zeta}\right) \tag{10.4-31}$$

$$z\text{-component} \quad 0 = -\frac{\partial P}{\partial \zeta} - \left(\varepsilon\frac{1}{\xi}\frac{\partial}{\partial \xi}(\xi \mathrm{T}_{rz}) + \frac{\partial \mathrm{T}_{zz}}{\partial \zeta}\right) \tag{10.4-32}$$

When the expansions for P and the T_{ij} are inserted into these equations and the coefficients of equal orders in ε equated, we obtain the following set of differential equations:

$$O(\varepsilon^{-1}): \qquad \frac{\partial P_{-1}}{\partial \zeta} = 0 \tag{10.4-33}$$

$$O(\varepsilon^{0}): \qquad \frac{\partial P_{-1}}{\partial \xi} + \frac{\partial}{\partial \zeta}\left(-\frac{\partial \hat{v}_{r0}}{\partial \zeta}\right)^{n} = 0 \tag{10.4-34}$$

$$\frac{\partial P_0}{\partial \zeta} + qM\frac{\partial}{\partial \zeta}\left(-\frac{\partial \hat{v}_{r0}}{\partial \zeta}\right)^{n'} = 0 \tag{10.4-35}$$

$$O(\varepsilon): \qquad \frac{\partial P_0}{\partial \xi} - (1-q)\frac{M}{\xi}\frac{\partial}{\partial \xi}\left[\xi\left(-\frac{\partial \hat{v}_{r0}}{\partial \zeta}\right)^{n'}\right] + \frac{\partial}{\partial \zeta}\left[-n\left(-\frac{\partial \hat{v}_{r0}}{\partial \zeta}\right)^{n-1}\frac{\partial \hat{v}_{r1}}{\partial \zeta}\right.$$
$$+ \tfrac{1}{2}M\left(-\frac{\partial \hat{v}_{r0}}{\partial \zeta}\right)^{n'-2}\left(\hat{v}_{r0}\frac{\partial^2 \hat{v}_{r0}}{\partial \zeta \partial \xi} + \hat{v}_{z1}\frac{\partial^2 \hat{v}_{r0}}{\partial \zeta^2}\right.$$
$$\left.\left. - (3-4q)\frac{\partial \hat{v}_{r0}}{\partial \zeta}\frac{\partial \hat{v}_{z1}}{\partial \zeta} - (1-4q)\frac{\partial \hat{v}_{r0}}{\partial \zeta}\frac{\partial \hat{v}_{r0}}{\partial \xi}\right)\right] = 0 \tag{10.4-36}$$

$$\frac{\partial P_1}{\partial \zeta} + \frac{1}{\xi}\frac{\partial}{\partial \xi}\left[\xi\left(-\frac{\partial \hat{v}_{r0}}{\partial \zeta}\right)^{n}\right] - 2\frac{\partial}{\partial \zeta}\left[\left(-\frac{\partial \hat{v}_{r0}}{\partial \zeta}\right)^{n-1}\frac{\partial \hat{v}_{z1}}{\partial \zeta}\right.$$
$$\left. - \tfrac{1}{2}M\left(-\frac{\partial \hat{v}_{r0}}{\partial \zeta}\right)^{n'-1}\left(\frac{\partial \hat{v}_{z1}}{\partial \zeta}\right)\right] = 0 \tag{10.4-37}$$

Before Eqs. 10.4-33 through 37 can be solved, we need to specify boundary conditions. These are

$$\text{At } z = h \qquad v_z = \dot{h}; \qquad v_r = 0 \tag{10.4-38}$$

$$\text{At } z = 0 \qquad \frac{\partial v_z}{\partial z} = 0; \qquad \frac{\partial v_r}{\partial z} = 0 \tag{10.4-39}$$

$$\text{At } r = R \text{ and } z = h \qquad \pi_{rr} = p_a \tag{10.4-40}$$

where p_a is atmospheric pressure. This last boundary condition is clearly an approximation since there is no fluid-air interface at $r = R$ for $t > 0$. We feel nonetheless that this is a reasonable choice at least for the early part of the experiment; this point is discussed further by McClelland and Finlayson[11] and at the end of this example. When the dimensionless expansions for velocity, stress, and pressure are combined with Eqs. 10.4-38 through 40, we obtain

$$\text{At } \zeta = 0 \qquad \frac{\partial \hat{v}_{zn}}{\partial \zeta} = \frac{\partial \hat{v}_{rn}}{\partial \zeta} = 0 \qquad (n \geq 0) \tag{10.4-41}$$

$$\text{At } \zeta = 1 \qquad \hat{v}_{z1} = -1; \qquad \hat{v}_{rn} = 0 \qquad (n \geq 0)$$
$$\hat{v}_{zn} = 0 \qquad (n > 1) \tag{10.4-42}$$

$$\text{At } \xi = 1, \zeta = 1 \qquad P_{-1} = 0$$
$$P_0 = P_a + (1-q)M\left(-\frac{\partial \hat{v}_{r0}}{\partial \zeta}\right)^{n'}_{\xi=1,\zeta=1} \tag{10.4-43}$$
$$P_n + T_{rr,n} = 0 \qquad (n \geq 1)$$

in which $T_{rr,n}$ is the nth order term in the expansion for T_{rr}.

We are now in a position to solve the perturbation equations. Before doing so we note that the objective of the calculation is to obtain the force on the upper plate. This is given by Eq. 4.2-64, which in dimensionless form is

$$\hat{F} = \frac{F}{\pi R^2 \eta^0 V/h} = 2\int_0^1 (P - P_a + \mathrm{T}_{zz})_{\zeta=1}\xi d\xi$$

$$= 2\int_0^1 \left[\varepsilon^{-1}P_{-1} + (P_0 - P_a) + qM\left(-\frac{\partial \hat{v}_{r0}}{\partial \zeta}\right)^{n'}\right]_{\zeta=1} \xi d\xi + O(\varepsilon) \tag{10.4-44}$$

$$= \frac{1}{\varepsilon}\hat{F}_{-1} + \hat{F}_0 + \cdots$$

From this we see that in order to get the first correction to the force, $\hat{F}_0$, we need to obtain only P_0 and $\hat{v}_{r0}$.

At lowest order we see immediately that $P_{-1} = P_{-1}(\xi)$. We next find at $O(\varepsilon^0)$ that

$$\hat{v}_{r0} = \left(-\frac{dP_{-1}}{d\xi}\right)^{1/n}\left(\frac{n}{n+1}\right)(1 - \zeta^{(1/n)+1}) \tag{10.4-45}$$

To obtain an equation for the pressure gradient we apply overall conservation of mass (cf. Eq. 4.2-61), which, when combined with the expansion for the radial velocity, gives

$$\int_0^1 \hat{v}_{r0}\, d\zeta = \tfrac{1}{2}\xi \tag{10.4-46}$$

$$\int_0^1 \hat{v}_{rn}\, d\zeta = 0 \qquad (n \geq 1) \tag{10.4-47}$$

Combining Eqs. 10.4-45 and 46 gives an ordinary differential equation for P_{-1}, which is easily solved together with the boundary condition in Eq. 10.4-43. Finally $\hat{v}_{z1}$ can be obtained from $\hat{v}_{r0}$ by means of the continuity equation. In this way we obtain

$$\hat{v}_{r0} = \tfrac{1}{2}\xi\left(\frac{2n+1}{n+1}\right)(1 - \zeta^{(1/n)+1}) \tag{10.4-48}$$

$$\hat{v}_{z1} = -\left(\frac{2n+1}{n+1}\right)\left(\zeta - \frac{n}{2n+1}\zeta^{(1/n)+2}\right) \tag{10.4-49}$$

$$P_{-1} = \left(\frac{2n+1}{2n}\right)^n\left(\frac{1}{n+1}\right)(1 - \xi^{n+1}) \tag{10.4-50}$$

Equations 10.4-48 to 50 are identical to the results obtained in Example 4.2-7 except for the p_a contribution to the pressure (Eq. 4.2-63), which does not enter in this analysis until the next order. Thus normal stress effects are not important at the lowest order in the force expression.

We now move to $O(\varepsilon)$ where we must solve the r-component of the equation of motion. All terms in Eq. 10.4-36 are now known except P_0 and $\hat{v}_{r1}$. These are found from Eqs. 10.4-35, 36, 41, 42, 43, and 47 in the same way as $\hat{v}_{r0}$ and P_{-1} were determined. The final result for P_0 is

$$P_0 = P_a - M\left(\frac{2n+1}{2n}\right)^{n'}\left\{1 - q\xi^{n'}\zeta^{n'/n} + \frac{K}{n'}(1 - \xi^{n'})\right\} \tag{10.4-51}$$

where

$$K = \frac{(3n + n' + 1) - n(2n + 1)(n' + 4 - 3q)}{(n + n')(2n + n' + 1)} \tag{10.4-52}$$

The first normal stress coefficient affects P_0 through M and n' in this result, and the influence of the second normal stress coefficient arises from the q-terms. Note that if $\Psi_2 = 0$ then $P_0 = P_a$, and the pressure distribution for the power-law fluid given in Eq. 4.2-63 is recovered.

Finally we develop the solution for the force by combining Eqs. 10.4-44, 48, 50, and 51. This leads to

$$\hat{F}_{-1} = \frac{1}{n + 3}\left(\frac{2n + 1}{2n}\right)^n \tag{10.4-53}$$

$$\hat{F}_0 = \frac{M}{(n' + 2)}\left(\frac{2n + 1}{2n}\right)^{n'}[(n' + 2) + K] \tag{10.4-54}$$

To find the separation of the plates as a function of time, we use the quasi-steady-state approximation, which allows us to obtain at each instant dh/dt from the force expression in Eqs. 10.4-44, 53, and 54. It is necessary to remove the h and $\dot{h}$ from the scaling of $\hat{F}$ in order to do this, and for that purpose we introduce the following additional dimensionless variables and groups:

$$\begin{gathered} \hat{t} = \frac{t}{\lambda}; \qquad \hat{h} = \frac{h}{h_0}; \qquad \varepsilon_0 = \frac{h_0}{R} \\ F^* = \frac{F\lambda^n}{\pi R^2 m} = \hat{F}\left(\frac{\lambda V}{h}\right)^n = \hat{F}\left(-\frac{d\hat{h}/d\hat{t}}{\varepsilon_0 \hat{h}^2}\right)^n \end{gathered} \tag{10.4-55}$$

By combining these definitions with the force expression we get

$$\boxed{\begin{aligned} F^* = {} & \frac{\varepsilon_0^{-(n+1)}}{(n + 3)}\left(\frac{2n + 1}{2n}\right)^n \frac{(-d\hat{h}/d\hat{t})^n}{\hat{h}^{2n+1}} \\ & + \frac{2\varepsilon_0^{-n'}}{(n' + 2)}\left(\frac{2n + 1}{2n}\right)^{n'}[(n' + 2) + K]\frac{(-d\hat{h}/d\hat{t})^{n'}}{\hat{h}^{2n'}} \end{aligned}} \tag{10.4-56}$$

which is the desired relation between F^*, $d\hat{h}/d\hat{t}$, and $\hat{h}$.

If the plate speed $\dot{h}$ were held constant during the squeeze flow experiment, then Eq. 10.4-56 could be used in a straightforward way to calculate the force as a function of time. On the other hand, when the force is held constant, as we consider it to be in this example, then Eq. 10.4-56 must be solved numerically for $\hat{h}(\hat{t})$. This is easily done following the method suggested by McClelland and Finlayson[11]. Let us interchange the dependent and independent variables in Eq. 10.4-56; that is, we consider $\hat{t}$ to be a function of $\hat{h}$. We then find $\hat{t}(\hat{h})$ by forward integration of

$$\frac{d\hat{t}}{d\hat{h}} = f(\hat{h}) \tag{10.4-57}$$

subject to the initial condition that

$$\text{At } \hat{h} = 1, \qquad \hat{t} = 0 \tag{10.4-58}$$

The value of $f(\hat{h})$ is found at each $\hat{h}$ from Eq. 10.4-56 by means of Newton's method.

The results of this integration are shown in Fig. 10.4-2 where they are compared with Leider's data[12] for a polyisobutylene solution. The value of q is arbitrarily chosen to be 0.1, since there are no

[12] P. J. Leider and R. B. Bird, University of Wisconsin Rheology Research Center Report No. 22 (1973).

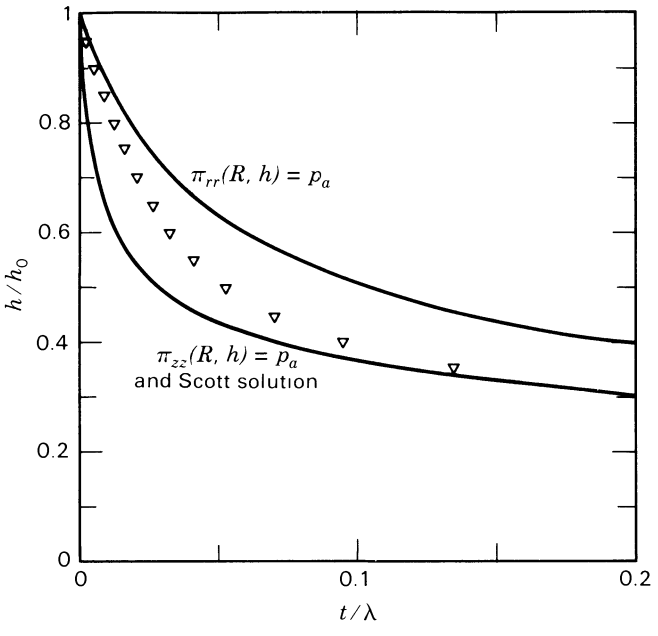

(a)

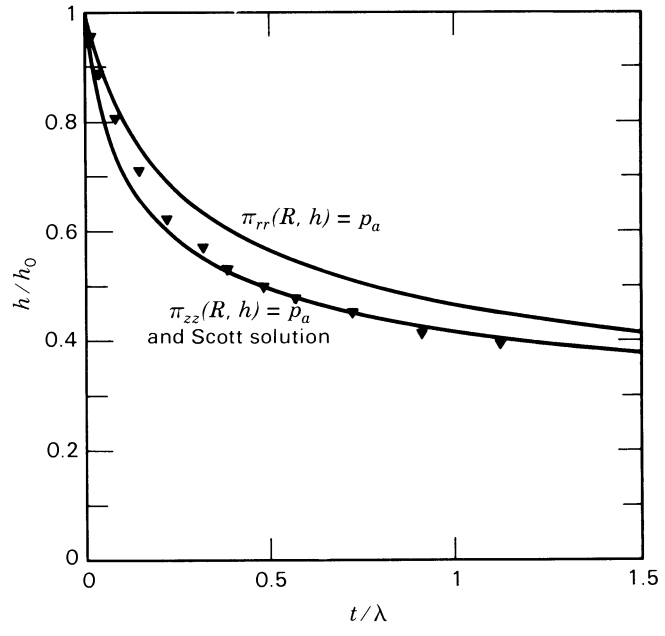

(b)

FIGURE 10.4-2. Comparison of calculated and experimental results for squeezing flow of a polyisobutylene solution with $q = 0.1$ and (*a*) $F^* = F\lambda^n/\pi R^2 m = 970$ and $R/h_0 = 91.7$; (*b*) $F^* = 0.265$ and $R/h_0 = 189.6$. The curve labeled $\pi_{rr}(R, h) = p_a$ is calculated from Eq. 10.4-56, which uses $\pi_{rr} = p_a$ at $r = R$, $z = h$; the curve labeled $\pi_{zz}(R, h) = p_a$ was obtained with $\pi_{zz} = p_a$ at $r = R$, $z = h$. The Scott solution from Eq. 4.2-65 is also shown for comparison. Data are from P. J. Leider and R. B. Bird, University of Wisconsin Rheology Research Center Report No. 22 (1973).

Ψ_2 data available on this particular solution; changing q by a factor of two in either direction does not affect $h(t)$ much. The calculated results are seen to describe the data accurately only for very short times. At long times, it is interesting that the data are well described by the Scott equation (Eq. 4.2-65).

We believe that the discrepancy between the results obtained from Eq. 10.4-56 and the data at moderate and long times may be due to the inappropriateness of the boundary condition, Eq. 10.4-40. When the experiment is first started, there is a free surface at $r = R$, so that requiring $\pi_{rr} = p_a$ is reasonable at $t = 0$. As fluid is squeezed out of the gap, the actual free surface will be beyond $r = R$, and it is questionable whether or not $\pi_{rr} = p_a$ at a position inside the fluid. To see how quickly deviations from this boundary condition might be expected, note that when the free surface has moved a distance h beyond the plate edge, the dimensionless gap will be roughly $\hat{h} \doteq (1 + \varepsilon_0)^{-1/2}$. For $\varepsilon_0 = 0.01$ this gives $\hat{h} \doteq 0.995$. Furthermore, the sensitivity of the solution to this boundary condition can be seen by replacing Eq. 10.4-40 by

$$\text{At } r = R \text{ and } z = h \qquad \pi_{zz} = p_a \tag{10.4-59}$$

This boundary condition might be reasonable if the free surface of the extruded material were nearly parallel to the plate surfaces and if velocity rearrangements near the plate rim could be ignored.[13] With this boundary condition, $[(n' + 2) + K]$ in Eq. 10.4-56 is replaced by K and the resulting solution for $\hat{h}(\hat{t})$ is seen in Fig. 10.4-2 to be very close to the Scott solution. The choice of an appropriate rim boundary condition is an unresolved issue in this problem. Experimentally, it might be feasible to circumvent this difficulty by using a partially filled gap.

Other possible sources of the discrepancy between theory and experiment are the quasi-steady-state approximation and the CEF constitutive equation. The latter should be used only for steady-state shear flows.

PROBLEMS

10A.1 Analysis of Capillary Viscometer Data[1]

The volumetric flow rate through a capillary tube has been measured at a series of imposed pressure drops for a 3.5% (weight) solution of carboxymethylcellulose in water at 303 K. The data have been corrected for end effects using the procedure of Example 10.2-3.

$4Q/\pi R^3$ (s^{-1})	τ_R (Pa)
250	220
350	255
500	298
700	341
900	382
1250	441
1750	509
2500	584
3500	670
5000	751
7000	825
9000	887
12500	1000
17500	1070
25000	1200

[13] D. V. Boger and M. M. Denn, *J. Non-Newtonian Fluid Mech.*, **6**, 163-185 (1980).

[1] Tabular data from A. G. Fredrickson, *Principles and Applications of Rheology*, 1964. Reprinted by permission of Prentice-Hall, Inc., Englewood Cliffs, NJ, pp. 309-310.

Construct a graph of $\log \eta$ vs. $\log \dot{\gamma}$ for this fluid. What is the slope of this curve in the power-law region?

10A.2 Normal Stress Measurements in the Cone-and-Plate Instrument

In Fig. 10A.2 data are shown on the radial variation of the total normal stress $\pi_{\theta\theta}$ exerted on the plate in the cone-and-plate device. The data are for a 2.5% polyacrylamide solution and were taken using flush-mounted pressure transducers at the positions indicated. The radius of the plate is 5 cm. From these data determine Ψ_1 and Ψ_2 for the polyacrylamide solution at the four shear rates shown.

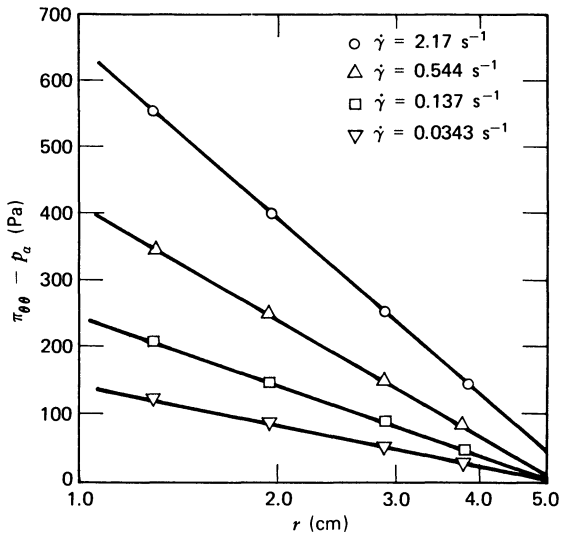

FIGURE 10A.2. Total normal stress on the plate relative to atmospheric pressure $\pi_{\theta\theta} - p_a$ versus distance from the center of the plate for a 2.5% polyacrylamide solution. [E. B. Christiansen and W. R. Leppard, *Trans. Soc. Rheol.*, **18**, 65-86 (1974).]

10A.3 Applicability of Concentric Cylinder Instrument Results

In order to use the formulas presented in Table 10.2-1D, the gap between the two cylinders of this instrument must be small. How must the ratio R_1/R_2 be restricted if the shear stress is to vary no more than 2% within the gap?

10A.4 Viscosity Measurements with an Epprecht Viscometer

An Epprecht viscometer utilizes a concentric cylinder geometry in which the inner cylinder is rotated at angular velocity W_1 and the outer cylinder is held in a fixed position. The shear stress at the inner cylinder τ_1 is measured for a series of rotation rates. Sample data[2] taken on a 1% solution of carboxymethylcellulose are given below. For the particular instrument used, the inner cylinder had a

[2] Tabular data from S. Middleman, *The Flow of High Polymers*, Wiley-Interscience, New York (1968), p. 23.

radius $R_1 = 1.54$ cm and the outer cylinder had a radius $R_2 = 1.94$ cm. Use the results of Problem 10C.2 to construct a plot of $\eta(\dot{\gamma})$ for this polymer solution.

τ_1(Pa)	W_1(rad/s)
4.1	2.63
5.2	3.53
6.5	4.64
8.1	6.19
10.1	8.17
13.6	11.8
17.0	15.9
20.7	20.9
25.4	28.0
30.9	36.9

10B.1 Forced Oscillation Measurements with the Cone-and-Plate Geometry

In Example 10.1-1 we showed how the complex viscosity could be determined from a parallel-plate system in which the upper plate was executing small-amplitude oscillations, and the torque $\mathscr{T}$ on the bottom, fixed plate was monitored. Rework that example for a cone-and-plate system (see Fig. 10.2-1) in which the upper cone is made to oscillate according to $\phi = \phi_0 \mathscr{R}e\{e^{i\omega t}\}$, in which $\phi_0 \ll 1$ is the small, real amplitude of oscillation. Show that the formulas analogous to Eqs. 10.1-11 and 12 are

$$\eta' = -\frac{3\vartheta_0 \mathscr{T}_0 \sin\delta}{2\pi R^3 \omega \phi_0} \tag{10B.1-1}$$

$$\eta'' = -\frac{3\vartheta_0 \mathscr{T}_0 \cos\delta}{2\pi R^3 \omega \phi_0} \tag{10B.1-2}$$

in which $\mathscr{T}_0$ is the amplitude of the oscillating torque defined in the first line of Eq. 10.1-10. Note that the phase angle δ is in the range $-\pi \leq \delta < \pi/2$.

10B.2 Inertial Effects in Oscillatory Parallel-Plate Flow

If inertial effects are allowed for in the oscillatory parallel-plate flow considered in Example 10.1-1, show that the torque is given by

$$\mathscr{T}_0(\cos\delta + i\sin\delta)\sin\alpha H = -\frac{\pi R^4}{2} i\omega\theta_0 \alpha\eta^* \tag{10B.2-1}$$

where $\alpha = \sqrt{(i\omega\rho/\eta^*)}$ and $\mathscr{T}_0$ is the real torque amplitude. Suggest an iterative scheme for solving this equation.

10B.3 Inertial Corrections in the Cone-and-Plate Instrument

In obtaining Eq. 10.2-7 for the total normal thrust in the cone-and-plate system, inertial forces were assumed to be negligible. The size of the error introduced in this way can be estimated theoretically in the following manner by considering the equation of motion for a Newtonian fluid:

a. Show that for a Newtonian fluid, the pressure distribution between the cone and plate (for small cone angles) is

$$p - p_a = \tfrac{1}{2}\rho W^2 R^2 \left(\frac{\vartheta}{\vartheta_0}\right)^2 \left(\frac{r^2}{R^2} - 1\right) \tag{10B.3-1}$$

b. Determine the average pressure in the gap[3] at any radial position $\bar{p}(r) = (1/\vartheta_0)\int_0^{\vartheta_0} p\, d\theta$ and use this result to compute the total normal thrust (over that due to atmospheric pressure) that a Newtonian fluid exerts on the plate

$$\mathscr{F}_{\text{Newtonian}} = -\frac{\pi}{12}\rho R^4 W^2 \tag{10B.3-2}$$

c. Interpret the result in **(b)**. The averaged form of Eq. 10B.3-1 has been compared with experimental data by Adams and Lodge,[4] who find a reasonable fit. It appears that this method slightly overestimates the inertial terms.

10B.4 End Correction for the Couette Viscometer

The assumption of tangential annular flow used in obtaining the results in Table 10.2-1D does not hold near the bottom of the viscometer. In order to compensate for this end effect, the bottom of the inner cylinder is actually constructed with a conical shape (see Fig. 10B.4); the flow at the bottom is thus a cone-and-plate flow. The gap is assumed to be narrow, that is, $(R_2 - R_1)/R_1 \ll 1$.

a. For what choice of the cone angle ϑ_0 is the shear rate uniform throughout the fluid?

b. Obtain an expression for η for this geometry that is analogous to Eq. D-1 in Table 10.2-1.

Answer: b. $\eta = \dfrac{\mathscr{T}(R_2 - R_1)}{2\pi R_1^3 H[1 + (R_1/3H)]W_1}$

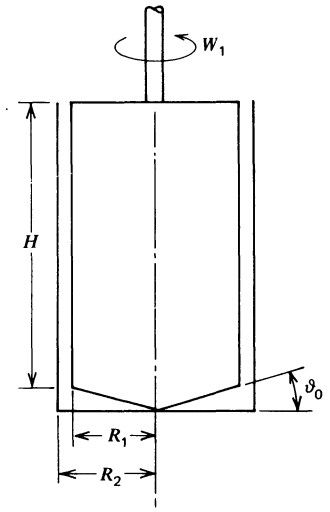

FIGURE 10B.4. Concentric cylinder viscometer with conical bottom. The inner cylinder rotates and the outer cylinder is fixed.

[3] This averaging procedure was first used by H. W. Greensmith and R. S. Rivlin, *Phil. Trans. Roy. Soc. London*, **A245**, 399-428 (1953), to fit experimental data for a torsional flow system. See also K. Walters, *Rheometry*, Chapman and Hall, London (1975), pp. 61-66.

[4] N. Adams and A. S. Lodge, *Phil. Trans. Roy. Soc. London*, **A256**, 149-184 (1964).

10B.5 Viscous Heating in a Concentric Cylinder Viscometer

Estimate the temperature rise caused by viscous heating in a concentric cylinder viscometer by considering steady tangential annular flow between two cylinders. The inner cylinder has radius κR and rotates with constant angular velocity W; the outer cylinder has radius R and is held fixed. In addition, the temperature of the outer cylinder is kept at T_0. It is assumed that the temperature rise is small enough so that the viscosity is not substantially altered by it. What is the maximum temperature rise in the fluid if $\kappa \doteq 1$ and no heat is transferred to the inner cylinder?

Answer: $T_{max} - T_0 = \dfrac{\eta R^2 W^2}{2k}$

10B.6 Centripetal Pumping between Parallel Disks[5]

Rework Problem 6B.14 by using the CEF constitutive equation. In this way verify Eq. F-1 in Table 10.2-1. Note that since the flow in this problem is viscometric, the CEF equation will be valid for a wide class of non-Newtonian fluids.

10B.7 The Truncated Cone-and-Plate Instrument[6]

The truncated cone-and-plate instrument shown in Fig. 10B.7 is a hybrid of the cone-and-plate and parallel-plate instruments. The normal force $\pi_{\theta\theta}$ is measured along the bottom plate by means of hole-mounted pressure transducers. Thus these readings are affected by the hole pressure, which depends on the shear rate. Denote the measured values by $\pi'_{\theta\theta}$; these are related to $\pi_{\theta\theta}$ by

$$p^* = \pi_{\theta\theta} - \pi'_{\theta\theta} \tag{10B.7-1}$$

where p^* is the hole pressure (see §2.3c). By paralleling the analyses in Examples 10.2-1 and 2, verify Eqs. G-1 through G-5 in Table 10.2-1. These formulas permit the truncated cone-and-plate device to be used to determine the first and second normal stress coefficients and the hole pressure as functions of the shear rate.

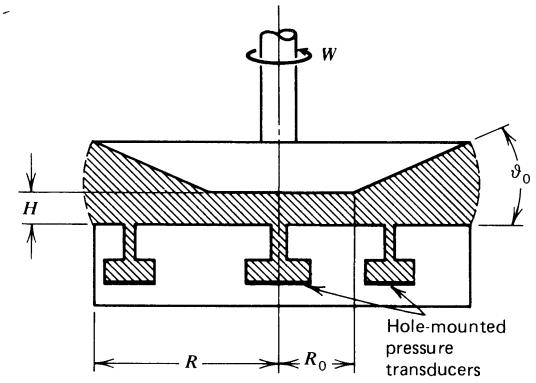

FIGURE 10B.7. The truncated cone-and-plate instrument.

10C.1 End Correction for a Capillary Viscometer[7]

Consider the operation of two capillary viscometers A and B (see Fig. 10.2-2). The reservoirs are identical and are located at the same elevation, but one is equipped with a tube of length L_A and the other a tube of length L_B. The radius of each tube is R, and the entrance angles are the same for the

[5] Y. Tomita and H. Katō, *Trans. Jpn. Soc. Mech. Eng.* (*Nippon Kikai Gakkai Ronbunshū*), **32**, 241, 1399–1408 (Sept. 1966); B. Maxwell and A. J. Scalora, *Mod. Plast.*, **37**(2), 107 (1959); P. A. Good, A. J. Schwartz, and C. W. Macosko, *AIChE J.*, **20**, 67–73 (1974).

[6] A. S. Lodge, *Rheol. Acta*, **10**, 554–556 (1971); A. S. Lodge and T. H. Hou, *Rheol. Acta*, **20**, 247–260 (1981).

[7] A. G. Fredrickson, *Principles and Applications of Rheology*, Prentice-Hall, Englewood Cliffs, NJ (1964), pp. 196–200.

two capillaries. Denote, respectively, by h_A and p_A the height of fluid in the reservoir and driving pressure (at the ram) for viscometer A. Use similar definitions for B. The ram speeds in the two viscometers are the same so that the flow rate Q through each of the two tubes is the same.

a. Apply the macroscopic mechanical energy balance[8] to the fluid in the viscometer, taking plane number 1 to be the tip of the ram and plane number 2 to be at the exit of the tube. For the purposes of this balance, take h to be constant. Show that for viscometer A

$$(\hat{\Phi}_{A_2} - \hat{\Phi}_{A_1}) + \frac{1}{2}\left(\frac{\langle v_z^3\rangle}{\langle v_z\rangle}\bigg|_{A_2} - \frac{\langle v_z^3\rangle}{\langle v_z\rangle}\bigg|_{A_1}\right) + \frac{1}{\rho Q}\int_{A_2} pv_z\,dS - \frac{p_A}{\rho} = -(\hat{E}_v)_A \tag{10C.1-1}$$

and that a similar relation holds for B. Here $\hat{\Phi}$ is the potential energy per unit mass, v_z is the axial velocity, $\langle v_z^3\rangle$ and $\langle v_z\rangle$ are cross-sectional averages of v_z^3 and v_z, and $\hat{E}_v$ is defined by

$$\hat{E}_v = -\frac{1}{\rho Q}\int_V (\boldsymbol{\tau}:\nabla \boldsymbol{v})\,dV \tag{10C.1-2}$$

b. Subtract the two mechanical energy balances to obtain

$$(\hat{\Phi}_{B_2} - \hat{\Phi}_{B_1}) - (\hat{\Phi}_{A_2} - \hat{\Phi}_{A_1}) - \frac{1}{\rho}(p_B - p_A) = +(\hat{E}_v)_A - (\hat{E}_v)_B \tag{10C.1-3}$$

c. Next, by splitting the total volume of each system into a volume in which there is steady shear flow plus volumes associated with the flow in the reservoir and in the entrance and exit regions, show that

$$(\hat{E}_v)_A - (\hat{E}_v)_B = \frac{2\pi(L_B - L_A)}{\rho Q}\int_0^R \tau_{rz}\left(\frac{dv_z}{dr}\right)r\,dr = -\frac{2}{\rho}\frac{\tau_R}{R}(L_B - L_A) \tag{10C.1-4}$$

Assume that $h_A = h_B$ in deriving this result. What other assumptions are needed?

d. Choose the reference potential to be at the bottom of the tube of length B so that $\hat{\Phi}_{B_2} = 0$. Use the resulting expressions for the potentials together with the results from **(b)** and **(c)** above to show

$$\tau_R = \left(\frac{p_B - p_A}{L_B - L_A} + \rho g\cos\beta\right)\frac{R}{2} \tag{10C.1-5}$$

where β is the angle between the tube axis and the vertical.

10C.2 Measurements in a Wide-Gap Couette Viscometer[9]

a. Show that for tangential annular flow between concentric cylinders with a wide gap, the appropriate generalizations of Eqs. D-1 and D-2 in Table 10.2-1 are

$$\Delta W = W_2 - W_1 = \frac{1}{2}\int_{\tau_1}^{\tau_2} \eta^{-1}(\tau)\,d\tau \tag{10C.2-1}$$

$$\Delta\pi_{rr} = \pi_{rr}(R_2) - \pi_{rr}(R_1) = \int_{R_1}^{R_2}\left(\rho\frac{v_\theta^2}{r} + \frac{\tau_{\theta\theta} - \tau_{rr}}{r}\right)dr \tag{10C.2-2}$$

In Eq. 10C.2-1, $\tau \equiv \tau_{r\theta} = \mathscr{T}/2\pi r^2 H$.

[8] See, for example, R. B. Bird, W. E. Stewart, and E. N. Lightfoot, *Transport Phenomena*, Wiley, New York (1960), pp. 211–214.

[9] B. D. Coleman, H. Markovitz, and W. Noll, *Viscometric Flows of Non-Newtonian Fluids*, Springer, New York (1966), pp. 42–44; S. Middleman, *The Flow of High Polymers*, Wiley-Interscience, New York (1968), pp. 19–25.

b. For wide gaps the above formulas may be conveniently inverted by differentiating with respect to the torque $\mathscr{T}$. The resulting expressions, valid for any value of $\mathscr{T}$, must also hold for a torque equal to $\beta\mathscr{T}$, where $\beta \equiv R_1^2/R_2^2$. Use this fact to obtain

$$\dot{\gamma}_{r\theta}(\tau_1) = \sum_{j=0}^{\infty} \left(2\mathscr{T}' \frac{\partial \Delta W}{\partial \mathscr{T}'} \right)\Bigg|_{\mathscr{T}' = \mathscr{T}\beta^j} \tag{10C.2-3}$$

$$(\tau_{\theta\theta} - \tau_{rr})|_{\tau_1} = \sum_{j=0}^{\infty} \left(2\mathscr{T}' \frac{\partial \Delta \pi_{rr}^{(c)}}{\partial \mathscr{T}'} \right)\Bigg|_{\mathscr{T}' = \mathscr{T}\beta^j} \tag{10C.2-4}$$

where

$$\Delta \pi_{rr}^{(c)} = \Delta \pi_{rr} - \int_{R_1}^{R_2} \rho \frac{v_\theta^2}{r}\, dr \tag{10C.2-5}$$

c. Explain how Eqs. 10C.2-3 and 4 can be used to interpret experimental data. Why are they useful only for wide gaps?